Informatics in Medicine Unlocked 49 (2024) 101548

Contents lists available at ScienceDirect

Informatics in Medicine Unlocked

journal homepage: www.elsevier.com/locate/imu

Non-optimal and optimal fractional control analysis of measles using real data

Fredrick Asenso Wireko [a], Joshua Kiddy K. Asamoah [a,*], Isaac Kwasi Adu [b], Sebastian Ndogum [a]

[a] Department of Mathematics, Kwame Nkrumah University of Science and Technology, Kumasi, Ghana
[b] Department of Mathematical Sciences, Kumasi Technical University, Ghana

ARTICLE INFO

Keywords:
Mathematical modeling
Disease modeling
Vaccination strategies
Compartmental modeling
Sensitivity analysis

ABSTRACT

This study employs fractional, non-optimal, and optimal control techniques to analyze measles transmission dynamics using real-world data. Thus, we develop a fractional-order compartmental model capturing measles transmission dynamics. We then formulate an optimal control problem to minimize the disease burden while considering constraints such as vaccination resources and intervention costs. The proposed model's positivity, boundedness, measles reproduction number, and stability are obtained. The sensitivity analysis using the partial rank correlation coefficient is shown for the fractional orders of 0.99 and 0.90. It is noticed that the rate of recruitment into the susceptible population (π), the rate at which individuals in the latent class become asymptomatic (α_1), and the transmission rate (β) contribute positively to the spread of the disease, while the rate at which individuals in the asymptomatic class become symptomatic (α_2), the vaccination rate for the first measles dose (γ_1), and the rate at which individuals in the latent class recover from measles (δ_1) contribute significantly to the reduction of measles in the community. Utilizing numerical simulations and sensitivity analyses, we identify optimal control strategies that balance the trade-offs between intervention efficacy, resource allocation, and societal costs. Our findings provide insights into the effectiveness of fractional optimal control strategies in mitigating measles outbreaks and contribute to developing more robust and adaptive disease control policies in real-world scenarios.

1. Introduction

Significant efforts have been made to eradicate infectious diseases through vaccination and education of the general populace. Yet, some of these diseases, like measles, have continued to rage destruction to human lives, especially the unvaccinated children under the age of five years and adults beyond 50 years [1]. The measles virus, classified as a member of the Morbillivirus genus in the Paramyxoviridae family, is a very contagious enveloped virus with a negative single-stranded RNA genome that affects the respiratory and the digestive tract [1,2]. Measles is highly contagious; up to 90% of those nearby or who have interacted with contaminated surfaces are prone to contracting the virus if they are not immune to the disease. The virus can stay in the environment for up to 2 h when an infected person contaminates the environment through mucus-induced coughing [3]. Symptoms, usually in the form of rashes, appear between ten to fourteen days after infection. They can lead to life-threatening complications in the form of pneumonia, sinusitis, otitis media, otosclerosis, tonsillitis, and sensorineural hearing loss [4]. Vaccination has been the driving force in preventing measles in many parts of the world, and it has averted about 56 million deaths between 2000 and 2021 alone. Unfortunately, these efforts were impeded due to the onset of COVID-19, which has drastically reduced the number of people vaccinated. In 2020, most children in African countries could not receive their first measles dose vaccine, and about 22.3 million children worldwide were not vaccinated [5,6].

Mathematical modeling has been vital in studying physical phenomena of a complex nature into simple and logical forms using graphical interpretations [7]. Such models, in effect, aid government and non-governmental organizations or even institutions in making informed decisions about the physical environment [8,9]. Many researchers have used mathematical models to understand the dynamics and transmission of the measles virus; for instance, Tilahun et al. [10] proposed a stochastic model of measles transmission with double dose vaccination, a five-compartmental model consisting of the standard SIR model with first vaccinated and second vaccinated compartments. They remarked that the disease-free equilibrium is asymptotically stable in deterministic and stochastic models. Additionally, sensitivity analyses were conducted to examine the impact of some parameters on the transmission of measles. However, they did not consider the duration of

* Corresponding author.
E-mail addresses: fredrick.wireko@knust.edu.gh (F.A. Wireko), jkkasamoah@knust.edu.gh (J.K.K. Asamoah).

https://doi.org/10.1016/j.imu.2024.101548
Received 20 April 2024; Received in revised form 4 July 2024; Accepted 6 July 2024
Available online 9 July 2024

exposure and the possibility of hospitalization, as individuals infected with the virus might need treatment before recovering due to the complications the disease can cause. Another model worth mentioning is Peter et al. [11]. They developed a measles transmission model comprising six compartments of susceptible, vaccinated, infected, hospitalized, and recovered individuals. They concluded that a stable endemic equilibrium exists if the Routh–Hurwitz condition is met and that the local and global stability is stable if the $\mathcal{R}_0 < 1$. Even though this model inculcated hospitalization as a way of treating infected individuals and prescribing vaccination to gain immunity against the virus, this model failed to meet the standard of measles vaccination policy. Thus, the interval between the first and second doses should be between six to twelve months as recommended by the World Health Organization [12]. Also, in the work of Kuddus et al. [13], they proposed a measles transmission model with a double-dose vaccination by incorporating the SEIR model with first and second-dose vaccinated individuals. They used the bacic reproduction number to determine the stability of the equilibrium points. They observed that early treatment of infected patients and vaccination are essential in containing the measles disease as the transmission rate propels the spread of measles among people. However, they did not regard that infected patients might get hospitalized from complications arising from the disease.

In addition, Diagne et al. [14] constructed a more holistic measles model with a non-linear incidence function, in which they conducted a theoretical analysis with optimal control analysis. In their model, the entire population was divided into six groups: individuals who were virus-susceptible, individuals who had gotten initial measles vaccination, those who received a second dose of the vaccine, the exposed class, the infected class, and the recovered class. They established that the model follows a forward bifurcation using the center manifold theory, and they also suggested an ideal control model with three control measures to lessen the measles virus's effects. The Pontryagin Maximum Principle was applied to assess the control model. On the other hand, the model failed to account for the treatment of infected individuals to boost their chances of survival and recovery.

It has, therefore, been an eminent quest as researchers forecast how long the disease will be in existence and seek to find reliable means of controlling the spread of the disease shortly. This has prompted researchers to develop non-optimal and optimal control models from diverse perspectives about infectious diseases [15]. As seen in Berhe et al. [16], a four-compartmental model with an optimal control strategy for the measles epidemic in a population was developed. In the work of Subhas et al. [17], they studied tuberculosis transmission dynamics with exogenous reinfections and endogenous reactivation. The researchers discovered their tuberculosis transmission model experiences Hopf bifurcation regarding contact and exogenous reinfection rates. Seidu et al. [18] focused on the dynamics of cholera in the presence of hyper-infective individuals. They identified the optimal combination of infection control measures, adherence to cleanliness procedures, treatment regulation, and bacterial-shedding restrictions necessary to manage the transmission of cholera effectively. Appiah et al. [19] studied the cost–benefit analysis of the COVID-19 vaccination model incorporating different infectivity reductions. The findings of Appiah et al. [19] enhanced our comprehension of COVID-19 epidemiology and offered valuable guidance on applying treatments to reduce the impact of COVID-19. Mathematical modeling of two strains Tuberculosis and COVID-19 vaccination model: A co-infection study with cost-effectiveness analysis was also presented in [20]. The survey in [20] investigates the durability of the co-infection model by analyzing the relationship between tuberculosis strains and COVID-19 reproduction numbers. They explored the impact of the drug-resistant and drug-sensitive strains of Tuberculosis on the co-infection of COVID-19 by examining the sensitivity of the parameters. Kumar et al. [21] studied the impact of media awareness and optimal strategy on the prevalence of tuberculosis. The model demonstrates the global asymptotic stability of the endemic equilibrium by building an appropriate Lyapunov function. Other works that studied the dynamics of various infectious diseases and made a significant contribution can be found in [22,22–28].

Notwithstanding the above, integer order operators have enormous limitations, such as their inability to measure memory effect and continuous data. This has, therefore, necessitated the need for fractional operators. Many biological systems have a constant data measurement and have consequently made the fractional operators of significant usage since fractional differential operators generalize the concept of derivatives [29]. Given this, researchers have proposed several fractional operators like the Caputo fractional operator, Atangana–Baleanu fractional operator in the Caputo sense, and Caputo–Fabrizio fractal-fractional operators, and have received enormous applications in studying infectious diseases. For instance, in [30,31], the transmission dynamics of gonorrhea disease were studied using fractional operators. Also, in [32], a fractional order mathematical model was constructed to study the heartwater transmission dynamics by emphasizing adult amblyopia and nymph ticks. The monkeypox disease was also extensively studied through fractional operators in [8,33]. Hamadjan et al. [34] studied the measles epidemic disease and its dynamics using the Caputo fractional operators. In their work, the population was stratified into six compartments, and they investigated the existence of a single stable solution using Caputo fractional operators. Their study reported the effect of natural occurrences contributing to the spread of the measles disease in societies. Considering the essence of memory effect in the study of epidemic models, Sania et al. [35] applied the Caputo fractional operator to study the dynamics of measles where the population was subdivided into four classes, that is, susceptible, vaccinated, infected and recovered. Their study also reported a reasonable effect of the fractional operator on the dynamics of the measles disease. Muhammad et al. [36] further used the Caputo fractional operator to study the measles disease where they introduced the exposed and hospital compartments, which Sania et al. [35] did not consider. They applied diverse approaches where the constant proportion (CP) model was transformed into a continuous proportion Caputo (CPC) model and then derived the eigenvectors of the CPC operator. Symmetric analysis was then carried out to study the model numerically. They reported that the CPC model significantly represented the physical environment more accurately than the integer-order models see, for instance, the work in [37–41] for more insight into the use of fractional derivatives.

Measles disease is reported to be one of the leading memory-dependent diseases in the world [42,43]. This is because the measles virus is highly contagious such that when the measles virus infects an individual, it targets the memory B cells, which are responsible for immune memory, and weakens or destroys them, therefore causing the loss of memory of previous infections and also permitting new measles infections to replace them, this is known as immune amnesia in epidemiology [44,45]. This studies, therefore, demonstrate a mathematical model for the measles disease using the Caputo fractional operator and fractional optimal control model to help minimize the spread of the measles disease in a population.

The rest of the paper is organized as follows: In Section 2, we give some primary results regarding the Caputo fractional derivative. Section 3 contains the model description, definition of the various parameters used in the model formulation, model flowchart, the invariant region, positivity of the solution, disease-free equilibrium points, and the reproduction number of the proposed model. In Section 4, we introduce the fractional Caputo model and the existence and uniqueness of the measles disease model with fractional operators. In Section 5, we presented the parameter estimation of the proposed model together with sensitivity analysis and fractional simulations. In Section 6, we presented the fractional optimal controls based on the sensitivity analysis. Finally, the conclusion and future analysis of the model is presented in 7.

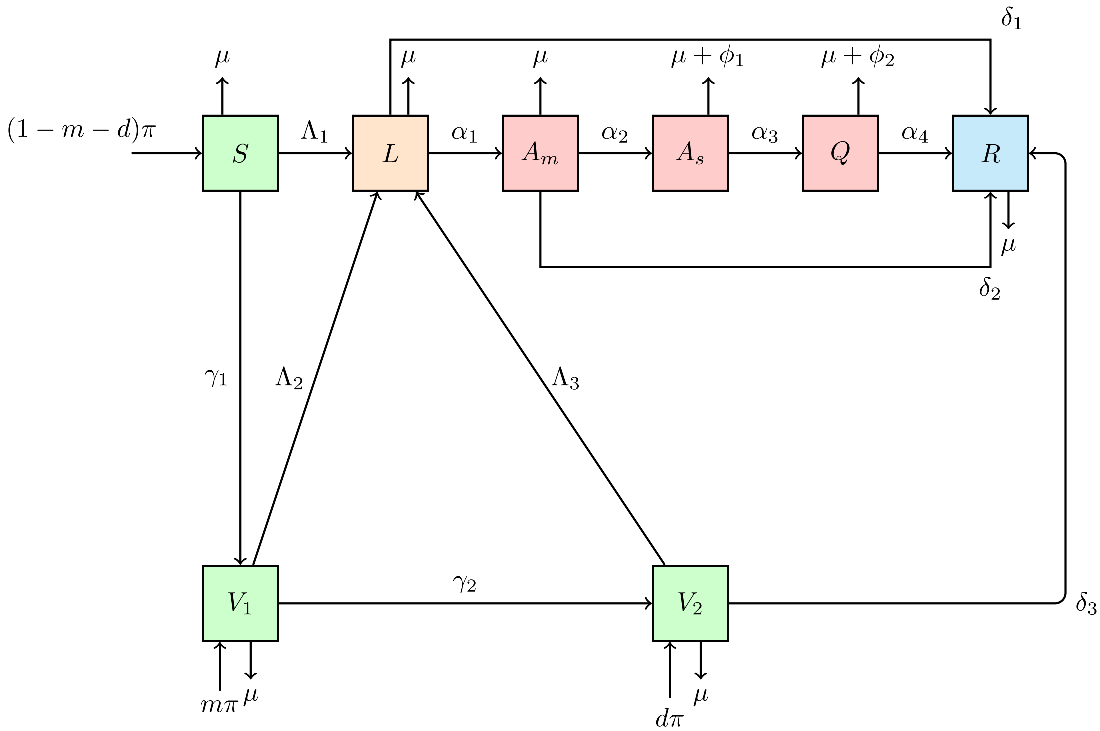

Fig. 1. Flow diagram of the model.

2. Basic results

This section focuses on highlighting some critical definitions of the development of the Caputo fractional measles disease model. We then derive these definitions from literature, see [46,47].

Definition 2.1. The fractional differentiation in the Caputo sense of the given function $\Omega(\curlyvee)$ of the order $\vartheta(\vartheta > 0)$ is defined as

$$\begin{cases} {}^{C}\mathcal{D}^{\vartheta}_{0,\curlyvee}\Omega(\curlyvee) = \frac{1}{\Gamma(n-\vartheta)}\int_0^{\curlyvee}(\curlyvee-\mu)^{n-\vartheta-1}\frac{d^n\Omega(\mu)}{d\mu^n}d\mu, & n-1<\mu<n, m\in\mathcal{N}, \\ \frac{d^n}{d\curlyvee^n}\Omega(\curlyvee), n=\mu, n\in\mathcal{N}. \end{cases}$$

where we have $\Gamma(m) = \int_0^{\infty} e^{-\curlyvee}\curlyvee^{m-1}\,d\curlyvee$, as the Euler's Gamma operator. Then we define the Caputo antiderivative with order $\vartheta > 0$ in the form,

$$I^{\vartheta}({}^{C}\mathcal{D}^{\vartheta}_{0,\curlyvee}\Omega(\curlyvee)) = \frac{1}{\Gamma(\vartheta)}\int_0^{\vartheta}\frac{\Omega(s)}{(\curlyvee-s)^{1-\vartheta}}ds,$$

with $\curlyvee > 0$.

3. Formulation of the model

In a population of social interaction, a deterministic model is formulated to describe the transmission of measles disease in a susceptible population. The total population $N(\curlyvee)$ is subdivided into eight (8) compartments at time $\curlyvee$, consisting of the susceptible population $S(\curlyvee)$, individuals that received the first dose of vaccination are denoted as $V_1(\curlyvee)$, those that received the second dose of vaccination is denoted by $V_2(\curlyvee)$, those in the latent class $L(\curlyvee)$. In the latent class, individuals are infected but not yet infectious, asymptomatic individuals $A_m(\curlyvee)$, symptomatic individuals $A_s(\curlyvee)$, infectious individuals that are isolated or quarantined $Q(\curlyvee)$, and the recovered individuals $R(\curlyvee)$. Individuals are recruited into the susceptible population through birth or immigration of unvaccinated individuals at the rate of $(1-m-d)\pi$. The first dose vaccination rate is denoted as γ_1 while others move to the latent compartment through the force of infection Λ_1. The efficacy of the measles vaccine is not 100 percent effective; therefore, individuals who have received the first dose of vaccination $V_1(t)$ are assumed to transition to the latent class with the force of infection Λ_2. Individuals receiving their second dose of vaccine transition to the second dose compartment at the rate of γ_2. It is also assumed that individuals in the second dose vaccine compartment $V_2(\curlyvee)$ get infected and moved to the latent class with the force of infection Λ_3. Also, people are infected with the measles virus through social interaction; hence, individuals infected without exhibiting any clinical signs enter the asymptomatic compartment at the rate of α_1. The asymptomatic population decreases due to people recovering from the diseases without showing symptoms at δ_2 and becoming infectious symptomatic at the rate of α_2 and then moving into the symptomatic compartment. Since infectious individuals with the measles virus suffer from complications from other illnesses, the symptomatic population declines due to an induced death rate of ϕ_1. In contrast, the others are isolated for treatment at the rate of α_3 with the measles-induced death rate of ϕ_2. Those who successfully get treated from the isolation centers recover at the rate of α_3. The total population at time $\curlyvee$, is given as $N(\curlyvee) = S(\curlyvee) + V_1(\curlyvee) + V_2(\curlyvee) + L(\curlyvee) + A_m(\curlyvee) + A_s(\curlyvee) + Q(\curlyvee) + R(\curlyvee)$. Table 1 gives the rest of the parameter description. The following assumptions were considered in developing the measles model in Fig. 1.

1. The transmission rate follows a Holling type II response; thus, the force of infection is given as

$$\Lambda_1 = \beta S\left(\frac{A_m}{1+\epsilon_1 Am} + \frac{As}{1+\epsilon_2 As}\right), \tag{1}$$

where β is the transmission rate, ϵ_1 and ϵ_2 characterizes the strength of the saturation effect.

2. Since the measles vaccine is not 100% effective, the efficacy of the vaccine is represented as $0 \le \epsilon_i \le 1$, where $\epsilon_i = 0$ means the vaccine does not provide protection and $\epsilon_i = 1$ means the measles vaccine provide 100% protection against the virus. Therefore, the force of infection in the vaccinated compartments is given as:

$$\Lambda_2 = (1-\tau_1)\beta V_1\left(\frac{Am}{1+\sigma V_1} + \frac{As}{1+\sigma V_1}\right), \tag{2}$$

$$\Lambda_3 = (1-\tau_2)\beta V_2\left(\frac{Am}{1+\sigma V_2} + \frac{As}{1+\sigma V_2}\right), \tag{3}$$

Table 1
Model parameters descriptions.

Parameters	Description	Parameters	Description
π	Rate of recruitment into the susceptible population	γ_1	Vaccination rate for first measles dose
γ_2	Vaccination rate for the second dose of measles vaccine	δ_1	The rate at which individuals in the latent class recover from the measles
δ_2	Recovery rate for asymptomatic individuals	δ_3	Vaccine-induced acquisition rate
α_1	Rate at which individuals in the latent class become asymptomatic	d	Fraction of newly recruited second dose vaccinated individuals
α_3	Rate of transition from symptomatic to isolation	α_2	Rate at which individuals in the asymptomatic class become symptomatic
α_4	Rate of recovery from isolation	τ_1	Efficacy of first dose of vaccine
τ_2	Efficacy of second dose of vaccine	ϵ_1	Inhibitory effect of susceptible
ϵ_2	Psychological effect of the infective	μ	Natural death rate
σ	Availability of measles vaccine in the population	ϕ_1	Measles-induced death rate for the symptomatic population
ϕ_2	Measles-induced death rate for the isolated population	m	Fraction of newly recruited first dose vaccinated individuals

where τ_1 and τ_2 are the efficacy of first and second dose vaccine respectively.

3. The natural death rate μ is considered constant in all the compartments, while the disease-induced death rate for symptomatic individuals ϕ_1 differs from those isolated for treatment ϕ_2.

From the above model description and assumptions, the system of equations without memory effects is given as follows;

$$\left.\begin{aligned}
\frac{dS}{d\curlyvee} &= (1-m-d)\pi - \beta S\left(\frac{A_m}{1+\epsilon_1 Am} + \frac{As}{1+\epsilon_2 As}\right) - (\mu+\gamma_1)S,\\
\frac{dV_1}{d\curlyvee} &= m\pi + \gamma_1 S - (1-\tau_1)\beta V_1\left(\frac{Am}{1+\sigma V_1} + \frac{As}{1+\sigma V_1}\right) - (\mu+\gamma_4)V_1,\\
\frac{dV_2}{d\curlyvee} &= d\pi + \gamma_2 V_1 - (1-\tau_2)\beta V_2\left(\frac{Am}{1+\sigma V_2} + \frac{As}{1+\sigma V_2}\right) - (\mu+\delta_3)V_2,\\
\frac{dL}{d\curlyvee} &= \beta S\left(\frac{A_m}{1+\epsilon_1 Am} + \frac{As}{1+\epsilon_2 As}\right) + (1-\tau_1)\beta V_1\left(\frac{Am}{1+\sigma V_1} + \frac{As}{1+\sigma V_1}\right)\\
&+ (1-\tau_2)\beta V_2\left(\frac{Am}{1+\sigma V_2} + \frac{As}{1+\sigma V_2}\right) - (\mu+\alpha_1+\delta_1)L,\\
\frac{dA_m}{d\curlyvee} &= \alpha_1 L - (\mu+\alpha_2+\delta_2)A_m,\\
\frac{dA_s}{d\curlyvee} &= \alpha_2 A_m - (\mu+\phi_1+\alpha_3)A_s,\\
\frac{dQ}{d\curlyvee} &= \alpha_3 A_s - (\mu+\phi_2+\alpha_4)Q,\\
\frac{dR}{d\curlyvee} &= \delta_1 L + \delta_2 A_m + \delta_3 V_2 + \alpha_4 Q - \mu R,
\end{aligned}\right\} \tag{4}$$

where the initial conditions are given as $S(0) = S^0, V_1(0) = V_1^0, V_2(0) = V_2^0, L(0) = L^0$,

$A_m(0) = A_m^0, A_s(0) = A_s^0, Q(0) = Q_0$ and $R(0) = R_0$.

3.1. Invariant region

To show that the total population is bounded in a region, we know that,

$$\frac{dN}{d\curlyvee} = \frac{dS}{d\curlyvee} + \frac{dV_1}{d\curlyvee} + \frac{dV_2}{d\curlyvee} + \frac{dL}{d\curlyvee} + \frac{dA_m}{d\curlyvee} + \frac{dA_s}{d\curlyvee} + \frac{dQ}{d\curlyvee} + \frac{dR}{d\curlyvee}. \tag{5}$$

Hence, making substitutions from Eq. (4) into Eq. (5), we obtained,

$$\begin{aligned}
\frac{dN}{d\curlyvee} &= (1-m-d)\pi - \beta S\left(\frac{A_m}{1+\epsilon_1 Am} + \frac{As}{1+\epsilon_2 As}\right)\\
&- (\mu+\gamma_1)S + m\pi + \gamma_1 S\\
&- (1-\tau_1)\beta V_1\left(\frac{Am}{1+\sigma V_1} + \frac{As}{1+\sigma V_1}\right) - (\mu+\gamma_4)V_1 + d\pi + \gamma_2 V_1\\
&- (1-\tau_2)\beta V_2\left(\frac{Am}{1+\sigma V_2} + \frac{As}{1+\sigma V_2}\right)\\
&- (\mu+\delta_3)V_2 + \beta S\left(\frac{A_m}{1+\epsilon_1 Am} + \frac{As}{1+\epsilon_2 As}\right)\\
&+ (1-\tau_1)\beta V_1\left(\frac{Am}{1+\sigma V_1} + \frac{As}{1+\sigma V_1}\right)\\
&+ (1-\tau_2)\beta V_2\left(\frac{Am}{1+\sigma V_2} + \frac{As}{1+\sigma V_2}\right) - (\mu+\alpha_1+\delta_1)L\\
&+ \alpha_1 L - (\mu+\alpha_2+\delta_2)A_m\\
&+ \alpha_2 A_m - (\mu+\phi_1+\alpha_3)A_s + \alpha_3 A_s\\
&- (\mu+\phi_2+\alpha_4)Q + \delta_1 L + \delta_2 A_m + \delta_3 V_2 + \alpha_4 Q - \mu R.
\end{aligned} \tag{6}$$

Simplifying Eq. (6) and grouping the terms, we obtained,

$$\frac{dN}{d\curlyvee} = \pi - \mu(S + V_1 + V_2 + L + A_m + A_s + Q + R) - \Phi_1 A_s - \phi_2 Q, \tag{7}$$

therefore if no death occurs due to measles-induced death rate, then,

$$\frac{dN}{d\curlyvee} \leq \pi - \mu N. \tag{8}$$

Using the integrating factor method to solve Eq. (8), we obtained

$$N(\curlyvee) \leq \frac{\pi}{\mu}. \tag{9}$$

Hence, the solution for the equation is bounded in the region

$$\varphi = \left\{ S + V_1 + V_2 + L + A_m + A_s + Q + R \in \mathcal{R}^8 : 0 \leq \frac{\pi}{\mu} \right\}. \tag{10}$$

3.2. Positivity of the solution

By using the model equations in (4), we used the method of integrating factors by starting with the first equation $\frac{dS}{d\curlyvee}$

$$\frac{dS}{d\curlyvee} = (1-m-d)\pi - \beta S\left(\frac{A_m}{1+\epsilon_1 Am} + \frac{As}{1+\epsilon_2 As}\right) - (\mu+\gamma_1)S. \quad (11)$$

Using the method of integrating factors to solve Eq. (11), we obtained

$$S(\curlyvee) = e^{-\int_0^t \left(\beta(\frac{A_m}{1+\epsilon_1 A_m} + \frac{A_s}{1+\epsilon_2 A_s}) - (\mu+\gamma_1)\right)d\curlyvee} \times \int_0^t \left((1-m-d)\pi \times e^{\int_0^t \left(\beta(\frac{A_m}{1+\epsilon_1 A_m} + \frac{A_s}{1+\epsilon_2 A_s}) - (\mu+\gamma_1)\right)d\curlyvee}\right), \quad (12)$$

the same workings showed that $V_1(0) \geq 0, V_2(0) \geq 0, L(0) \geq 0, A_m(0) \geq 0, A_s(0) \geq 0, Q(0) \geq 0, R(0) \geq 0$ for all $t \geq 0$.

3.3. Disease-free equilibrium points

At the disease-free equilibrium (DFE), the infected classes are zero, that is, $L(\curlyvee) = 0, A_m(\curlyvee) = 0, A_S(\curlyvee) = 0, Q(\curlyvee) = 0$. The equilibrium points are then obtained by putting the L.H.S of the system of Eqs. (4) to zero. Hence, the DFE points $(S^*, V_1^*, V_2^*, L^*, A_m^*, A_s^*, Q^*, R^*)$

$$= \left(\frac{\pi(1-m-d)}{(\gamma_1+\mu)}, \frac{\pi(\gamma_1+m\mu-d\gamma_1)}{(\mu+\gamma_1)(\mu+\gamma_4)}, \frac{\mu^2 d\pi + \gamma_1\gamma_2\pi + \gamma_2\ m\mu\pi + \gamma_1\mu d\pi + \gamma_2\mu d\pi}{(\delta_3+\mu)(\gamma_1+\mu)(\gamma_4+\mu)}, 0, 0, 0, 0, \frac{\tau_2\delta_3 V_2^*}{\mu}\right).$$

3.4. Basic reproduction number

From the infective classes from Eq. (4), we apply the next generation matrix to the system and obtained

$$\mathcal{F} = \begin{bmatrix} \beta S\left(\frac{A_m}{1+\epsilon_1 Am} + \frac{As}{1+\epsilon_2 As}\right) + (1-\tau_1)\beta V_1\left(\frac{Am}{1+\sigma V_1} + \frac{As}{1+\sigma V_1}\right) + (1-\tau_2)\beta V_2\left(\frac{Am}{1+\sigma V_2} + \frac{As}{1+\sigma V_2}\right) \\ 0 \\ 0 \\ 0 \end{bmatrix},$$

$$\mathcal{V} = \begin{bmatrix} (\mu+\alpha_1+\delta_1)L \\ -\alpha_1 L + (\mu+\alpha_2+\delta_2)A_m \\ -\alpha_2 A_m + (\mu+\phi_1+\alpha_3)A_s \\ -\alpha_3 A_s + (\mu+\phi_2+\alpha_4)Q \end{bmatrix}.$$

Finding the Jacobian of $\mathcal{F}$ and $\mathcal{V}$ at disease-free equilibrium, we obtained,

$$F = \begin{bmatrix} 0 & S\beta - \frac{V_1\beta(\tau_1-1)}{V_1\sigma+1} - \frac{V_2\beta(\tau_2-1)}{V_2\sigma+1} & S\beta - \frac{V_1\beta(\tau_1-1)}{V_1\sigma+1} - \frac{V_2\beta(\tau_2-1)}{V_2\sigma+1} & 0 \\ 0 & 0 & 0 & 0 \\ 0 & 0 & 0 & 0 \\ 0 & 0 & 0 & 0 \end{bmatrix},$$

$$V = \begin{bmatrix} (\mu+\alpha_1+\delta_1) & 0 & 0 & 0 \\ \alpha_1 & (\mu+\alpha_2+\delta_2) & 0 & 0 \\ 0 & \alpha_2 & (\mu+\phi_1+\alpha_3) & 0 \\ 0 & 0 & \alpha_3 & (\mu+\phi_2+\alpha_4) \end{bmatrix}.$$

The basic reproduction number is the supremum of the eigenvalues of FV^{-1}. That is

$$\rho(FV^{-1}) = \mathcal{R}_0 = \frac{\alpha_1}{xy}\left[\left(\frac{V_1^*\beta(\tau_1-1)}{V_1^*\sigma+1} - S^*\beta + \frac{V_2^*\beta(\tau_2-1)}{V_2^*\sigma+1}\right) + \frac{\alpha_1\alpha_2}{z}\left(\frac{V_1^*\beta(\tau_1-1)}{V_1^*\sigma+1} - S^*\beta + \frac{V_2^*\beta(\tau_2-1)}{V_2^*\sigma+1}\right)\right],$$

where $x = (\mu+\alpha_1+\delta_1), y = (\mu+\alpha_2+\delta_2), z = (\mu+\phi_1+\alpha_3)$.

4. Non-integer order representation of the measles model

The integer order measles model (4) is reformulated using fractional operators in this section. Fractional systems provide veracious and circumstantiated facts on the dynamics of a biological process, especially in reporting on memory processes in such systems. In the case of measles, the virus fights the immune system by attacking the memory cell B, which over time replaces the memory of previous infections with new measles virus infections [45]. Therefore, this suggests that we can provide robust and accurate information on the dynamics of the measles disease by employing fractional operators. The memory effect is significant in infectious disease modeling as individuals can acquire an immunity or lose it over time, impacting the disease's spread. Furthermore, fractional calculus offers a versatile framework for explaining phenomena characterized by long-range dependencies and non-local interactions, frequently observed in the spread of infectious diseases. Models that use fractional derivatives better capture the complex dynamics of measles outbreaks, including factors like vaccination effects, demographic variety, and spatial layout. Fractional order derivative models provide crucial insights for creating effective control measures and treatments by improving the accuracy of representing the essential dynamics of measles transmission. Therefore, using the Caputo interpretation, the integer-order measles model (4) is reformulated in the fractional system. What follows is an explanation of the Caputo fractional order measles model;

$$\begin{aligned}
{}^C\mathcal{D}^{\vartheta}_{0,\curlyvee}S(\curlyvee) &= (1-m^{\vartheta}-d^{\vartheta})\pi^{\vartheta} - \beta^{\vartheta}S\left(\frac{A_m}{1+\epsilon_1^{\vartheta}Am} + \frac{As}{1+\epsilon_2^{\vartheta}As}\right) \\
&\quad - (\mu^{\vartheta}+\gamma_1^{\vartheta})S, \\
{}^C\mathcal{D}^{\vartheta}_{0,\curlyvee}V_1(\curlyvee) &= m^{\vartheta}\pi^{\vartheta} + \gamma_1^{\vartheta}S - (1-\tau_1^{\vartheta})\beta^{\vartheta}V_1\left(\frac{Am}{1+\sigma^{\vartheta}V_1} + \frac{As}{1+\sigma^{\vartheta}V_1}\right) \\
&\quad - (\mu^{\vartheta}+\gamma_4^{\vartheta})V_1, \\
{}^C\mathcal{D}^{\vartheta}_{0,\curlyvee}V_2(\curlyvee) &= d^{\vartheta}\pi^{\vartheta} + \gamma_2^{\vartheta}V_1 - (1-\tau_2^{\vartheta})\beta^{\vartheta}V_2\left(\frac{Am}{1+\sigma^{\vartheta}V_2} + \frac{As}{1+\sigma^{\vartheta}V_2}\right) \\
&\quad - (\mu^{\vartheta}+\delta_3^{\vartheta})V_2, \\
{}^C\mathcal{D}^{\vartheta}_{0,\curlyvee}L(\curlyvee) &= \beta^{\vartheta}S\left(\frac{A_m}{1+\epsilon_1^{\vartheta}Am} + \frac{As}{1+\epsilon_2^{\vartheta}As}\right) \\
&\quad + (1-\tau_1^{\vartheta})\beta^{\vartheta}V_1\left(\frac{Am}{1+\sigma^{\vartheta}V_1} + \frac{As}{1+\sigma^{\vartheta}V_1}\right) \\
&\quad + (1-\tau_2^{\vartheta})\beta^{\vartheta}V_2\left(\frac{Am}{1+\sigma^{\vartheta}V_2} + \frac{As}{1+\sigma^{\vartheta}V_2}\right) - (\mu^{\vartheta}+\alpha_1^{\vartheta}+\delta_1^{\vartheta})L, \\
{}^C\mathcal{D}^{\vartheta}_{0,\curlyvee}A_m(\curlyvee) &= \alpha_1^{\vartheta}L - (\mu^{\vartheta}+\alpha_2^{\vartheta}+\delta_2^{\vartheta})A_m, \\
{}^C\mathcal{D}^{\vartheta}_{0,\curlyvee}A_s(\curlyvee) &= \alpha_2^{\vartheta}A_m - (\mu^{\vartheta}+\phi_1^{\vartheta}+\alpha_3^{\vartheta})A_s, \\
{}^C\mathcal{D}^{\vartheta}_{0,\curlyvee}Q(\curlyvee) &= \alpha_3^{\vartheta}A_s - (\mu^{\vartheta}+\phi_2^{\vartheta}+\alpha_4^{\vartheta})Q, \\
{}^C\mathcal{D}^{\vartheta}_{0,\curlyvee}R(\curlyvee) &= \delta_1^{\vartheta}L + \delta_2^{\vartheta}A_m + \delta_3^{\vartheta}V_2 + \alpha_4^{\vartheta}Q - \mu^{\vartheta}R.
\end{aligned} \quad (13)$$

with the initial values given as $S(0) = S^0, V_1(0) = V_1^0, V_2(0) = V_2^0, L(0) = L^0, A_m(0) = A_m^0, A_s(0) = A_s^0, Q(0) = Q_0$ and $R(0) = R_0$.

4.1. Existence and uniqueness

Utilizing the fixed point theory, this section delves into whether the solution to the fractional measles disease model, as defined by Caputo (13), exists and remains unique. Let us start by defining the norm $\mathbb{B}(\Theta)$ that is, a Banach space, and also, a continuous real-valued function given in the domain $\Theta(0,a)$ with a defined sub norm. In addition, we have $\mathcal{L} = \mathbb{B}(\Theta_1)\times\mathbb{B}(\Theta_2)\times\mathbb{B}(\Theta_3)\times\mathbb{B}(\Theta_4)\times\mathbb{B}(\Theta_5)\times\mathbb{B}(\Theta_6)\times\mathbb{B}(\Theta_7)\times\mathbb{B}(\Theta_8)$ on the norm $\|(S,V_1,V_2,L,A_m,A_s,Q,R)\| = \|S\|+\|V_1\|+\|V_2\|+\|L\|+\|A_m\|+\|A_s\|+\|Q\|,+\|R\|$ and also $\|S\| = \sup_{t\in\Theta}|S|, \|V_1\| = \sup_{t\in\Theta}|V_1|, \|V_2\| = \sup_{t\in\Theta}|V_2|, \|A_m\| = \sup_{t\in\Theta}|A_m|, \|A_s\| = \sup_{t\in\Theta}|A_s|, \|Q\| = \sup_{t\in\Theta}|Q|, \|R\| = \sup_{t\in\Theta}|R|$. We then go on to apply the Caputo fractional operators on the non-linear fractional model (13); we have;

$$\begin{aligned}
&\mathcal{S}(\Upsilon)-\mathcal{S}(0)\\
&={}^{C}\mathcal{D}^{\vartheta}_{\Upsilon}\left[(1-m^{\vartheta}-d^{\vartheta})\pi^{\vartheta}-\beta^{\vartheta}S\left(\frac{A_m}{1+\epsilon_1^{\vartheta}Am}+\frac{As}{1+\epsilon_2^{\vartheta}As}\right)-(\mu^{\vartheta}+\gamma_1^{\vartheta})S\right],\\
&\mathcal{V}_1(\Upsilon)-\mathcal{V}_1(0)\\
&={}^{C}\mathcal{D}^{\vartheta}_{\Upsilon}\left[m^{\vartheta}\pi^{\vartheta}+\gamma_1^{\vartheta}S-(1-\tau_1^{\vartheta})\beta^{\vartheta}V_1\left(\frac{Am}{1+\sigma^{\vartheta}V_1}+\frac{As}{1+\sigma^{\vartheta}V_1}\right)-(\mu^{\vartheta}+\gamma_4^{\vartheta})V_1\right],\\
&\mathcal{V}_2(\Upsilon)-\mathcal{V}_2(0)={}^{C}\mathcal{D}^{\vartheta}_{\Upsilon}\left[d^{\vartheta}\pi^{\vartheta}+\gamma_2^{\vartheta}V_1-(1-\tau_2^{\vartheta})\beta^{\vartheta}V_2\left(\frac{Am}{1+\sigma^{\vartheta}V_2}+\frac{As}{1+\sigma^{\vartheta}V_2}\right)\right.\\
&\left.-(\mu^{\vartheta}+\delta_3^{\vartheta})V_2\right],\\
&\mathcal{L}(\Upsilon)-\mathcal{L}(0)={}^{C}\mathcal{D}^{\vartheta}_{\Upsilon}[\beta^{\vartheta}S\left(\frac{A_m}{1+\epsilon_1^{\vartheta}Am}+\frac{As}{1+\epsilon_2^{\vartheta}As}\right)+(1-\tau_1^{\vartheta})\beta^{\vartheta}V_1\left(\frac{Am}{1+\sigma^{\vartheta}V_1}\right.\\
&\left.+\frac{As}{1+\sigma^{\vartheta}V_1}\right)+(1-\tau_2^{\vartheta})\beta^{\vartheta}V_2\left(\frac{Am}{1+\sigma^{\vartheta}V_2}+\frac{As}{1+\sigma^{\vartheta}V_2}\right)-(\mu^{\vartheta}+\alpha_1^{\vartheta}+\delta_1^{\vartheta})L],\\
&\mathcal{A}_m(\Upsilon)-\mathcal{A}_m(0)={}^{C}\mathcal{D}^{\vartheta}_{\Upsilon}\left[\alpha_1^{\vartheta}L-(\mu^{\vartheta}+\alpha_2^{\vartheta}+\delta_2^{\vartheta})A_m\right],\\
&\mathcal{A}_s(\Upsilon)-\mathcal{A}_s(0)={}^{C}\mathcal{D}^{\vartheta}_{\Upsilon}\left[\alpha_2^{\vartheta}A_m-(\mu^{\vartheta}+\phi_1^{\vartheta}+\alpha_3^{\vartheta})A_s\right],\\
&\mathcal{Q}(\Upsilon)-\mathcal{Q}(0)={}^{C}\mathcal{D}^{\vartheta}_{\Upsilon}\left[\alpha_3^{\vartheta}A_s-(\mu^{\vartheta}+\phi_2^{\vartheta}+\alpha_4^{\vartheta})Q\right],\\
&\mathcal{R}(\Upsilon)-\mathcal{R}(0)={}^{C}\mathcal{D}^{\vartheta}_{\Upsilon}\left[\delta_1^{\vartheta}L+\delta_2^{\vartheta}A_m+\delta_3^{\vartheta}V_2+\alpha_4^{\vartheta}Q-\mu^{\vartheta}R\right].
\end{aligned}\tag{14}$$

To standardize Eq. (14), we suppose that

$$\begin{aligned}
\mathcal{M}_1&=(1-m^{\vartheta}-d^{\vartheta})\pi^{\vartheta}-\beta^{\vartheta}S\left(\frac{A_m}{1+\epsilon_1^{\vartheta}Am}+\frac{As}{1+\epsilon_2^{\vartheta}As}\right)-(\mu^{\vartheta}+\gamma_1^{\vartheta})S,\\
\mathcal{M}_2&=m^{\vartheta}\pi^{\vartheta}+\gamma_1^{\vartheta}S-(1-\tau_1^{\vartheta})\beta^{\vartheta}V_1\left(\frac{Am}{1+\sigma^{\vartheta}V_1}+\frac{As}{1+\sigma^{\vartheta}V_1}\right)-(\mu^{\vartheta}+\gamma_4^{\vartheta})V_1,\\
\mathcal{M}_3&=d^{\vartheta}\pi^{\vartheta}+\gamma_2^{\vartheta}V_1-(1-\tau_2^{\vartheta})\beta^{\vartheta}V_2\left(\frac{Am}{1+\sigma^{\vartheta}V_2}+\frac{As}{1+\sigma^{\vartheta}V_2}\right)-(\mu^{\vartheta}+\delta_3^{\vartheta})V_2,\\
\mathcal{M}_4&=\beta^{\vartheta}S\left(\frac{A_m}{1+\epsilon_1^{\vartheta}Am}+\frac{As}{1+\epsilon_2^{\vartheta}As}\right)+(1-\tau_1^{\vartheta})\beta^{\vartheta}V_1\left(\frac{Am}{1+\sigma^{\vartheta}}V_1+\frac{As}{1+\sigma^{\vartheta}V_1}\right)\\
&\quad+(1-\tau_2^{\vartheta})\beta^{\vartheta}V_2\left(\frac{Am}{1+\sigma^{\vartheta}V_2}+\frac{As}{1+\sigma^{\vartheta}V_2}\right)-(\mu^{\vartheta}+\alpha_1^{\vartheta}+\delta_1^{\vartheta})L,\\
\mathcal{M}_5&=\alpha_1^{\vartheta}L-(\mu^{\vartheta}+\alpha_2^{\vartheta}+\delta_2^{\vartheta})A_m,\\
\mathcal{M}_6&=\alpha_2^{\vartheta}A_m-(\mu^{\vartheta}+\phi_1^{\vartheta}+\alpha_3^{\vartheta})A_s,\\
\mathcal{M}_7&=\alpha_3^{\vartheta}A_s-(\mu^{\vartheta}+\phi_2^{\vartheta}+\alpha_4^{\vartheta})Q,\\
\mathcal{M}_8&=\delta_1^{\vartheta}L+\delta_2^{\vartheta}A_m+\delta_3^{\vartheta}V_2+\alpha_4^{\vartheta}Q-\mu^{\vartheta}R.
\end{aligned}\tag{15}$$

Considering the expressions in Eq. (14) and applying the definition of the Caputo integral operator, we then reformulate Eq. (13) in the form.

$$\begin{aligned}
S(\Upsilon)-S(0)&=\frac{1}{\Gamma(\vartheta)}\int_0^{\Upsilon}\frac{\mathcal{M}_1(\vartheta,\varphi,S(\varphi))}{(\Upsilon-\varphi)^{1-\vartheta}}d\varphi,\\
V_1(\Upsilon)-V_1(0)&=\frac{1}{\Gamma(\vartheta)}\int_0^{\Upsilon}\frac{\mathcal{M}_2(\vartheta,\varphi,S(\varphi))}{(\Upsilon-\varphi)^{1-\vartheta}}d\varphi,\\
V_2(\Upsilon)-V_2(0)&=\frac{1}{\Gamma(\vartheta)}\int_0^{\Upsilon}\frac{\mathcal{M}_3(\vartheta,\varphi,S(\varphi))}{(\Upsilon-\varphi)^{1-\vartheta}}d\varphi,\\
L(\Upsilon)-L(0)&=\frac{1}{\Gamma(\vartheta)}\int_0^{\Upsilon}\frac{\mathcal{M}_4(\vartheta,\varphi,S(\varphi))}{(\Upsilon-\varphi)^{1-\vartheta}}d\varphi,\\
A_m(\Upsilon)-A_m(0)&=\frac{1}{\Gamma(\vartheta)}\int_0^{\Upsilon}\frac{\mathcal{M}_5(\vartheta,\varphi,S(\varphi))}{(\Upsilon-\varphi)^{1-\vartheta}}d\varphi,\\
A_s(\Upsilon)-A_s(0)&=\frac{1}{\Gamma(\vartheta)}\int_0^{\Upsilon}\frac{\mathcal{M}_6(\vartheta,\varphi,S(\varphi))}{(\Upsilon-\varphi)^{1-\vartheta}}d\varphi,\\
Q(\Upsilon)-Q(0)&=\frac{1}{\Gamma(\vartheta)}\int_0^{\Upsilon}\frac{\mathcal{M}_7(\vartheta,\varphi,S(\varphi))}{(\Upsilon-\varphi)^{1-\vartheta}}d\varphi,\\
R(\Upsilon)-R(0)&=\frac{1}{\Gamma(\vartheta)}\int_0^{\Upsilon}\frac{\mathcal{M}_8(\vartheta,\varphi,S(\varphi))}{(\Upsilon-\varphi)^{1-\vartheta}}d\varphi.
\end{aligned}\tag{16}$$

Now, we proceed by assuming that the Lipschitz condition of boundedness is satisfied given that

$$\mathcal{M}_1(S,\varphi),\mathcal{M}_2(V_1,\varphi),\mathcal{M}_3(V_2,\varphi),\mathcal{M}_4(L,\varphi),\mathcal{M}_5(A_m,\varphi),$$
$$\mathcal{M}_6(A_s,\varphi),\mathcal{M}_7(Q,\varphi),$$

and $\mathcal{K}_8(R,\varphi)$ if and only if there exists a supremum for the given functions $S(\Upsilon),V_1(\Upsilon),V_2(\Upsilon),A_m(\Upsilon),A_s(\Upsilon),Q(\Upsilon)$ and $R(\Upsilon)$. To establish this supposition, we start by considering the dual functions $S(\Upsilon)$ and $S^{\circledast}$ and taking note that;

$$\xi_1^{\vartheta}=\left(\frac{A_m}{1+\epsilon_1^{\vartheta}Am}+\frac{As}{1+\epsilon_2^{\vartheta}As}\right),\quad \xi_2^{\vartheta}=\left(\frac{Am}{1+\sigma^{\vartheta}V_1}+\frac{As}{1+\sigma^{\vartheta}V_1}\right)$$

and $\xi_3^{\vartheta}=\left(\frac{Am}{1+\sigma^{\vartheta}V_2}+\frac{As}{1+\sigma^{\vartheta}V_2}\right)$,

then we have;

$$\begin{aligned}
&\|\mathcal{M}_1(\vartheta,\Upsilon,S(\Upsilon))-\mathcal{M}_1(\vartheta,\Upsilon,S^{\circledast}(\Upsilon))\|\\
&=\|(1-m^{\vartheta}-d^{\vartheta})\pi^{\vartheta}-\beta^{\vartheta}\xi_1^{\vartheta}S-(\mu^{\vartheta}+\gamma_1^{\vartheta})S\|\\
&\le\|-\beta^{\vartheta}\xi_1^{\vartheta}S-(\mu^{\vartheta}+\gamma_1^{\vartheta})S\|\\
&\le\|-[\beta^{\vartheta}\xi_1^{\vartheta}+(\mu^{\vartheta}+\gamma_1^{\vartheta})](S(\Upsilon)-S^{\circledast}(\Upsilon)).
\end{aligned}$$

Now, let us take $\chi_1:=-[\beta^{\vartheta}\xi_1^{\vartheta}+(\mu^{\vartheta}+\gamma_1^{\vartheta})]$, we then have

$$\|\mathcal{M}_1(\vartheta,\Upsilon,S(\Upsilon))-\mathcal{M}_1(\vartheta,\Upsilon,S^{\circledast}(\Upsilon))\|\le\|\chi_1(S(\Upsilon)-S^{\circledast}(\Upsilon))\|.$$

By following a similar approach, we obtain the following for the remaining dual functions as;

$$\begin{aligned}
\|\mathcal{M}_2(\vartheta,\Upsilon,V_1(\Upsilon))-\mathcal{M}_2(\vartheta,\Upsilon,V_1^{\circledast}(\Upsilon))\|&\le\|\chi_2(V_1(\Upsilon)-V_1^{\circledast}(\Upsilon))\|,\\
\|\mathcal{M}_3(\vartheta,\Upsilon,V_2(\Upsilon))-\mathcal{M}_3(\vartheta,\Upsilon,V_2^{\circledast}(\Upsilon))\|&\le\|\chi_3(V_2(\Upsilon)-V_2^{\circledast}(\Upsilon))\|,\\
\|\mathcal{M}_4(\vartheta,\Upsilon,L(\Upsilon))-\mathcal{M}_4(\vartheta,\Upsilon,L^{\circledast}(\Upsilon))\|&\le\|\chi_4(L(\Upsilon)-L^{\circledast}(\Upsilon))\|,\\
\|\mathcal{M}_5(\vartheta,\Upsilon,A_m(\Upsilon))-\mathcal{M}_5(\vartheta,\Upsilon,A_m^{\circledast}(\Upsilon))\|&\le\|\chi_5(A_m(\Upsilon)-A_m^{\circledast}(\Upsilon))\|,\\
\|\mathcal{M}_6(\vartheta,\Upsilon,A_s(\Upsilon))-\mathcal{M}_6(\vartheta,\Upsilon,A_s^{\circledast}(\Upsilon))\|&\le\|\chi_1(A_s(\Upsilon)-A_s^{\circledast}(\Upsilon))\|,\\
\|\mathcal{M}_7(\vartheta,\Upsilon,Q(\Upsilon))-\mathcal{M}_7(\vartheta,\Upsilon,Q^{\circledast}(\Upsilon))\|&\le\|\chi_1(Q(\Upsilon)-Q^{\circledast}(\Upsilon))\|,\\
\|\mathcal{M}_8(\vartheta,\Upsilon,R(\Upsilon))-\mathcal{M}_8(\vartheta,\Upsilon,R^{\circledast}(\Upsilon))\|&\le\|\chi_1(R(\Upsilon)-R^{\circledast}(\Upsilon))\|,
\end{aligned}\tag{17}$$

where $\chi_2=-[(1-\tau_1^{\vartheta})\beta^{\vartheta}\xi_1^{\vartheta}+(\mu^{\vartheta}+\gamma_4^{\vartheta})]$, $\chi_3=(1-\tau_2^{\vartheta})\beta^{\vartheta}\xi_2^{\vartheta}-(\mu^{\vartheta}+\delta_3^{\vartheta})$, $\chi_4=-(\mu^{\vartheta}+\alpha_1^{\vartheta}+\delta_1^{\vartheta})$, $\chi_5=(\mu^{\vartheta}+\alpha_2^{\vartheta}+\delta_2^{\vartheta})$, $\chi_6=-(\mu^{\vartheta}+\phi_1^{\vartheta}+\alpha_3^{\vartheta})$, $\chi_7=-(\mu^{\vartheta}+\phi_2^{\vartheta}+\alpha_4^{\vartheta})$ and $\chi_8=-\mu^{\vartheta}$. From the above discussions, we therefore posit that the Lipschitz condition of boundedness is well established for $\mathcal{M}_1,\mathcal{M}_2,\mathcal{M}_3,\mathcal{M}_4,\mathcal{M}_5,\mathcal{M}_6,\mathcal{M}_7$, and $\mathcal{M}_8$. Following the above, Eq. (16) can be written iteratively in this manner;

$$\begin{aligned}
S_{\iota}(\Upsilon)&=\frac{1}{\Gamma(\vartheta)}\int_0^{\Upsilon}\frac{\mathcal{M}_1(\vartheta,\varphi,S_{\iota-1}(\varphi))}{(\Upsilon-\varphi)^{1-\vartheta}}d\varphi,\\
V_{1_{\iota}}(\Upsilon)&=\frac{1}{\Gamma(\vartheta)}\int_0^{\Upsilon}\frac{\mathcal{M}_1(\vartheta,\varphi,V_{1_{\iota-1}}(\varphi))}{(\Upsilon-\varphi)^{1-\vartheta}}d\varphi,\\
V_{2_{\iota}}(\Upsilon)&=\frac{1}{\Gamma(\vartheta)}\int_0^{\Upsilon}\frac{\mathcal{M}_1(\vartheta,\varphi,V_{1_{\iota-1}}(\varphi))}{(\Upsilon-\varphi)^{1-\vartheta}}d\varphi,\\
L_{\iota}(\Upsilon)&=\frac{1}{\Gamma(\vartheta)}\int_0^{\Upsilon}\frac{\mathcal{M}_1(\vartheta,\varphi,L_{\iota-1}(\varphi))}{(\Upsilon-\varphi)^{1-\vartheta}}d\varphi,\\
A_{m_{\iota}}(\Upsilon)&=\frac{1}{\Gamma(\vartheta)}\int_0^{\Upsilon}\frac{\mathcal{M}_1(\vartheta,\varphi,A_{m_{\iota-1}}(\varphi))}{(\Upsilon-\varphi)^{1-\vartheta}}d\varphi,\\
A_{s_{\iota}}(\Upsilon)&=\frac{1}{\Gamma(\vartheta)}\int_0^{\Upsilon}\frac{\mathcal{M}_1(\vartheta,\varphi,A_{s_{\iota-1}}(\varphi))}{(\Upsilon-\varphi)^{1-\vartheta}}d\varphi,\\
Q_{\iota}(\Upsilon)&=\frac{1}{\Gamma(\vartheta)}\int_0^{\Upsilon}\frac{\mathcal{M}_1(\vartheta,\varphi,Q_{\iota-1}(\varphi))}{(\Upsilon-\varphi)^{1-\vartheta}}d\varphi,\\
R_{\iota}(\Upsilon)&=\frac{1}{\Gamma(\vartheta)}\int_0^{\Upsilon}\frac{\mathcal{M}_1(\vartheta,\varphi,R_{\iota-1}(\varphi))}{(\Upsilon-\varphi)^{1-\vartheta}}d\varphi,
\end{aligned}\tag{18}$$

this is related to the following initial values $S_0(\Upsilon)=S(0),V_{1_0}(\Upsilon)=V_1(0),V_{2_0}(\Upsilon)=V_2(0),L_0(\Upsilon)=L(0),A_{m_0}(\Upsilon)=A_m(0),A_{s_0}(\Upsilon)=A_s(0)$, $Q_0(\Upsilon)=Q(0),R_0(\Upsilon)=R(0)$. By successively computing the differences yields;

$$\begin{aligned}
Y_{S,\iota} &= S_\iota(\curlyvee) - S_{\iota-1}(\curlyvee) = \frac{1}{\Gamma(\vartheta)}\int_0^{\curlyvee} \frac{\mathcal{M}_1(\vartheta,\varphi,S_{\iota-1}(\varphi)) - \mathcal{M}_1(\vartheta,\varphi,S_{\iota-2}(\varphi))}{(\curlyvee-\varphi)^{1-\vartheta}}d\varphi,\\
Y_{V_1,\iota} &= V_{1_\iota}(\curlyvee) - V_{1_{\iota-1}}(\curlyvee) = \frac{1}{\Gamma(\vartheta)}\int_0^{\curlyvee} \frac{\mathcal{M}_2(\vartheta,\varphi,V_{1_{\iota-1}}(\varphi)) - \mathcal{M}_2(\vartheta,\varphi,V_{1_{\iota-2}}(\varphi))}{(\curlyvee-\varphi)^{1-\vartheta}}d\varphi,\\
Y_{V_2,\iota} &= V_{2_\iota}(\curlyvee) - V_{2_{\iota-1}}(\curlyvee) = \frac{1}{\Gamma(\vartheta)}\int_0^{\curlyvee} \frac{\mathcal{M}_3(\vartheta,\varphi,V_{2_{\iota-1}}(\varphi)) - \mathcal{M}_3(\vartheta,\varphi,V_{2_{\iota-2}}(\varphi))}{(\curlyvee-\varphi)^{1-\vartheta}}d\varphi,\\
Y_{L,\iota} &= L_\iota(\curlyvee) - L_{\iota-1}(\curlyvee) = \frac{1}{\Gamma(\vartheta)}\int_0^{\curlyvee} \frac{\mathcal{M}_4(\vartheta,\varphi,S_{\iota-1}(\varphi)) - \mathcal{M}_4(\vartheta,\varphi,L_{\iota-2}(\varphi))}{(\curlyvee-\varphi)^{1-\vartheta}}d\varphi,\\
Y_{A_m,\iota} &= A_{m_\iota}(\curlyvee) - A_{m_{\iota-1}}(\curlyvee) = \frac{1}{\Gamma(\vartheta)}\int_0^{\curlyvee} \frac{\mathcal{M}_5(\vartheta,\varphi,A_{m_{\iota-1}}(\varphi)) - \mathcal{M}_5(\vartheta,\varphi,A_{m_{\iota-2}}(\varphi))}{(\curlyvee-\varphi)^{1-\vartheta}}d\varphi,\\
Y_{A_s,\iota} &= A_{s_\iota}(\curlyvee) - A_{s_{\iota-1}}(\curlyvee) = \frac{1}{\Gamma(\vartheta)}\int_0^{\curlyvee} \frac{\mathcal{M}_6(\vartheta,\varphi,A_{s_{\iota-1}}(\varphi)) - \mathcal{M}_6(\vartheta,\varphi,A_{s_{\iota-2}}(\varphi))}{(\curlyvee-\varphi)^{1-\vartheta}}d\varphi,\\
Y_{Q,\iota} &= Q_\iota(\curlyvee) - Q_{\iota-1}(\curlyvee) = \frac{1}{\Gamma(\vartheta)}\int_0^{\curlyvee} \frac{\mathcal{M}_7(\vartheta,\varphi,Q_{\iota-1}(\varphi)) - \mathcal{M}_7(\vartheta,\varphi,Q_{\iota-2}(\varphi))}{(\curlyvee-\varphi)^{1-\vartheta}}d\varphi,\\
Y_{R,\iota} &= R_\iota(t) - R_{\iota-1}(\curlyvee) = \frac{1}{\Gamma(\vartheta)}\int_0^{\curlyvee} \frac{\mathcal{M}_8(\vartheta,\varphi,R_{\iota-1}(\varphi)) - \mathcal{M}_8(\vartheta,\varphi,R_{\iota-2}(\varphi))}{(\curlyvee-\varphi)^{1-\vartheta}}d\varphi.
\end{aligned} \tag{19}$$

We then have

$$\begin{aligned}
S_\iota(\curlyvee) &= \sum_{j=0}^{\iota} Y_{S,\iota}(\curlyvee), V_{1_\iota}(\curlyvee) = \sum_{j=0}^{\iota} Y_{V_1,\iota}(\curlyvee), V_{2_\iota}(\curlyvee)\\
&= \sum_{j=0}^{\iota} Y_{V_2,\iota}(\curlyvee), L_\iota(\curlyvee) = \sum_{j=0}^{\iota} Y_{L,\iota}(\curlyvee),\\
A_{m_\iota}(\curlyvee) &= \sum_{j=0}^{\iota} Y_{A_m,\iota}(\curlyvee), A_{s_\iota}(\curlyvee) = \sum_{j=0}^{\iota} Y_{A_s,\iota}(\curlyvee), Q_\iota(\curlyvee) = \sum_{j=0}^{\iota} Y_{Q,\iota}(\curlyvee), R_\iota(t)\\
&= \sum_{j=0}^{\iota} Y_{R,\iota}(\curlyvee).
\end{aligned}$$

Now, let us assume that

$$\begin{aligned}
Y_{S,\iota-1} &= S_{\iota-1}(\curlyvee) - S_{\iota-2}(\curlyvee), Y_{V_1,\iota-1} = V_{1_{\iota-1}}(\curlyvee) - V_{1_{\iota-2}}(\curlyvee),\\
Y_{V_2,\iota-1} &= V_{2_{\iota-1}}(\curlyvee) - V_{2_{\iota-2}}(\curlyvee), Y_{L,\iota-1} = L_{\iota-1}(\curlyvee) - L_{\iota-2}(\curlyvee),\\
Y_{A_m,\iota-1} &= A_{m_{\iota-1}}(\curlyvee) - A_{m_{\iota-2}}(\curlyvee), Y_{A_s,\iota-1} = A_{s_{\iota-1}}(\curlyvee) - A_{s_{\iota-2}}(\curlyvee),\\
Y_{Q,\iota-1} &= Q_{\iota-1}(\curlyvee) - Q_{\iota-2}(\curlyvee), Y_{R,\iota-1} = R_{\iota-1}(\curlyvee) - R_{\iota-2}(\curlyvee),
\end{aligned}$$

and also considering Eq. (16) and Eq. (17), we then obtain;

$$\begin{aligned}
\|Y_{S,\iota}(\curlyvee)\| &= \frac{1}{\Gamma(\vartheta)}\chi_1\int_0^{\curlyvee}\frac{\|Y_{S,\iota-1}(\varphi)\|}{(\curlyvee-\varphi)^{\vartheta}}d\varphi,\\
\|Y_{V_1,\iota}(\curlyvee)\| &= \frac{1}{\Gamma(\vartheta)}\chi_1\int_0^{\curlyvee}\frac{\|Y_{V_1,\iota-1}(\varphi)\|}{(\curlyvee-\varphi)^{\vartheta}}d\varphi,\\
\|Y_{V_2,\iota}(\curlyvee)\| &= \frac{1}{\Gamma(\vartheta)}\chi_1\int_0^{\curlyvee}\frac{\|Y_{V_2,\iota-1}(\varphi)\|}{(\curlyvee-\varphi)^{\vartheta}}d\varphi,\\
\|Y_{L,\iota}(\curlyvee)\| &= \frac{1}{\Gamma(\vartheta)}\chi_1\int_0^{\curlyvee}\frac{\|Y_{L,\iota-1}(\varphi)\|}{(\curlyvee-\varphi)^{\vartheta}}d\varphi,\\
\|Y_{A_m,\iota}(\curlyvee)\| &= \frac{1}{\Gamma(\vartheta)}\chi_1\int_0^{\curlyvee}\frac{\|Y_{A_m,\iota-1}(\varphi)\|}{(\curlyvee-\varphi)^{\vartheta}}d\varphi,\\
\|Y_{A_s,\iota}(\curlyvee)\| &= \frac{1}{\Gamma(\vartheta)}\chi_1\int_0^{\curlyvee}\frac{\|Y_{A_s,\iota-1}(\varphi)\|}{(\curlyvee-\varphi)^{\vartheta}}d\varphi\\
\|Y_{Q,\iota}(\curlyvee)\| &= \frac{1}{\Gamma(\vartheta)}\chi_1\int_0^{\curlyvee}\frac{\|Y_{Q,\iota-1}(\varphi)\|}{(\curlyvee-\varphi)^{\vartheta}}d\varphi,\\
\|Y_{R,\iota}(\curlyvee)\| &= \frac{1}{\Gamma(\vartheta)}\chi_1\int_0^{\curlyvee}\frac{\|Y_{R,\iota-1}(\varphi)\|}{(\curlyvee-\varphi)^{\vartheta}}d\varphi.
\end{aligned} \tag{20}$$

By stating the theorem below, we look forward to establishing the uniqueness of the fractional measles disease model.

Theorem 4.1. *There exists exactly one solution to the Caputo fractional measles model (13), and this solution is unique under the assumption that*

$$\frac{\beta^{\vartheta}}{\Gamma(\vartheta)+1}\chi_i < 1, \quad i = 1,2,3,\dots,8, \tag{21}$$

whenever $\curlyvee \in [0,a]$.

Proof. It has been arguably shown that the compartmental functions $S(\curlyvee), V_1(\curlyvee), V_2(\curlyvee), L(t), A_m(\curlyvee), A_s(\curlyvee), Q(\curlyvee)$ and $R(\curlyvee)$ are limited and also the functions $\mathcal{M}_1, \mathcal{M}_2, \mathcal{M}_3, \mathcal{M}_4, \mathcal{M}_5, \mathcal{M}_6, \mathcal{M}_7, \mathcal{M}_8$ satisfies the Lipschitz criterion of boundedness. Through a recursive approach Eq. (19) yields the results below;

$$\begin{aligned}
\|Y_{S,\iota}(\curlyvee)\| &\le \|S_0(\curlyvee)\|\left(\frac{\alpha^{\vartheta}}{\Gamma(\vartheta)}\chi_1\right)^{\iota},\\
\|Y_{V_1,\iota}(\curlyvee)\| &\le \|V_{1_0}(\curlyvee)\|\left(\frac{\alpha^{\vartheta}}{\Gamma(\vartheta)}\chi_2\right)^{\iota},\\
\|Y_{V_2,\iota}(\curlyvee)\| &\le \|V_{2_0}(\curlyvee)\|\left(\frac{\alpha^{\vartheta}}{\Gamma(\vartheta)}\chi_3\right)^{\iota},\\
\|Y_{L,\iota}(\curlyvee)\| &\le \|L_0(\curlyvee)\|\left(\frac{\alpha^{\vartheta}}{\Gamma(\vartheta)}\chi_4\right)^{\iota},\\
\|Y_{A_m,\iota}(\curlyvee)\| &\le \|A_{m_0}(\curlyvee)\|\left(\frac{\alpha^{\vartheta}}{\Gamma(\vartheta)}\chi_5\right)^{\iota},\\
\|Y_{A_s,\iota}(\curlyvee)\| &\le \|A_{s_0}(\curlyvee)\|\left(\frac{\alpha^{\vartheta}}{\Gamma(\vartheta)}\chi_6\right)^{\iota},\\
\|Y_{Q,\iota}(\curlyvee)\| &\le \|Q_0(\curlyvee)\|\left(\frac{\alpha^{\vartheta}}{\Gamma(\vartheta)}\chi_7\right)^{\iota},\\
\|Y_{R,\iota}(\curlyvee)\| &\le \|R_0(\curlyvee)\|\left(\frac{\alpha^{\vartheta}}{\Gamma(\vartheta)}\chi_8\right)^{\iota}.
\end{aligned} \tag{22}$$

From the above relations, we have

$$\begin{aligned}
&\|Y_{S,\iota}(\curlyvee)\| \longrightarrow 0, && \|Y_{A_m,\iota}(\curlyvee)\| \longrightarrow 0,\\
&\|Y_{V_1,\iota}(\curlyvee)\| \longrightarrow 0, && \|Y_{A_s,\iota}(\curlyvee)\| \longrightarrow 0,\\
&\|Y_{V_2,\iota}(\curlyvee)\| \longrightarrow 0, && \|Y_{Q,\iota}(\curlyvee)\| \longrightarrow 0,\\
&\|Y_{L,\iota}(\curlyvee)\| \longrightarrow 0, && \|Y_{R,\iota}(\curlyvee)\| \longrightarrow 0,
\end{aligned} \tag{23}$$

where $\iota \longrightarrow 0$. To conclude, we make use of the principle of triangle inequality in line with Eq. (21), and this gives;

$$\begin{aligned}
\|S_{\iota+\mu}(\curlyvee) - S_\iota(\curlyvee)\| &\le \sum_{j=\iota+1}^{\iota+\mu}\mathcal{B}_1 = \frac{\mathcal{B}_1^{\iota+1} - \mathcal{B}_1^{\iota+\iota+1}}{1-\mathcal{B}_1},\\
\|V_{1_{\iota+\mu}}(\curlyvee) - V_{1_\iota}(\curlyvee)\| &\le \sum_{j=\iota+1}^{\iota+\mu}\mathcal{B}_2 = \frac{\mathcal{B}_2^{\iota+1} - \mathcal{B}_2^{\iota+\iota+1}}{1-\mathcal{B}_2},\\
\|V_{2_{\iota+\mu}}(\curlyvee) - V_{2_\iota}(\curlyvee)\| &\le \sum_{j=\iota+1}^{\iota+\mu}\mathcal{B}_3 = \frac{\mathcal{B}_3^{\iota+1} - \mathcal{B}_3^{\iota+\iota+1}}{1-\mathcal{B}_3},\\
\|L_{\iota+\mu}(\curlyvee) - L_\iota(\curlyvee)\| &\le \sum_{j=\iota+1}^{\iota+\mu}\mathcal{B}_4 = \frac{\mathcal{B}_4^{\iota+1} - \mathcal{B}_4^{\iota+\iota+1}}{1-\mathcal{B}_4},\\
\|A_{m_{\iota+\mu}}(\curlyvee) - A_{s_\iota}(\curlyvee)\| &\le \sum_{j=\iota+1}^{\iota+\mu}\mathcal{B}_5 = \frac{\mathcal{B}_5^{\iota+1} - \mathcal{B}_5^{\iota+\iota+1}}{1-\mathcal{B}_5},\\
\|A_{s_{\iota+\mu}}(\curlyvee) - A_{s_\iota}(\curlyvee)\| &\le \sum_{j=\iota+1}^{\iota+\mu}\mathcal{B}_6 = \frac{\mathcal{B}_6^{\iota+1} - \mathcal{B}_6^{\iota+\iota+1}}{1-\mathcal{B}_6},\\
\|L_{\iota+\mu}(\curlyvee) - L_\iota(\curlyvee)\| &\le \sum_{j=\iota+1}^{\iota+\mu}\mathcal{B}_7 = \frac{\mathcal{B}_7^{\iota+1} - \mathcal{B}_7^{\iota+\iota+1}}{1-\mathcal{B}_7},\\
\|R_{\iota+\mu}(\curlyvee) - R_\iota(\curlyvee)\| &\le \sum_{j=\iota+1}^{\iota+\mu}\mathcal{B}_8 = \frac{\mathcal{B}_8^{\iota+1} - \mathcal{B}_8^{\iota+\iota+1}}{1-\mathcal{B}_8},
\end{aligned} \tag{24}$$

where we define $\mathcal{B}_i = \frac{\beta^{\vartheta}}{\Gamma(\vartheta)+1}\chi_i$, $i = 1,2,3,\dots,8$. From the above expressions, the sequences

$S_\iota, S_\iota, V_{1_\upsilon}, V_{2_\upsilon}, L_\iota, A_{m_\iota}, A_{s_\iota}, Q_\iota$ and R_ι are said to be Cauchy sequences in the Banach space $\mathbb{B}(\Theta)$. Therefore, the solutions uniformly converge. Now, from the concept of limit, we observe that the sequences (17) are limited, which implies that the fractional Caputo measles disease model (13) has only one solution. Hence, the proof. □

4.2. Stability analysis of the measles model in Caputo fractional operator

In this section, we carry out an explicit investigation into the stability analysis of the fractional Caputo measles disease model (13). Stability analysis is essential in studying the dynamics of biological systems as it has been reported in the literature that the biological processes these biological systems undergo mostly exhibit memory effect [48]. Also, many biological systems do not have exact solutions and are approximate. These approximations sometimes incur some errors, where a perturbation in the neighborhood may explode the solution set, which could best be studied through stability analysis. Therefore, to be able to accurately capture these memory effects exhibited by these biological systems and also minimize these mathematical errors, we apply the Hyers–Ulam (HU) and Hyers–Ulam–Rassias (HUR) stability criteria [49,50]. We, therefore, follow the approach in [51,52] to study the stability of the fractional Caputo measles disease model (13).

Definition 4.1. The fractional Caputo measles model (13) is HU stable if there exists $0 < \mathcal{D}_{Q_i} \in \mathbb{R}$ for $i = 1,2,3,\dots,8$ such that, $\forall \kappa_i > 0$ and $\forall (S^{\circledast\circledast}, V_1^{\circledast\circledast}, V_2^{\circledast\circledast}, L^{\circledast\circledast}, A_m^{\circledast\circledast}, A_s^{\circledast\circledast}, Q^{\circledast\circledast}, R^{\circledast\circledast}) \in \mathcal{X}$ satisfying

$$
\begin{aligned}
&|{}^C\mathcal{D}^{\vartheta}_{0,\Upsilon} S^{\circledast\circledast}(\Upsilon) - \mathcal{A}_1(S^{\circledast\circledast}(\Upsilon), V_1^{\circledast\circledast}(\Upsilon), V_2^{\circledast\circledast}(\Upsilon), L^{\circledast\circledast}(\Upsilon),\\
&A_m^{\circledast\circledast}(\Upsilon), A_s^{\circledast\circledast}(\Upsilon), Q^{\circledast\circledast}(\Upsilon), R^{\circledast\circledast}(\Upsilon))| && < \kappa_1,\\
&|{}^C\mathcal{D}^{\vartheta}_{0,\Upsilon} V_1^{\circledast\circledast}(\Upsilon) - \mathcal{A}_2(S^{\circledast\circledast}(\Upsilon), V_1^{\circledast\circledast}(\Upsilon), V_2^{\circledast\circledast}(\Upsilon), L^{\circledast\circledast}(\Upsilon),\\
&A_m^{\circledast\circledast}(\Upsilon), A_s^{\circledast\circledast}(\Upsilon), Q^{\circledast\circledast}(\Upsilon), R^{\circledast\circledast}(\Upsilon))| && < \kappa_2,\\
&|{}^C\mathcal{D}^{\vartheta}_{0,\Upsilon} V_2^{\circledast\circledast}(\Upsilon) - \mathcal{A}_3(S^{\circledast\circledast}(\Upsilon), V_1^{\circledast\circledast}(\Upsilon), V_2^{\circledast\circledast}(\Upsilon), L^{\circledast\circledast}(\Upsilon),\\
&A_m^{\circledast\circledast}(\Upsilon), A_s^{\circledast\circledast}(\Upsilon), Q^{\circledast\circledast}(\Upsilon), R^{\circledast\circledast}(\Upsilon))| && < \kappa_3,\\
&|{}^C\mathcal{D}^{\vartheta}_{0,\Upsilon} L^{\circledast\circledast}(\Upsilon) - \mathcal{A}_4(S^{\circledast\circledast}(\Upsilon), V_1^{\circledast\circledast}(\Upsilon), V_2^{\circledast\circledast}(\Upsilon), L^{\circledast\circledast}(\Upsilon),\\
&A_m^{\circledast\circledast}(\Upsilon), A_s^{\circledast\circledast}(\Upsilon), Q^{\circledast\circledast}(\Upsilon), R^{\circledast\circledast}(\Upsilon))| && < \kappa_4,\\
&|{}^C\mathcal{D}^{\vartheta}_{0,\Upsilon} A_m^{\circledast\circledast}(\Upsilon) - \mathcal{A}_1(S^{\circledast\circledast}(\Upsilon), V_1^{\circledast\circledast}(\Upsilon), V_2^{\circledast\circledast}(\Upsilon), L^{\circledast\circledast}(\Upsilon),\\
&A_m^{\circledast\circledast}(\Upsilon), A_s^{\circledast\circledast}(\Upsilon), Q^{\circledast\circledast}(\Upsilon), R^{\circledast\circledast}(\Upsilon))| && < \kappa_5,\\
&|{}^C\mathcal{D}^{\vartheta}_{0,\Upsilon} A_s^{\circledast\circledast}(\Upsilon) - \mathcal{A}_1(S^{\circledast\circledast}(\Upsilon), V_1^{\circledast\circledast}(\Upsilon), V_2^{\circledast\circledast}(\Upsilon), L^{\circledast\circledast}(\Upsilon),\\
&A_m^{\circledast\circledast}(\Upsilon), A_s^{\circledast\circledast}(\Upsilon), Q^{\circledast\circledast}(\Upsilon), R^{\circledast\circledast}(\Upsilon))| && < \kappa_6,\\
&|{}^C\mathcal{D}^{\vartheta}_{0,\Upsilon} Q^{\circledast\circledast}(\Upsilon) - \mathcal{A}_1(S^{\circledast\circledast}(\Upsilon), V_1^{\circledast\circledast}(\Upsilon), V_2^{\circledast\circledast}(\Upsilon), L^{\circledast\circledast}(\Upsilon),\\
&A_m^{\circledast\circledast}(\Upsilon), A_s^{\circledast\circledast}(\Upsilon), Q^{\circledast\circledast}(\Upsilon), R^{\circledast\circledast}(\Upsilon))| && < \kappa_7,\\
&|{}^C\mathcal{D}^{\vartheta}_{0,\Upsilon} SR^{\circledast\circledast}(\Upsilon) - \mathcal{A}_1(S^{\circledast\circledast}(\Upsilon), V_1^{\circledast\circledast}(\Upsilon), V_2^{\circledast\circledast}(\Upsilon), L^{\circledast\circledast}(\Upsilon),\\
&A_m^{\circledast\circledast}(\Upsilon), A_s^{\circledast\circledast}(\Upsilon), Q^{\circledast\circledast}(\Upsilon), R^{\circledast\circledast}(\Upsilon))| && < \kappa_8,
\end{aligned}
\tag{25}
$$

and there also exists $S(\Upsilon), V_1(\Upsilon), V_2(\Upsilon), L(\Upsilon), A_m(\Upsilon), A_s(\Upsilon), Q(\Upsilon), R(\Upsilon) \in \mathcal{X}$ which implies that the fractional Caputo measles model will be

$$
\begin{aligned}
&|S^{\circledast\circledast}(\Upsilon) - S(\Upsilon)| < \mathcal{D}_{\mathcal{E}_1}\kappa_1, |V_1^{\circledast\circledast}(\Upsilon) - V_1(\Upsilon)| < \mathcal{D}_{\mathcal{E}_2}\kappa_2,\\
&|V_2^{\circledast\circledast}(\Upsilon) - V_2(\Upsilon)| < \mathcal{D}_{\mathcal{E}_3}\kappa_3, |L^{\circledast\circledast}(\Upsilon) - L(\Upsilon)| < \mathcal{D}_{\mathcal{E}_4}\kappa_4,\\
&|A_m^{\circledast\circledast}(\Upsilon) - A_m(\Upsilon)| < \mathcal{D}_{\mathcal{E}_5}\kappa_5, |A_s^{\circledast\circledast}(\Upsilon) - A_s(\Upsilon)| < \mathcal{D}_{\mathcal{E}_6}\kappa_6,\\
&|Q^{\circledast\circledast}(\Upsilon) - Q(\Upsilon)| < \mathcal{D}_{\mathcal{E}_7}\kappa_7, |R^{\circledast\circledast}(\Upsilon) - R(\Upsilon)| < \mathcal{D}_{\mathcal{E}_8}\kappa_8.
\end{aligned}
\tag{26}
$$

Remark 4.1. We suppose that $(S^{\circledast\circledast}(\Upsilon), V_1^{\circledast\circledast}(\Upsilon), V_2^{\circledast\circledast}(\Upsilon), L^{\circledast\circledast}(\Upsilon), A_m^{\circledast\circledast}(\Upsilon), A_s^{\circledast\circledast}(\Upsilon), Q^{\circledast\circledast}(\Upsilon), R^{\circledast\circledast}(\Upsilon)) \in \mathcal{X}$ is a solution to Eq. (20) if and only if we have $\ell_1, \ell_2, \ell_3, \ell_4, \ell_5, \ell_6, \ell_7, \ell_8 \in \mathcal{C}([0, M], \mathbb{R})$ in such a way that $\forall \Upsilon \in (M, (j)).|\varrho_j(\Upsilon)| < \rho_j$ for $j = 1,2,3,\dots,8$, given

$$
\begin{aligned}
{}^C\mathcal{D}^{\vartheta}_{0,\Upsilon} S^{\circledast\circledast}(\Upsilon) &= \mathcal{A}_1(S^{\circledast\circledast}(\Upsilon), V_1^{\circledast\circledast}(\Upsilon), V_2^{\circledast\circledast}(\Upsilon), L^{\circledast\circledast}(\Upsilon), A_m^{\circledast\circledast}(\Upsilon),\\
&\quad A_s^{\circledast\circledast}(\Upsilon), Q^{\circledast\circledast}(\Upsilon), R^{\circledast\circledast}(\Upsilon))| + \ell_1(\Upsilon),\\
{}^C\mathcal{D}^{\vartheta}_{0,\Upsilon} V_1^{\circledast\circledast}(\Upsilon) &= \mathcal{A}_2(S^{\circledast\circledast}(\Upsilon), V_1^{\circledast\circledast}(\Upsilon), V_2^{\circledast\circledast}(\Upsilon), L^{\circledast\circledast}(\Upsilon), A_m^{\circledast\circledast}(\Upsilon),\\
&\quad A_s^{\circledast\circledast}(\Upsilon), Q^{\circledast\circledast}(\Upsilon), R^{\circledast\circledast}(\Upsilon))| + \ell_2(\Upsilon),\\
{}^C\mathcal{D}^{\vartheta}_{0,\Upsilon} V_3^{\circledast\circledast}(\Upsilon) &= \mathcal{A}_3(S^{\circledast\circledast}(\Upsilon), V_1^{\circledast\circledast}(\Upsilon), V_2^{\circledast\circledast}(\Upsilon), L^{\circledast\circledast}(\Upsilon), A_m^{\circledast\circledast}(\Upsilon),\\
&\quad A_s^{\circledast\circledast}(\Upsilon), Q^{\circledast\circledast}(\Upsilon), R^{\circledast\circledast}(\Upsilon))| + \ell_3(\Upsilon),\\
{}^C\mathcal{D}^{\vartheta}_{0,\Upsilon} V_2^{\circledast\circledast}(\Upsilon) &= \mathcal{A}_4(S^{\circledast\circledast}(\Upsilon), V_1^{\circledast\circledast}(\Upsilon), V_2^{\circledast\circledast}(\Upsilon), L^{\circledast\circledast}(\Upsilon), A_m^{\circledast\circledast}(\Upsilon),\\
&\quad A_s^{\circledast\circledast}(\Upsilon), Q^{\circledast\circledast}(\Upsilon), R^{\circledast\circledast}(\Upsilon))| + \ell_4(\Upsilon),\\
{}^C\mathcal{D}^{\vartheta}_{0,\Upsilon} L^{\circledast\circledast}(\Upsilon) &= \mathcal{A}_5(S^{\circledast\circledast}(\Upsilon), V_1^{\circledast\circledast}(\Upsilon), V_2^{\circledast\circledast}(\Upsilon), L^{\circledast\circledast}(\Upsilon), A_m^{\circledast\circledast}(\Upsilon),\\
&\quad A_s^{\circledast\circledast}(\Upsilon), Q^{\circledast\circledast}(\Upsilon), R^{\circledast\circledast}(\Upsilon))| + \ell_5(\Upsilon),\\
{}^C\mathcal{D}^{\vartheta}_{0,\Upsilon} A_s^{\circledast\circledast}(\Upsilon) &= \mathcal{A}_6(S^{\circledast\circledast}(\Upsilon), V_1^{\circledast\circledast}(\Upsilon), V_2^{\circledast\circledast}(\Upsilon), L^{\circledast\circledast}(\Upsilon), A_m^{\circledast\circledast}(\Upsilon),\\
&\quad A_s^{\circledast\circledast}(\Upsilon), Q^{\circledast\circledast}(\Upsilon), R^{\circledast\circledast}(\Upsilon))| + \ell_6(\Upsilon),\\
{}^C\mathcal{D}^{\vartheta}_{0,\Upsilon} Q^{\circledast\circledast}(\Upsilon) &= \mathcal{A}_7(S^{\circledast\circledast}(\Upsilon), V_1^{\circledast\circledast}(\Upsilon), V_2^{\circledast\circledast}(\Upsilon), L^{\circledast\circledast}(\Upsilon), A_m^{\circledast\circledast}(\Upsilon),\\
&\quad A_s^{\circledast\circledast}(\Upsilon), Q^{\circledast\circledast}(\Upsilon), R^{\circledast\circledast}(\Upsilon))| + \ell_7(\Upsilon),\\
{}^C\mathcal{D}^{\vartheta}_{0,\Upsilon} R^{\circledast\circledast}(\Upsilon) &= \mathcal{A}_8(S^{\circledast\circledast}(\Upsilon), V_1^{\circledast\circledast}(\Upsilon), V_2^{\circledast\circledast}(\Upsilon), L^{\circledast\circledast}(\Upsilon), A_m^{\circledast\circledast}(\Upsilon),\\
&\quad A_s^{\circledast\circledast}(\Upsilon), Q^{\circledast\circledast}(\Upsilon), R^{\circledast\circledast}(\Upsilon))| + \ell_8(\Upsilon),
\end{aligned}
\tag{27}
$$

Definition 4.2. The fractional Caputo measles model (13) is HUR stable if we have Φ_i for $i = 1,2,3,\dots,8$ whenever $D_{\mathcal{E}_i,\Phi_i} > 0 \in \mathbb{R}$ for $i = 1,2,3,\dots,8$ such that for every $\kappa_i > 0$ and for all $(S^{\circledast\circledast}, V_1^{\circledast\circledast}, V_2^{\circledast\circledast}, L^{\circledast\circledast}, A_m^{\circledast\circledast}, A_s^{\circledast\circledast}, Q^{\circledast\circledast}, R^{\circledast\circledast}) \in \mathbb{X}$ satisfying

$$
\begin{aligned}
&|{}^C\mathcal{D}^{\vartheta}_{0,\Upsilon} S^{\circledast\circledast}(\Upsilon) - \mathcal{A}_1(S^{\circledast\circledast}(\Upsilon), V_1^{\circledast\circledast}(\Upsilon), V_2^{\circledast\circledast}(\Upsilon), L^{\circledast\circledast}(\Upsilon), A_m^{\circledast\circledast}(\Upsilon),\\
&A_s^{\circledast\circledast}(\Upsilon), Q^{\circledast\circledast}(\Upsilon), R^{\circledast\circledast}(\Upsilon))| < \kappa_1\Phi_1(\Upsilon),\\
&|{}^C\mathcal{D}^{\vartheta}_{0,\Upsilon} V_1^{\circledast\circledast}(\Upsilon) - \mathcal{A}_1(S^{\circledast\circledast}(\Upsilon), V_1^{\circledast\circledast}(\Upsilon), V_2^{\circledast\circledast}(\Upsilon), L^{\circledast\circledast}(\Upsilon), A_m^{\circledast\circledast}(\Upsilon),\\
&A_s^{\circledast\circledast}(\Upsilon), Q^{\circledast\circledast}(\Upsilon), R^{\circledast\circledast}(\Upsilon))| < \kappa_1\Phi_1(\Upsilon),\\
&|{}^C\mathcal{D}^{\vartheta}_{0,\Upsilon} V_2^{\circledast\circledast}(\Upsilon) - \mathcal{A}_1(S^{\circledast\circledast}(\Upsilon), V_1^{\circledast\circledast}(\Upsilon), V_2^{\circledast\circledast}(\Upsilon), L^{\circledast\circledast}(\Upsilon), A_m^{\circledast\circledast}(\Upsilon),\\
&A_s^{\circledast\circledast}(\Upsilon), Q^{\circledast\circledast}(\Upsilon), R^{\circledast\circledast}(\Upsilon))| < \kappa_1\Phi_1(\Upsilon),\\
&|{}^C\mathcal{D}^{\vartheta}_{0,\Upsilon} L^{\circledast\circledast}(\Upsilon) - \mathcal{A}_1(S^{\circledast\circledast}(\Upsilon), V_1^{\circledast\circledast}(\Upsilon), V_2^{\circledast\circledast}(\Upsilon), L^{\circledast\circledast}(\Upsilon), A_m^{\circledast\circledast}(\Upsilon),\\
&A_s^{\circledast\circledast}(\Upsilon), Q^{\circledast\circledast}(\Upsilon), R^{\circledast\circledast}(\Upsilon))| < \kappa_1\Phi_1(\Upsilon),\\
&|{}^C\mathcal{D}^{\vartheta}_{0,\Upsilon} A_m^{\circledast\circledast}(\Upsilon) - \mathcal{A}_1(S^{\circledast\circledast}(\Upsilon), V_1^{\circledast\circledast}(\Upsilon), V_2^{\circledast\circledast}(\Upsilon), L^{\circledast\circledast}(\Upsilon), A_m^{\circledast\circledast}(\Upsilon),\\
&A_s^{\circledast\circledast}(\Upsilon), Q^{\circledast\circledast}(\Upsilon), R^{\circledast\circledast}(\Upsilon))| < \kappa_1\Phi_1(\Upsilon),\\
&|{}^C\mathcal{D}^{\vartheta}_{0,\Upsilon} A_s^{\circledast\circledast}(\Upsilon) - \mathcal{A}_1(S^{\circledast\circledast}(\Upsilon), V_1^{\circledast\circledast}(\Upsilon), V_2^{\circledast\circledast}(\Upsilon), L^{\circledast\circledast}(\Upsilon), A_m^{\circledast\circledast}(\Upsilon),\\
&A_s^{\circledast\circledast}(\Upsilon), Q^{\circledast\circledast}(\Upsilon), R^{\circledast\circledast}(\Upsilon))| < \kappa_1\Phi_1(\Upsilon),\\
&|{}^C\mathcal{D}^{\vartheta}_{0,\Upsilon} Q^{\circledast\circledast}(\Upsilon) - \mathcal{A}_1(S^{\circledast\circledast}(\Upsilon), V_1^{\circledast\circledast}(\Upsilon), V_2^{\circledast\circledast}(\Upsilon), L^{\circledast\circledast}(\Upsilon), A_m^{\circledast\circledast}(\Upsilon),\\
&A_s^{\circledast\circledast}(\Upsilon), Q^{\circledast\circledast}(\Upsilon), R^{\circledast\circledast}(\Upsilon))| < \kappa_1\Phi_1(\Upsilon),\\
&|{}^C\mathcal{D}^{\vartheta}_{0,\Upsilon} R^{\circledast\circledast}(\Upsilon) - \mathcal{A}_1(S^{\circledast\circledast}(\Upsilon), V_1^{\circledast\circledast}(\Upsilon), V_2^{\circledast\circledast}(\Upsilon), L^{\circledast\circledast}(\Upsilon), A_m^{\circledast\circledast}(\Upsilon),\\
&A_s^{\circledast\circledast}(\Upsilon), Q^{\circledast\circledast}(\Upsilon), R^{\circledast\circledast}(\Upsilon))| < \kappa_1\Phi_1(\Upsilon),
\end{aligned}
\tag{28}
$$

moreover, we suppose that $S(\Upsilon), V_1(\Upsilon), V_2(\Upsilon), L(\Upsilon), A_m(\Upsilon), A_s(\Upsilon), Q(\Upsilon), R(\Upsilon), \in \mathcal{X}$ satisfies the fractional Caputo measles model (13) as stated

$$
\begin{aligned}
&|S^{\circledast\circledast}(\Upsilon) - S(\Upsilon)| < \mathcal{D}_{\mathcal{E}_1,\Phi_1}\kappa_1\Phi_1(\Upsilon),\\
&|V_1^{\circledast\circledast}(\Upsilon) - V_1(\Upsilon)| < \mathcal{D}_{\mathcal{E}_2,\Phi_2}\kappa_2\Phi_2(\Upsilon),\\
&|V_2^{\circledast\circledast}(\Upsilon) - V_2(\Upsilon)| < \mathcal{D}_{\mathcal{E}_3,\Phi_3}\kappa_3\Phi_3(\Upsilon),\\
&|L^{\circledast\circledast}(\Upsilon) - L(\Upsilon)| < \mathcal{D}_{\mathcal{E}_4,\Phi_4}\kappa_4\Phi_4(\Upsilon),\\
&|A_m^{\circledast\circledast}(\Upsilon) - A_m(\Upsilon)| < \mathcal{D}_{\mathcal{E}_5,\Phi_5}\kappa_5\Phi_5(\Upsilon),\\
&|A_s^{\circledast\circledast}(\Upsilon) - A_s(\Upsilon)| < \mathcal{D}_{\mathcal{E}_6,\Phi_6}\kappa_6\Phi_6(\Upsilon),\\
&|Q^{\circledast\circledast}(\Upsilon) - Q(\Upsilon)| < \mathcal{D}_{\mathcal{E}_7,\Phi_7}\kappa_7\Phi_7(\Upsilon),\\
&|R^{\circledast\circledast}(\Upsilon) - R(\Upsilon)| < \mathcal{D}_{\mathcal{E}_8,\Phi_8}\kappa_8\Phi_8(\Upsilon),
\end{aligned}
\tag{29}
$$

Remark 4.2. We suppose that $(S^{\circledast\circledast}, V_1^{\circledast\circledast}, V_2^{\circledast\circledast}, L^{\circledast\circledast}, A_m^{\circledast\circledast}, A_s^{\circledast\circledast}, Q^{\circledast\circledast}, R^{\circledast\circledast}) \in \mathcal{X}$ is a solution to Eq. (23) if and only if we have $\ell_1, \ell_2, \ell_3, \ell_4, \ell_5, \ell_6, \ell_7, \ell_8 \in C([0, M], \mathbb{R})$ in relation with $(S^{\circledast\circledast}, V_1^{\circledast\circledast}, V_2^{\circledast\circledast}, L^{\circledast\circledast}, A_m^{\circledast\circledast}, A_s^{\circledast\circledast}, Q^{\circledast\circledast}, R^{\circledast\circledast}) \in \mathcal{X}$ such that $\forall \Upsilon \in M$: $(i).|\ell_j(t)| < \Phi_j(t)\kappa_j$ for $j = 1, 2, 3, \ldots, 8$, given

$$\begin{aligned}
{}^C\mathcal{D}^{\vartheta}_{0,\Upsilon} S^{\circledast\circledast}(\vartheta) &= \mathcal{A}_1(S^{\circledast\circledast}(\Upsilon), V_1^{\circledast\circledast}(\Upsilon), V_2^{\circledast\circledast}(\Upsilon), L^{\circledast\circledast}(\Upsilon), A_m^{\circledast\circledast}(\Upsilon),\\
&\quad A_s^{\circledast\circledast}(\Upsilon), Q^{\circledast\circledast}(\Upsilon), R^{\circledast\circledast}(\Upsilon))| + \ell_1(\Upsilon),\\
{}^C\mathcal{D}^{\vartheta}_{0,\Upsilon} V_1^{\circledast\circledast}(\vartheta) &= \mathcal{A}_2(S^{\circledast\circledast}(\Upsilon), V_1^{\circledast\circledast}(\Upsilon), V_2^{\circledast\circledast}(\Upsilon), L^{\circledast\circledast}(\Upsilon), A_m^{\circledast\circledast}(\Upsilon),\\
&\quad A_s^{\circledast\circledast}(\Upsilon), Q^{\circledast\circledast}(\Upsilon), R^{\circledast\circledast}(\Upsilon))| + \ell_2(\Upsilon),\\
{}^C\mathcal{D}^{\vartheta}_{0,\Upsilon} V_3^{\circledast\circledast}(\vartheta) &= \mathcal{A}_3(S^{\circledast\circledast}(\Upsilon), V_1^{\circledast\circledast}(\Upsilon), V_2^{\circledast\circledast}(\Upsilon), L^{\circledast\circledast}(\Upsilon), A_m^{\circledast\circledast}(\Upsilon),\\
&\quad A_s^{\circledast\circledast}(\Upsilon), Q^{\circledast\circledast}(\Upsilon), R^{\circledast\circledast}(\Upsilon))| + \ell_3(\Upsilon),\\
{}^C\mathcal{D}^{\vartheta}_{0,\Upsilon} V_2^{\circledast\circledast}(\vartheta) &= \mathcal{A}_4(S^{\circledast\circledast}(\Upsilon), V_1^{\circledast\circledast}(\Upsilon), V_2^{\circledast\circledast}(\Upsilon), L^{\circledast\circledast}(\Upsilon), A_m^{\circledast\circledast}(\Upsilon),\\
&\quad A_s^{\circledast\circledast}(\Upsilon), Q^{\circledast\circledast}(\Upsilon), R^{\circledast\circledast}(\Upsilon))| + \ell_4(\Upsilon),\\
{}^C\mathcal{D}^{\vartheta}_{0,\Upsilon} L^{\circledast\circledast}(\vartheta) &= \mathcal{A}_5(S^{\circledast\circledast}(\Upsilon), V_1^{\circledast\circledast}(\Upsilon), V_2^{\circledast\circledast}(\Upsilon), L^{\circledast\circledast}(\Upsilon), A_m^{\circledast\circledast}(\Upsilon),\\
&\quad A_s^{\circledast\circledast}(\Upsilon), Q^{\circledast\circledast}(\Upsilon), R^{\circledast\circledast}(\Upsilon))| + \ell_5(\Upsilon),\\
{}^C\mathcal{D}^{\vartheta}_{0,\Upsilon} A_s^{\circledast\circledast}(\vartheta) &= \mathcal{A}_6(S^{\circledast\circledast}(\Upsilon), V_1^{\circledast\circledast}(\Upsilon), V_2^{\circledast\circledast}(\Upsilon), L^{\circledast\circledast}(\Upsilon), A_m^{\circledast\circledast}(\Upsilon),\\
&\quad A_s^{\circledast\circledast}(\Upsilon), Q^{\circledast\circledast}(\Upsilon), R^{\circledast\circledast}(\Upsilon))| + \ell_6(\Upsilon),\\
{}^C\mathcal{D}^{\vartheta}_{0,\Upsilon} Q^{\circledast\circledast}(\vartheta) &= \mathcal{A}_7(S^{\circledast\circledast}(\Upsilon), V_1^{\circledast\circledast}(\Upsilon), V_2^{\circledast\circledast}(\Upsilon), L^{\circledast\circledast}(\Upsilon), A_m^{\circledast\circledast}(\Upsilon),\\
&\quad A_s^{\circledast\circledast}(\Upsilon), Q^{\circledast\circledast}(\Upsilon), R^{\circledast\circledast}(\Upsilon))| + \ell_7(\Upsilon),\\
{}^C\mathcal{D}^{\vartheta}_{0,\Upsilon} R^{\circledast\circledast}(\vartheta) &= \mathcal{A}_8(S^{\circledast\circledast}(\Upsilon), V_1^{\circledast\circledast}(\Upsilon), V_2^{\circledast\circledast}(\Upsilon), L^{\circledast\circledast}(\Upsilon), A_m^{\circledast\circledast}(\Upsilon),\\
&\quad A_s^{\circledast\circledast}(\Upsilon), Q^{\circledast\circledast}(\Upsilon), R^{\circledast\circledast}(\Upsilon))| + \ell_8(\Upsilon).
\end{aligned} \tag{30}$$

Theorem 4.2. *The measles disease model with Caputo fractional operators is HU stable under the condition that* $N := [0, T]$ *in a manner that* $\varphi\hbar_i$ *for* $i = 1, 2, 3, \ldots, 8$, *and* $\hbar_i$ *and* φ *are defined to be* $\hbar_1$: $\hbar_1 = \beta^{\vartheta}\xi_1^{\vartheta} - (\mu^{\vartheta} + \gamma_1^{\vartheta})$, $\hbar_2 = -(1-\tau_1^{\vartheta})\beta^{\vartheta}\xi_2^{\vartheta} - (\mu^{\vartheta}+\gamma_4^{\vartheta})$, $\hbar 3 = (1-\tau_2^{\vartheta})\beta^{\vartheta}\xi_3^{\vartheta} - (\mu^{\vartheta}+\delta_3^{\vartheta})$, $\hbar 4 = -(\mu^{\vartheta}+\alpha_1^{\vartheta}+\delta_1^{\vartheta})$, $\hbar_5 = -(\mu^{\vartheta}+\alpha_2^{\vartheta}+\delta_2^{\vartheta})$, $\hbar_6 = -(\mu^{\vartheta}+\phi_1^{\vartheta}+\alpha_3^{\vartheta})$, $\hbar_7 = -(\mu^{\vartheta}+\phi_2^{\vartheta}+\alpha_4^{\vartheta})$ *and* $\hbar_8 = -\mu^{\vartheta}$ *and* $\varphi := \frac{T^{\vartheta}}{\Gamma(\vartheta)+1}$, *let us suppose* $P1$ *to be valid, where* $P1$ *contains* $\|S(\Upsilon)\| < \hbar_1, \|V_1(\Upsilon)\| < \hbar_2, \|V_2(\Upsilon)\| < \hbar_3, \|L(\Upsilon)\| < \hbar_4, \|A_m(\Upsilon)\| < \hbar_5 \|, \|A_s(\Upsilon)\| < \hbar_6, \|Q(\Upsilon)\| < \hbar_7, \|R(\Upsilon)\| < \hbar_8$.

Proof. We prove this theorem by first letting $\Psi > 0$ and also $S^{\circledast,\circledast} \in \mathcal{Y}$ in a manner that

$$|{}^C\mathcal{D}^{\vartheta}_{0,\Upsilon} S^{\circledast\circledast}(\Upsilon) - \mathcal{A}_1 S^{\circledast\circledast}(\Upsilon), V_1^{\circledast\circledast}(\Upsilon), V_2^{\circledast\circledast}(\Upsilon), L^{\circledast\circledast}(\Upsilon), A_m^{\circledast\circledast}(\Upsilon),\\ A_s^{\circledast\circledast}(\Upsilon), Q^{\circledast\circledast}(\Upsilon), R^{\circledast\circledast}(\Upsilon)| < \Psi_1,$$

we then have σ_1 following from the knowledge of Remark 4.1, this then leads to;

$${}^C\mathcal{D}^{\vartheta}_{0,\Upsilon} S^{\circledast\circledast}(\eth) = \mathcal{A}_1 S^{\circledast\circledast}(\Upsilon), V_1^{\circledast\circledast}(\Upsilon), V_2^{\circledast\circledast}(\Upsilon), L^{\circledast\circledast}(\Upsilon), A_m^{\circledast\circledast}(\Upsilon),\\ A_s^{\circledast\circledast}(\Upsilon), Q^{\circledast\circledast}(\Upsilon), R^{\circledast\circledast}(\Upsilon) + \sigma_1,$$

and we define $|\sigma_1 \le \Psi_1|$. Then,

$$\begin{aligned}
S(\Upsilon) &= S_0 + \frac{1}{\Gamma(\vartheta)}\int_0^{\Upsilon}(\Upsilon-\zeta)^{\vartheta-1}\\
&\times \mathcal{A}_1(S^{\circledast\circledast}(\zeta), V_1^{\circledast\circledast}(\zeta), V_2^{\circledast\circledast}(\zeta), L^{\circledast\circledast}(\zeta), A_m^{\circledast\circledast}(\zeta), A_s^{\circledast\circledast}(\zeta), Q^{\circledast\circledast}(\zeta), R^{\circledast\circledast}(\zeta))d\zeta\\
&+ \frac{1}{\Gamma(\vartheta)}\int_0^{\Upsilon}(\Upsilon-\zeta)^{\vartheta-1}\sigma_1(\zeta)d\zeta.
\end{aligned} \tag{31}$$

Referring from Theorem 4.2, we then suppose $S \in \mathcal{Y}$ to be a unique solution of the measles disease model with Caputo fractional operators. This reformulate $S(\Upsilon)$ in the form

$$\begin{aligned}
S(\Upsilon) &= S_0 + \frac{1}{\Gamma(\vartheta)}\int_0^{\Upsilon}(\Upsilon-\zeta)^{\vartheta-1}\\
&\times \mathcal{A}_1(S^{\circledast\circledast}(\zeta), V_1^{\circledast\circledast}(\zeta), V_2^{\circledast\circledast}(\zeta), L^{\circledast\circledast}(\zeta), A_m^{\circledast\circledast}(\zeta),\\
&A_s^{\circledast\circledast}(\zeta), Q^{\circledast\circledast}(\zeta), R^{\circledast\circledast}(\zeta))d\zeta,
\end{aligned} \tag{32}$$

this suffices that,

$$\begin{aligned}
&|S^{\circledast\circledast}(\Upsilon) - S(\Upsilon)| \le \frac{1}{\Gamma(\vartheta)}\int_0^{\Upsilon}(\Upsilon-\zeta)^{\vartheta-1}|\ell_1(\Upsilon)|d\zeta\\
&+ \frac{1}{\Gamma(\vartheta)}\int_0^{\Upsilon}(\Upsilon-\zeta)^{\vartheta-1}\\
&\times |\mathcal{A}_1(S^{\circledast\circledast}(\zeta), V_1^{\circledast\circledast}(\zeta), V_2^{\circledast\circledast}(\zeta), L^{\circledast\circledast}(\zeta), A_m^{\circledast\circledast}(\zeta), A_s^{\circledast\circledast}(\zeta), Q^{\circledast\circledast}(\zeta), R^{\circledast\circledast}(\zeta))\\
&- \mathcal{A}_1(S(\zeta), V_1(\zeta), V_2(\zeta), L(\zeta), A_m(\zeta),\\
&A_s(\zeta), Q(\zeta), R(\zeta))d\zeta\\
&\le \varrho\kappa_1 + \varrho\hbar_1\|S^{\circledast\circledast} - S\|.
\end{aligned} \tag{33}$$

By imposing sup norm on the inequality above, this yields, $\|S^{\circledast\circledast} - S\| - \varrho\hbar_1\|S^{\circledast\circledast} - S\| \le \varrho\kappa_1$ which leads to;

$$\|S^{\circledast\circledast} - S\| \le \frac{\varrho\kappa_1}{1-\varrho\hbar_1}.$$

We further assume that $D_{\mathcal{E}_1}\kappa_1 = \frac{\Phi\kappa_1}{1-\varrho\hbar_1}$, then we have the norm $\|S^{\circledast\circledast} - S\| \le D_{\mathcal{E}_1}\kappa_1$. From a similar approach, we obtain the following norms;

$$\begin{aligned}
\|V_1^{\circledast\circledast} - V_1\| &\le D_{\mathcal{E}_2}\kappa_2,\\
\|V_2^{\circledast\circledast} - V_2\| &\le D_{\mathcal{E}_3}\kappa_3,\\
\|L^{\circledast\circledast} - L\| &\le D_{\mathcal{E}_4}\kappa_4,\\
\|A_m^{\circledast\circledast} - A_m\| &\le D_{\mathcal{E}_5}\kappa_5,\\
\|A_s^{\circledast\circledast} - A_s\| &\le D_{\mathcal{E}_6}\kappa_6,\\
\|Q^{\circledast\circledast} - Q\| &\le D_{\mathcal{E}_7}\kappa_7,\\
\|R^{\circledast\circledast} - R\| &\le D_{\mathcal{E}_8}\kappa_8.
\end{aligned} \tag{34}$$

Let us take it that $D_{\mathcal{E}_i}\kappa_i = \frac{\varrho\kappa_i}{1-\varrho\hbar_i}$ for $i = 2, 3, \ldots, 8$. Therefore, the measles disease model with Caputo fractional operators satisfies the Hyers–Ulam stability criterion. □

Theorem 4.3. *Supposing that we have* (D') *and that there is an increasing monotonic function* $\Omega_i \in C([0, T], \mathbb{R}^+)$ *for* $i = 1, 2, 3 \cdots, 8$ *and there also exists* $\prod_{\Omega_i} > 0$ *in a manner that* $\forall \Upsilon \in T$, *there is* ${}^C I^{\vartheta}_{0,\Upsilon}\Omega_i(\Upsilon) < \prod_{\Omega_i}\Omega_i(\Upsilon)$ *for* $i = 1, 2, 3, \ldots, 8$. *By further assuming that* $(G1)$ *is valid, it is then in order to say that the measles disease model with fractional operators meets the Hyers–Ulam–Rassias stability criterion.*

Proof. Now, we begin to prove this theorem by first assuming that $\kappa > 0$ and also $S^{\circledast,\circledast} \in \mathcal{Y}$ indicates that

$$|{}^C D^{\vartheta}_{0,\Upsilon} S^{\circledast\circledast}(\vartheta) - \mathcal{A}_1(S^{\circledast\circledast}(\Upsilon), V_1^{\circledast\circledast}(\Upsilon), V_2^{\circledast\circledast}(\Upsilon), L^{\circledast\circledast}(\Upsilon), A_m^{\circledast\circledast}(\Upsilon),\\ A_s^{\circledast\circledast}(\Upsilon), Q^{\circledast\circledast}(\Upsilon), R^{\circledast\circledast}(\Upsilon))| < \kappa_1\Omega_1(\Upsilon),$$

then, there is ℓ_1 following Remark (3.2) and this yields

$${}^C D^{\vartheta}_{0,\Upsilon} S^{\circledast\circledast}(\Upsilon) = \mathcal{A}_1(S^{\circledast\circledast}(\Upsilon), V_1^{\circledast\circledast}(\Upsilon), V_2^{\circledast\circledast}(\Upsilon), L^{\circledast\circledast}(\Upsilon), A_m^{\circledast\circledast}(\Upsilon),\\ A_s^{\circledast\circledast}(\Upsilon), Q^{\circledast\circledast}(\Upsilon), R^{\circledast\circledast}(\Upsilon)) + \ell_1,$$

where $|\ell_1(\Upsilon)| \le \kappa_1\Omega_1(\Upsilon)$. Thus,

$$\begin{aligned}
S^{\circledast\circledast}(\Upsilon) &= S_0 + \frac{1}{\Gamma(\vartheta)}\int_0^{\Upsilon}(\Upsilon-\zeta)^{\vartheta-1}\\
&\times \mathcal{A}_1(S^{\circledast\circledast}(\zeta), V_1^{\circledast\circledast}(\zeta), V_2^{\circledast\circledast}(\zeta), L^{\circledast\circledast}(\zeta), A_m^{\circledast\circledast}(\zeta),\\
&A_s^{\circledast\circledast}(\zeta), Q^{\circledast\circledast}(\zeta), R^{\circledast\circledast}(\zeta))d\zeta\\
&+ \frac{1}{\Gamma(\vartheta)}\int_0^{\Upsilon}(\Upsilon-\zeta)^{\vartheta-1}\ell_1(\zeta)d\zeta.
\end{aligned} \tag{35}$$

Also recalling from theorem (3.1) we assume that $S \in \mathcal{Y}$ has a unique solution for the measles disease Caputo fractional model. $S(\Upsilon)$ is then rewritten in the form

$$\begin{aligned}
S(\Upsilon) &= S_0 + \frac{1}{\Gamma(\vartheta)}\int_0^{\Upsilon}(\Upsilon-\zeta)^{\vartheta-1}\\
&\times \mathcal{A}_1(S^{\circledast\circledast}(\zeta), V_1^{\circledast\circledast}(\zeta), V_2^{\circledast\circledast}(\zeta), L^{\circledast\circledast}(\zeta), A_m^{\circledast\circledast}(\zeta),\\
&A_s^{\circledast\circledast}(\zeta), Q^{\circledast\circledast}(\zeta), R^{\circledast\circledast}(\zeta))d\zeta,
\end{aligned} \tag{36}$$

and this leads to,

$$|S^{\circledast\circledast}(\Upsilon)-S(\Upsilon)| \leq \frac{1}{\Gamma(\vartheta)}\int_0^{\Upsilon}(\Upsilon-\zeta)^{\vartheta-1}|\ell_1(\Upsilon)|d\zeta$$
$$+\frac{1}{\Gamma(\vartheta)}\int_0^{\vartheta}(\Upsilon-\zeta)^{\vartheta-1}$$
$$\times|\mathcal{A}_1(S^{\circledast\circledast}(\zeta),V_1^{\circledast\circledast}(\zeta),V_2^{\circledast\circledast}(\zeta),L^{\circledast\circledast}(\zeta),A_m^{\circledast\circledast}(\zeta),A_s^{\circledast\circledast}(\zeta),Q^{\circledast\circledast}(\zeta),R^{\circledast\circledast}(\zeta))$$
$$-\mathcal{A}_1(S(\zeta),V_1(\zeta),V_2(\zeta),L(\zeta),A_m(\zeta),A_s(\zeta),Q(\zeta),R(\zeta))d\zeta$$
$$\leq\prod_{\Omega_1}\kappa_1\Omega_1(\Upsilon)+\varrho\hbar_1\|S^{\circledast\circledast}-S\|. \tag{37}$$

Again, we apply the knowledge of norm on the inequality above, and this yields, $\|S^{\circledast\circledast}-S\|-\varrho\hbar_1\|S^{\circledast\circledast}-S\| \leq \prod_{\Omega_1}\kappa_1\Omega_1(\Upsilon)$ which then suffices that;

$$\|S^{\circledast\circledast}-S\| \leq \frac{\prod_{\Omega_1}\kappa_1\Omega_1(\Upsilon)}{1-\varrho\hbar_1}.$$

By assuming also that $D_{\mathcal{E}_1,\Omega_1}=\frac{\Pi_{\Omega_1}}{1-\varrho\hbar_1}$, yields the norm $\|S^{\circledast\circledast}-S\| \leq \kappa_1 D_{\mathcal{E}_1,\Omega_1}\omega_1(\Upsilon)$. From a similar approach, we derive the following norms;

$$\begin{aligned}
&\|V_1^{\circledast\circledast}-V_1\| \leq D_{\mathcal{E}_2,\Omega_2}\kappa_2\Omega_2(\Upsilon),\\
&\|V_2^{\circledast\circledast}-V_2\| \leq D_{\mathcal{E}_3,\Omega_3}\kappa_3\Omega_3(\Upsilon),\\
&\|L^{\circledast\circledast}-L\| \leq D_{\mathcal{E}_4,\Omega_4}\kappa_4\Omega_4(\Upsilon),\\
&\|A_s^{\circledast\circledast}-A_s\| \leq D_{\mathcal{E}_5,\Omega_5}\kappa_5\Omega_5(\Upsilon),\\
&\|A_m^{\circledast\circledast}-A_m\| \leq D_{\mathcal{E}_6,\Omega_6}\kappa_6\Omega_6(\Upsilon),\\
&\|L^{\circledast\circledast}-L\| \leq D_{\mathcal{E}_7,\Omega_7}\kappa_7\Omega_7(\Upsilon),\\
&\|R^{\circledast\circledast}-R\| \leq D_{\mathcal{E}_8,\Omega_8}\kappa_8\Omega_8(\Upsilon),
\end{aligned} \tag{38}$$

by supposing that $D_{\mathcal{E}_i,\Omega_i}=\frac{\Pi_{\Omega_i}}{1-\varrho\hbar_i}$ for $i=2,3,\dots,8$. This undoubtedly suffices that the measles disease model with Caputo fractional operators satisfies the HUR stability criterion. This ends the proof. □

5. Parameter estimation

Mathematical modeling of infectious diseases is meant to aid in predicting the future transmission dynamics of the disease. To achieve this goal, researchers employ the concept of parameter estimation through the least squares approach to derive parameter values that are realistic and reliable. Parameter estimation by the least squares approach is a robust and most acceptable means as compared to the interpolation approach and others that produce high error margins and sometimes even yield impracticable parameter values [53,54]. As given in [55], we mostly assume the domain values to be true values for the least squares approach, whereas the functional values may be noisy. We then obtain reliable data in time series for at least one compartment of the disease that preferably exhibits the widespread presence of the disease. Initial guesses for the parameter values to be fitted are then pre-estimated. The solution curve is fitted from the data chosen in a manner that makes the residual error insignificant or very minimal. Let us take our observed values to be ξ_Υ and the model's solution set to be $\mathcal{U}(\Upsilon,\xi)$, then the residual error is defined as;

$$\mathcal{U}^*(\xi)=\sum_{\Upsilon=1}^{n}(\xi_\Upsilon-\mathcal{U}(\Upsilon,\xi))^2. \tag{39}$$

The data used for fitting the parameter values is given in Table 2; this was obtained from the World Health Organization [56]. We employed the following initial values for the state variables; $S(0)=33\,422\,824, V_1(0)=20\,000, V_2(0)=600, L(0)=200, A_m(0)=0, A_s(0)=32\,246, Q(0)=0$, and $R(0)=0$. The total population for the measles disease model presented in this work is defined as $N=S(0)+V_1(0)+V_2(0)+L(0)+A_m(0)+A_s(0)+Q(0)+R(0)$. According to [57], the total population of Ghana as of the year 2022 was 33 475 870. Also, the life expectancy of Ghanaians as of 2022 was 64.68 years, indicating that the natural death rate of this model could be defined as $\mu=\frac{1}{64.68}=0.015$. This implies that the corresponding recruitment rate defined by $\pi=\mu\times N$ is obtained to be 525 438. The model's parameter estimation reported a basic reproductive number for measles disease to be 4.32 with a mean square error of 0.000185; this indicates that the parameters estimated are reliable and could help in future predictions on the transmission dynamics of the measles disease. The parameter estimated values are given in Table 3.

Table 2
Measles disease prevalence data.

Year	Measles cases	Year	Measles cases
1990	32 246	2006	420
1991	17 135	2007	6
1992	39 933	2008	82
1993	34 641	2009	101
1994	34 821	2010	641
1995	40 276	2011	120
1996	34 273	2012	1613
1997	37 261	2013	319
1998	23 335	2014	124
1999	15 987	2015	23
2000	23 068	2016	32
2001	13 476	2017	19
2002	12 289	2018	34
2003	1939	2019	1274
2004	60	2020	88
2005	435	2021	52
2022	395		

Table 3
Model parameters descriptions.

Parameters	Value	Source	Parameters	Value	Source
π	525 438	Estimated	μ	0.015	Estimated
γ_1	0.00727	Fitted	γ_4	0.036834	Fitted
δ_1	0.082331	Fitted	δ_2	0.049824	Fitted
δ_3	0.000462	Fitted	α_1	0.0074	Fitted
α_2	0.178305	Fitted	α_3	0.3	Fitted
α_4	0.0000661	Fitted	τ_1	0.111737	Fitted
τ_2	4.3×10^{-14}	Fitted	ϵ_1	0.003316	Fitted
ϵ_2	0.4	Fitted	σ	1.223×10^{-5}	Fitted
ϕ_1	0.536911	Fitted	ϕ_2	0.033982	Fitted
m	0.004213	Fitted	n	0.001950	Fitted
β	0.000011	Fitted			

5.1. Numerical simulation of non-optimal control model

Here, we show the numerical fit of the proposed model with real data and the corresponding residuals. The importance of residuals in Caputo fractional analysis of measles using real data cannot be overstated, as they serve as a crucial diagnostic tool for model validation, parameter estimation, and predictive accuracy assessment. In Fig. 2, we plotted the model solution in the infected compartment with cumulative measles cases. Fig. 2(a) shows that the model solution fits relatively well with the observed data. Fig. 2(b) shows that the residuals are randomly distributed and can be used for prediction. Fig. 3 shows the sensitivity analysis in regards to the measles reproduction number $\mathcal{R}_0$. Fig. 3(a) shows that $\pi,\alpha_1,\beta,\tau_1,\tau_2$ and γ_2 contribute positively to the spread of measles with $\alpha_2,\alpha_3,\sigma,m,d,\gamma_1,\mu,\phi_1,\delta_1,\delta_2$, and δ_3 contributing negatively to the spread of secondary infection when the fraction order is 0.99. Fig. 3(b) shows that $\pi,\alpha_1,\beta,\tau_1,\tau_2$ and m contribute positively to the spread of measles with $\alpha_2,\alpha_3,\sigma,d,\gamma_1,\gamma_2,\mu,\phi_1,\delta_1,\delta_2$, and δ_3 contributing negatively to the spread of secondary infection when the fraction order is 0.90. This indicates that a change in memory affects the intensity (positive or negative correlation) of the parameters m and γ_2; thus, the proportion of newly recruited first-dose vaccinated individuals and vaccination ate for the second dose of measles vaccine.

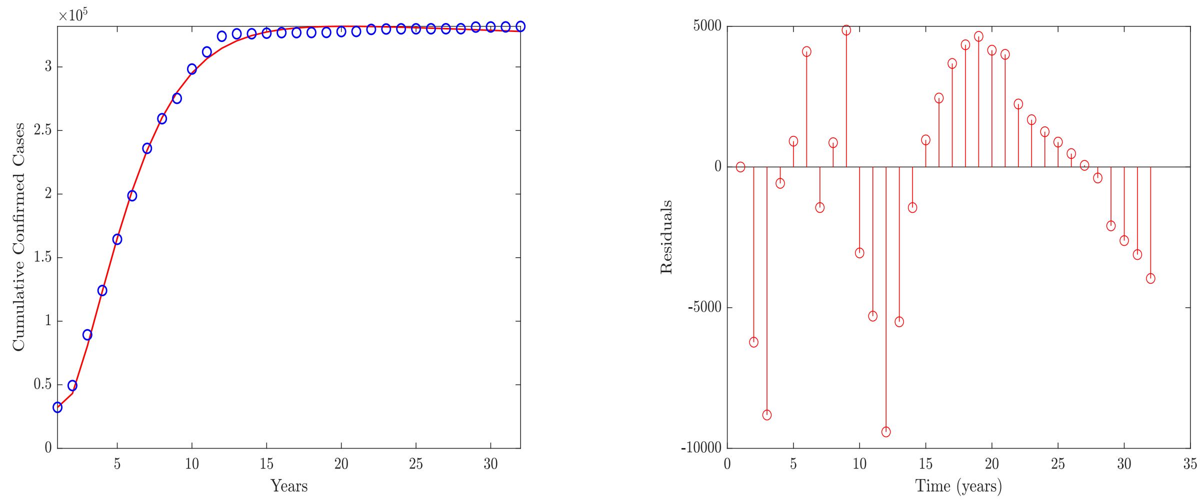

(a) Measles reported data

(b) Residual plot

Fig. 2. Time series fitting reported data from WHO [56].

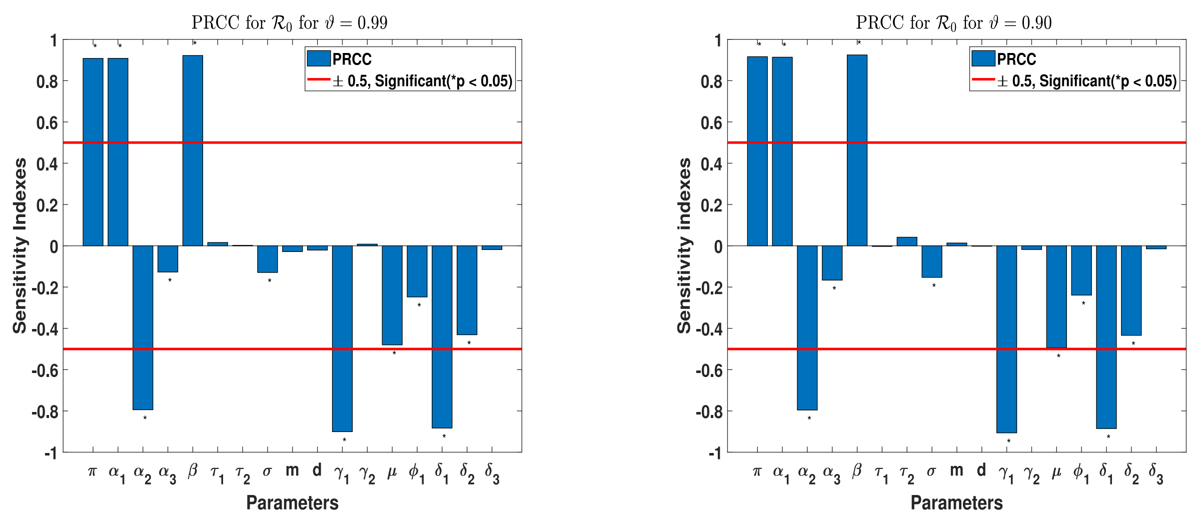

(a) PRCC plot of the measles reproduction expression.

(b) PRCC plot of the measles reproduction expression.

Fig. 3. PRCC plot for fractional order 0.99 and 0.90 respectively.

Fig. 4 shows the effects of simultaneously varying some parameters in the measles reproduction number with a memory order of 0.90. Fig. 4(a) shows the effect of varying β and γ_1 on $\mathcal{R}_0$. It indicates that an increase in the first dose of the measles vaccine reduces the number of secondary infections. Still, with an increase in the transmission rate, β increases the number of secondary infections. Fig. 4(b) shows the effect of varying β and γ_2 on $\mathcal{R}_0$. This indicates that a minimal rate of a second dose of the measles vaccine increases the number of secondary infections. Still, a reduction in the transmission rate, β, reduces the number of secondary infections. Also, Fig. 4(b) indicates that zero transmission rate leads to a zero number of secondary infections. Fig. 4(c) shows the effect of varying β and α_1 on $\mathcal{R}_0$.

Fig. 4(c) indicates that, a simultaneous increase in the rate at which individuals in the latent class become asymptomatic, α_1, and the transmission rate β increase the number of secondary infection in the population. Fig. 4(d) indicates that simultaneous increase in the rate of first dose vaccine γ_1 and second dose vaccine γ_2 reduces the number of secondary infection in the population. Fig. 5 shows the effect of varying the rate at which individuals in the asymptomatic class become symptomatic, α_2. Fig. 5(a) shows the effects of varying α_2, the latent compartment $L(t)$. It shows that an increase in α_2 reduces the number of latent individuals after the first year of the disease. Fig. 5(b) shows the effects of varying α_2, the asymptomatic compartment at time t, $A_m(t)$. It shows that an increase in α_2 reduces the number of asymptomatic individuals after one and half years of the disease outbreak. Fig. 5(c) shows the effects of varying α_2, the symptomatic compartment at time t, $A_s(t)$. It shows that an increase in α_2 first increases the number of symptomatic individuals for one and half years and later reduces the

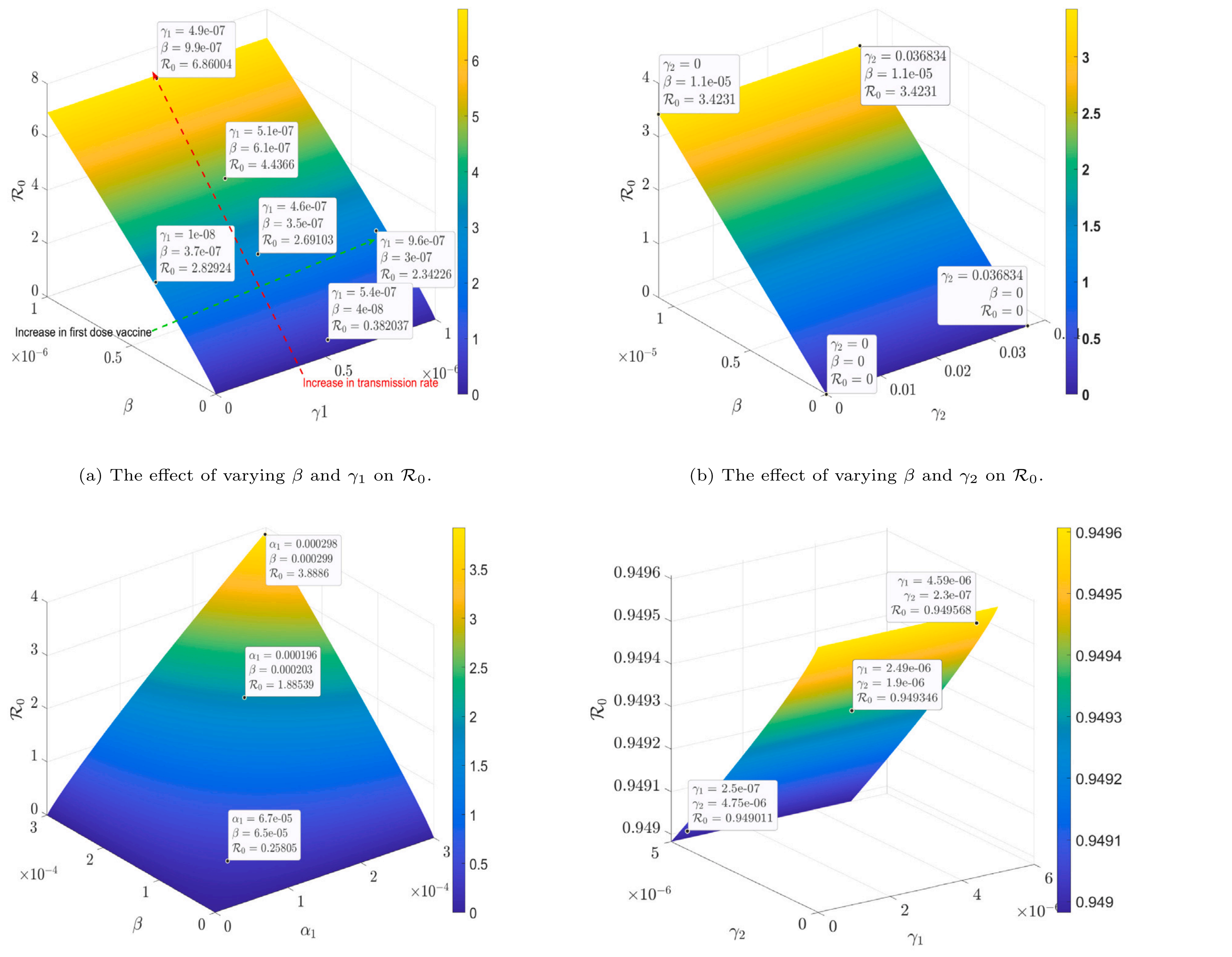

(a) The effect of varying β and γ_1 on $\mathcal{R}_0$.

(b) The effect of varying β and γ_2 on $\mathcal{R}_0$.

(c) The effect of varying β and α_1 on $\mathcal{R}_0$.

(d) The effect of varying γ_1 and γ_2 on $\mathcal{R}_0$.

Fig. 4. Effects of varying some parameters in the measles reproduction number simultaneously with memory order of 0.90.

number of symptomatic individuals after one and half years of the disease outbreak. Fig. 5(d) shows the effects of varying α_2 on, the isolated or quarantined compartment at time t, $Q(t)$. It shows that an increase in α_2 first increases the number of isolated or quarantined individuals for two and half years and later reduces the number of isolated or quarantined individuals after two and half years of the disease outbreak. Fig. 6 shows the effect of varying the rate at which individuals in the asymptomatic class become symptomatic, α_2, and the effect of varying the rate at which individuals in the latent class recover from the measles, δ_1 on the first and second dose vaccinated individuals respectively.

Fig. 6(a), 6(b), 6(c) and Fig. 6(d) indicate that an increase in these (Rate at which individuals in the asymptomatic class become symptomatic, α_2 and the rate at which individuals in the latent class recover from the measles, δ_1) parameters increase the number of vaccinated individuals.

Fig. 7 shows the effect of memory on the $S(t), V_1(t), V_2(t)$, and $L(t)$, respectively. Considering $\vartheta \in [0.90 : 0.01 : 1]$. Fig. 7(a) shows that a change in the memory index by 0.01 affects the number of susceptible individuals. This indicates that the number of healthy individuals can be overestimated when considering the integer order within five years of the disease outbreak. Fig. 7(b) suggests that the number of individuals who receive the first dose of vaccine slightly increases for the first year and afterward reduces. This memory dynamics shows that individuals should be advised to go for the first dose of vaccination after the first year of the measles outbreak in Ghana. Fig. 7(c) suggests that the number of individuals who receive a second dose of vaccine slightly increases for one and half years and afterward reduces. This memory dynamics shows that individuals should be advised to go for their second vaccination dose to reduce the intensity of the measles outbreak in Ghana. Fig. 7(d) shows that a change in the memory index by 0.01 affects the number of latent individuals for more than two years before finally reducing. Fig. 8 shows the effect of memory on the $A_m(t), A_s(t), Q(t)$, and $R(t)$, respectively. Considering $\vartheta \in [0.90 : 0.01 : 1]$. Fig. 8(a) shows that a change in the memory index by 0.01 affects the number of asymptomatic individuals for three years before finally reducing. Fig. 8(b) shows that a change in the memory index by 0.01 affects the number of symptomatic individuals for more than three years before finally reducing in intensity. Fig. 8(c) shows that a change in the memory index affects the number of quarantined individuals for more than three years before any crisscrossing. Fig. 8(d) shows that a change in the memory index affects the number of recovered individuals for almost four years before any crisscrossing effects set in.

6. Fractional optimal control of the measles model

Measles is a highly contagious disease that spreads swiftly when it enters a population. Based on the PRCC plot in Fig. 3, the following four control measures are implemented to lessen the disease spread. These controls consist of media campaign, $u_1(\Upsilon)$, first dose of measles vaccine, $u_2(\Upsilon)$, second dose of measles vaccine, $u_3(\Upsilon)$ and isolation centers for treatment purposes, $u_4(\Upsilon)$. Using the Caputo fractional derivative, the Caputo optimal control equation (constraints) is given as,

$$
\begin{aligned}
{}^{C}\mathcal{D}^{\vartheta}_{0,\Upsilon}S(\Upsilon) &= (1-m^{\vartheta}-d^{\vartheta})\pi^{\vartheta} - (1-u_1(\Upsilon))\beta^{\vartheta}S\left(\frac{A_m}{1+\epsilon_1^{\vartheta}Am}+\frac{As}{1+\epsilon_2^{\vartheta}As}\right)\\
&- (\mu^{\vartheta}+u_2(\Upsilon)+\gamma_1^{\vartheta})S,\\
{}^{C}\mathcal{D}^{\vartheta}_{0,\Upsilon}V_1(\Upsilon) &= m^{\vartheta}\pi^{\vartheta} + (u_2(\Upsilon)+\gamma_1^{\vartheta})S\\
&- (1-\tau_1^{\vartheta})(1-u_1(\Upsilon))\beta^{\vartheta}V_1\left(\frac{Am}{1+\sigma^{\vartheta}V_1}+\frac{As}{1+\sigma^{\vartheta}V_1}\right)\\
&- (\mu^{\vartheta}+u_3+(\Upsilon)\gamma_1^{\vartheta})V_1,\\
{}^{C}\mathcal{D}^{\vartheta}_{0,\Upsilon}V_2(\Upsilon) &= d^{\vartheta}\pi^{\vartheta} + u_3(\Upsilon)+\gamma_1^{\vartheta}V_1\\
&- (1-\tau_2^{\vartheta})(1-u_1(\Upsilon))\beta^{\vartheta}V_2\left(\frac{Am}{1+\sigma^{\vartheta}V_2}+\frac{As}{1+\sigma^{\vartheta}V_2}\right) - (\mu^{\vartheta}+\tau_2^{\vartheta}\delta_3^{\vartheta})V_2,\\
{}^{C}\mathcal{D}^{\vartheta}_{0,\Upsilon}L(\Upsilon) &= (1-u_1(\Upsilon))\beta^{\vartheta}S\left(\frac{A_m}{1+\epsilon_1^{\vartheta}Am}+\frac{As}{1+\epsilon_2^{\vartheta}As}\right)\\
&+ (1-\tau_1^{\vartheta})(1-u_1(\Upsilon))\beta^{\vartheta}V_1\left(\frac{Am}{1+\sigma^{\vartheta}V_1}+\frac{As}{1+\sigma^{\vartheta}V_1}\right)\\
&+ (1-\tau_2^{\vartheta})(1-u_1(\Upsilon))\beta^{\vartheta}V_2\left(\frac{Am}{1+\sigma^{\vartheta}V_2}+\frac{As}{1+\sigma^{\vartheta}V_2}\right)\\
&- (\mu^{\vartheta}+\alpha_1^{\vartheta}+\delta_1^{\vartheta})L,\\
{}^{C}\mathcal{D}^{\vartheta}_{0,\Upsilon}A_m(\Upsilon) &= \alpha_1^{\vartheta}L - (\mu^{\vartheta}+\alpha_2^{\vartheta}+\delta_2^{\vartheta})A_m,\\
{}^{C}\mathcal{D}^{\vartheta}_{0,\Upsilon}A_s(\Upsilon) &= \alpha_2^{\vartheta}A_m - (\mu^{\vartheta}+\phi_1^{\vartheta}+u_4+\alpha_3^{\vartheta})A_s,\\
{}^{C}\mathcal{D}^{\vartheta}_{0,\Upsilon}Q(\Upsilon) &= (u_4+\alpha_3^{\vartheta})A_s - (\mu^{\vartheta}+\phi_2^{\vartheta}+\alpha_4^{\vartheta})Q,\\
{}^{C}\mathcal{D}^{\vartheta}_{0,\Upsilon}R(\Upsilon) &= \delta_1^{\vartheta}L + \delta_2^{\vartheta}A_m + \tau_2^{\vartheta}\delta_3^{\vartheta}V_2 + \alpha_4^{\vartheta}Q - \mu^{\vartheta}R.
\end{aligned} \tag{40}
$$

With initial conditions $S(\Upsilon)\geq 0, V_1(0)\geq 0, V_2(0)\geq 0, L(0)\geq 0, A_m(0)\geq 0, A_s(0)\geq 0, Q(0)\geq 0, R(0)\geq 0$. The optimal control model in (40) is subject to the objective function

$$
J(u_1,u_2,u_3) = min\int_0^T \left(B_1L + B_2A_m + B_3A_s + B_4Q + \frac{1}{2}C_1u_1^2 + \frac{1}{2}C_2u_2^2 + \frac{1}{2}C_3u_3^2 + \frac{1}{2}C_4u_4^2\right)dt, \tag{41}
$$

where B_1, B_2, B_3, B_4 are the weight constants related to the infected measles population and C_1, C_2, C_3, and C_4 are the costs associated with setting up isolation centers for treating infected individuals and the cost of procuring or manufacturing measles vaccines comprising the first dose and the second dose of the measles vaccine. To minimize the cost function, we determined the optional controls $u_1^{\odot}, u_2^{\odot}, u_3^{\odot}, u_4^{\odot}$ such that.

$$
J(u_1^{\odot}, u_2^{\odot}, u_3^{\odot}, u_4^{\odot}) = \inf\{J(u_1,u_2,u_3,u_4)|u_i\in U\},
$$

where $U = \{(u_1,u_2,u_3,u_4)|u_i(t)$ is Lebesgue measurable on the interval $[0, \text{T}]$, $0\leq u_i\leq 1, i=1,2,3,4\}$. We used Pontryagin's maximum principle to obtain the optimal control solution u_1,u_2,u_3,u_4 that minimizes the objective function. The Hamiltonian of the Caputo fractional control is obtained as

$$
\begin{aligned}
\mathcal{H} &= B_1L + B_2A_m + B_3A_s + B_4Q + \frac{1}{2}C_1u_1^2 + \frac{1}{2}C_2u_2^2 + \frac{1}{2}C_3u_3^2 + \frac{1}{2}C_4u_4^2\\
&+ \lambda_1\left((1-m^{\vartheta}-d^{\vartheta})\pi^{\vartheta} - (1-u_1(\Upsilon))\beta^{\vartheta}S\left(\frac{A_m}{1+\epsilon_1^{\vartheta}Am}+\frac{As}{1+\epsilon_2^{\vartheta}As}\right)\right.\\
&\left. - (\mu^{\vartheta}+u_2(\Upsilon)+\gamma_1^{\vartheta})S\right)\\
&+ \lambda_2\left(m^{\vartheta}\pi^{\vartheta} + (u_2(\Upsilon)+\gamma_1^{\vartheta})S\right.\\
&\left. - (1-\tau_1^{\vartheta})(1-u_1(\Upsilon))\beta^{\vartheta}V_1\left(\frac{Am}{1+\sigma^{\vartheta}V_1}+\frac{As}{1+\sigma^{\vartheta}V_1}\right) - (\mu^{\vartheta}+u_3+(\Upsilon)\gamma_1^{\vartheta})V_1\right)\\
&+ \lambda_3\left(d^{\vartheta}\pi^{\vartheta} + u_3(\Upsilon)+\gamma_1^{\vartheta}V_1\right.\\
&- (1-\tau_2^{\vartheta})(1-u_1(\Upsilon))\beta^{\vartheta}V_2\left(\frac{Am}{1+\sigma^{\vartheta}V_2}+\frac{As}{1+\sigma^{\vartheta}V_2}\right)\\
&\left. - (\mu^{\vartheta}+\tau_2^{\vartheta}\delta_3^{\vartheta})V_2\right)\\
&+ \lambda_4\left((1-u_1(\Upsilon))\beta^{\vartheta}S\left(\frac{A_m}{1+\epsilon_1^{\vartheta}Am}+\frac{As}{1+\epsilon_2^{\vartheta}As}\right)\right.\\
&+ (1-\tau_1^{\vartheta})(1-u_1(\Upsilon))\beta^{\vartheta}V_1\left(\frac{Am}{1+\sigma^{\vartheta}V_1}+\frac{As}{1+\sigma^{\vartheta}V_1}\right)\\
&+ (1-\tau_2^{\vartheta})(1-u_1(\Upsilon))\beta^{\vartheta}V_2\left(\frac{Am}{1+\sigma^{\vartheta}V_2}+\frac{As}{1+\sigma^{\vartheta}V_2}\right)\\
&\left. - (\mu^{\vartheta}+\alpha_1^{\vartheta}+\delta_1^{\vartheta})L\right)\\
&+ \lambda_5\left(\alpha_1^{\vartheta}L - (\mu^{\vartheta}+\alpha_2^{\vartheta}+\delta_2^{\vartheta})A_m\right)\\
&+ \lambda_6\left(\alpha_2^{\vartheta}A_m - (\mu^{\vartheta}+\phi_1^{\vartheta}+u_4+\alpha_3^{\vartheta})A_s\right)\\
&+ \lambda_7\left((u_4+\alpha_3^{\vartheta})A_s - (\mu^{\vartheta}+\phi_2^{\vartheta}+\alpha_4^{\vartheta})Q\right)\\
&+ \lambda_8\left(\delta_1^{\vartheta}L + \delta_2^{\vartheta}A_m + \tau_2^{\vartheta}\delta_3^{\vartheta}V_2 + \alpha_4^{\vartheta}Q - \mu^{\vartheta}R\right).
\end{aligned} \tag{42}
$$

Where λ_i, i=1, 2, ...8, are the adjoined variables to be determined by taking the partial derivative of the Hamiltonian with respect to the state variables $S, V_1, V_2, A_m, A_s, Q, R$. The optimal conditions of Eqs. (40) and (41) according to Caputo Fractional derivative are stated as follows

$$
\begin{aligned}
&{}^{C}\mathcal{D}^{\vartheta}_{0,\Upsilon}S(\Upsilon) = \frac{\partial\mathcal{H}}{\partial\lambda_1}(\Upsilon), {}^{C}\mathcal{D}^{\vartheta}_{0,\Upsilon}V_1(\Upsilon)\\
&= \frac{\partial\mathcal{H}}{\partial\lambda_2}(\Upsilon), {}^{C}\mathcal{D}^{\vartheta}_{0,\Upsilon}V_2(\Upsilon) = \frac{\partial\mathcal{H}}{\partial\lambda_3}(\Upsilon), {}^{C}\mathcal{D}^{\vartheta}_{0,\Upsilon}L(\Upsilon) = \frac{\partial\mathcal{H}}{\partial\lambda_4}(\Upsilon),\\
&{}^{C}\mathcal{D}^{\vartheta}_{0,\Upsilon}A_m(\Upsilon) = \frac{\partial\mathcal{H}}{\partial\lambda_5}(\Upsilon), {}^{C}\mathcal{D}^{\vartheta}_{0,\Upsilon}A_s(\Upsilon) = \frac{\partial\mathcal{H}}{\partial\lambda_6}(\Upsilon), {}^{C}\mathcal{D}^{\vartheta}_{0,\Upsilon}Q(\Upsilon)\\
&= \frac{\partial\mathcal{H}}{\partial\lambda_7}(\Upsilon), {}^{C}\mathcal{D}^{\vartheta}_{0,\Upsilon}R(\Upsilon) = \frac{\partial\mathcal{H}}{\partial\lambda_8}(\Upsilon),
\end{aligned} \tag{43}
$$

$$
\begin{aligned}
&\Upsilon^{C}\mathcal{D}^{\vartheta}_{T}\lambda_1(\Upsilon) = -\frac{\partial\mathcal{H}}{\partial S}(\Upsilon), \Upsilon^{C}\mathcal{D}^{\vartheta}_{T}\lambda_2(\Upsilon)\\
&= -\frac{\partial\mathcal{H}}{\partial V_1}(\Upsilon), \Upsilon^{C}\mathcal{D}^{\vartheta}_{T}\lambda_3(\Upsilon) = -\frac{\partial\mathcal{H}}{\partial V_2}(\Upsilon), \Upsilon^{C}\mathcal{D}^{\vartheta}_{T}\lambda_4(\Upsilon) = -\frac{\partial\mathcal{H}}{\partial L}(\Upsilon)\\
&\Upsilon^{C}\mathcal{D}^{\vartheta}_{T}\lambda_5(\Upsilon) = -\frac{\partial\mathcal{H}}{\partial A_m}(\Upsilon), \Upsilon^{C}\mathcal{D}^{\vartheta}_{T}\lambda_6(\Upsilon) = -\frac{\partial\mathcal{H}}{\partial A_s}(\Upsilon), \Upsilon^{C}\mathcal{D}^{\vartheta}_{T}\lambda_7(\Upsilon)\\
&= -\frac{\partial\mathcal{H}}{\partial Q}(\Upsilon), \Upsilon^{C}\mathcal{D}^{\vartheta}_{T}\lambda_8(\Upsilon) = -\frac{\partial\mathcal{H}}{\partial R}(\Upsilon).
\end{aligned} \tag{44}
$$

Theorem 6.1. *Let the solutions of the state system be* $S^{\odot}, V_1^{\odot}, V_2^{\odot}, L^{\odot}, A_m^{\odot}, A_s^{\odot}, Q^{\odot}, R^{\odot}$ *and the specified optional controls are* u_1, u_2, u_3, u_4*. Then there exists the following adjoints* $\lambda_i, i=1,2,\dots,8$ *that satisfies*

$$
\begin{aligned}
&{}_{\Upsilon}^{C} \mathcal{D}_T^{\vartheta} \lambda_1^{\odot}(\Upsilon) = (u_1-1)\beta^{\vartheta}\left(\frac{A_m}{1+\epsilon_1^{\vartheta} A_m}+\frac{A_s}{1+\epsilon_2^{\vartheta} A_s}\right)(\lambda_1^{\odot}-\lambda_4^{\odot})\\
&+\lambda_1^{\odot}(\mu^{\vartheta}+u_1+\gamma_1^{\vartheta})-\lambda_2^{\odot}(u_2+\gamma_1^{\vartheta}),\\
&{}_{\Upsilon}^{C} \mathcal{D}_T^{\vartheta} \lambda_2^{\odot}(\Upsilon) = (u_1-1)(\tau_1^{\vartheta}-1)\beta^{\vartheta}\left(\frac{A_m}{1+\sigma^{\vartheta} V_1}+\frac{A_s}{1+\sigma^{\vartheta} V_1}\right)(\lambda_4^{\odot}-\lambda_2^{\odot})\\
&-\lambda_3^{\odot}(u_3+\gamma_4^{\vartheta})\\
&+(u_1-1)(\tau_1^{\vartheta}-1)\beta^{\vartheta} V_1\left(\frac{A_m\sigma^{\vartheta}}{(1+\sigma^{\vartheta}V_1)^2}+\frac{A_s\sigma^{\vartheta}}{(1+\sigma^{\vartheta}V_1)^2}\right)(\lambda_2^{\odot}-\lambda_4^{\odot})\\
&+\lambda_2^{\odot}(\mu^{\vartheta}+u_3+\gamma_4^{\vartheta}),\\
&{}_{\Upsilon}^{C} \mathcal{D}_T^{\vartheta} \lambda_3^{\odot}(\Upsilon) = (u_1-1)(\tau_2^{\vartheta}-1)\beta^{\vartheta}\left(\frac{A_m}{1+\sigma^{\vartheta} V_2}+\frac{A_s}{1+\sigma^{\vartheta} V_2}\right)(\lambda_4^{\odot}-\lambda_3^{\odot})\\
&+\lambda_3^{\odot}(\mu^{\vartheta}+\tau_2^{\vartheta}\delta_3^{\vartheta})-\lambda_8^{\odot}\tau_2^{\vartheta}\delta_3^{\vartheta}\\
&+(u_1-1)(\tau_2^{\vartheta}-1)\beta^{\vartheta} V_2\left(\frac{A_m\sigma^{\vartheta}}{(1+\sigma^{\vartheta}V_2)^2}+\frac{A_s\sigma^{\vartheta}}{(1+\sigma^{\vartheta}V_2)^2}\right)(\lambda_3^{\odot}-\lambda_4^{\odot}),\\
&{}_{\Upsilon}^{C} \mathcal{D}_T^{\vartheta} \lambda_4^{\odot}(\Upsilon) = \lambda_4^{\odot}(\mu^{\vartheta}+\alpha_1^{\vartheta}+\delta_1^{\vartheta})-\lambda_5^{\odot}\alpha_1^{\vartheta}-\lambda_8^{\odot}\delta_1^{\vartheta}-B_1,\\
&{}_{\Upsilon}^{C} \mathcal{D}_T^{\vartheta} \lambda_5^{\odot}(\Upsilon) = \frac{(u_1-1)\beta^{\vartheta} S}{(\epsilon_1^{\vartheta}A_m+1)^2}(\lambda_1^{\odot}-\lambda_4^{\odot})\\
&+(u_1-1)(1-\tau_1^{\vartheta})\left(\frac{\beta^{\vartheta}V_1}{1+\sigma^{\vartheta}V_1}\right)(\lambda_2^{\odot}-\lambda_4^{\odot})-\lambda_6^{\odot}\alpha_2^{\vartheta}\\
&+(u_1-1)(1-\tau_2^{\vartheta})\left(\frac{\beta^{\vartheta}V_2}{1+\sigma^{\vartheta}V_2}\right)(\lambda_3^{\odot}-\lambda_4^{\odot})+\lambda_5^{\odot}(\mu^{\vartheta}+\alpha_2^{\vartheta}+\delta_2^{\vartheta})\lambda_6^{\odot}\delta_2^{\vartheta}-B_2,\\
&{}_{\Upsilon}^{C} \mathcal{D}_T^{\vartheta} \lambda_6^{\odot}(\Upsilon) = \frac{(u_1-1)\beta^{\vartheta} S}{(\epsilon_2^{\vartheta}A_s+1)^2}(\lambda_1^{\odot}-\lambda_4^{\odot})\\
&+(u_1-1)(1-\tau_1^{\vartheta})\left(\frac{\beta^{\vartheta}V_1}{1+\sigma^{\vartheta}V_1}\right)(\lambda_2^{\odot}-\lambda_4^{\odot})-\lambda_7^{\odot}(u_4+\alpha_3^{\vartheta})\\
&+(u_1-1)(1-\tau_2^{\vartheta})\left(\frac{\beta^{\vartheta}V_2}{1+\sigma^{\vartheta}V_2}\right)(\lambda_3^{\odot}-\lambda_4^{\odot})\\
&+\lambda_6^{\odot}(\mu^{\vartheta}+\phi_1^{\vartheta}+u_4+\alpha_3^{\vartheta})-B_3,\\
&{}_{\Upsilon}^{C} \mathcal{D}_T^{\vartheta} \lambda_7^{\odot}(\Upsilon) = \lambda_7^{\odot}(\mu^{\vartheta}+\phi_2^{\vartheta}+\alpha_4^{\vartheta})-\lambda_8^{\odot}\alpha_4^{\vartheta}-B_4\\
&{}_{\Upsilon}^{C} \mathcal{D}_T^{\vartheta} \lambda_8^{\odot}(\Upsilon) = \lambda_7^{\odot}\mu^{\vartheta}.
\end{aligned}
\tag{45}
$$

The optimality requirement is satisfied by the controls $u_1^{\odot}, u_2^{\odot}, u_3^{\odot}, u_4^{\odot}$

$$
\begin{aligned}
u_1^{\odot} &= \sup\left\{0, \inf\left(1, -\frac{\mathcal{M}_1}{C_1}\right)\right\},\\
u_2^{\odot} &= \sup\left\{0, \inf\left(1, \frac{S\,(\lambda_1^{\odot}-\lambda_2^{\odot})}{C_2}\right)\right\},\\
u_3^{\odot} &= \sup\left\{0, \inf\left(1, \frac{V_1\,(\lambda_2^{\odot}-\lambda_3^{\odot})}{C_3}\right)\right\},\\
u_4^{\odot} &= \sup\left\{0, \inf\left(1, \frac{A_s\,(\lambda_6^{\odot}-\lambda_7^{\odot})}{C_4}\right)\right\},
\end{aligned}
$$

where

$$
\begin{aligned}
\mathcal{M}_1 =\;&\lambda_4^{\odot}\left(\frac{V_1\beta^{\vartheta}\left(\tau_1^{\vartheta}-1\right)\left(A_s+A_m\right)}{V_1\sigma^{\vartheta}+1}-\frac{S\beta^{\vartheta}\left(A_mA_s\epsilon_1^{\vartheta}+A_mA_s\epsilon_2^{\vartheta}+A_s+A_m\right)}{\left(A_m\epsilon_1^{\vartheta}+1\right)\left(A_s\epsilon_2^{\vartheta}+1\right)}\right.\\
&\left.+\frac{V_2\,\beta^{\vartheta}\left(\tau_2^{\vartheta}-1\right)\left(A_s+A_m\right)}{V_2\sigma^{\vartheta}+1}\right)\\
&-\frac{V_1\beta^{\vartheta}\lambda_2^{\odot}\left(\tau_1^{\vartheta}-1\right)\left(A_s+A_m\right)}{V_1\,\sigma^{\vartheta}+1}-\frac{V_2\beta^{\vartheta}\,\lambda_3^{\odot}\left(\tau_2^{\vartheta}-1\right)\left(A_s+A_m\right)}{V_2\sigma^{\vartheta}+1}\\
&+\frac{S\,\beta^{\vartheta}\,\left(A_m\,A_s\,\epsilon_1^{\vartheta}+A_mA_s\epsilon_2^{\vartheta}+A_s+A_m\right)}{\left(A_m\epsilon_1^{\vartheta}+1\right)\,\left(A_s\epsilon_2^{\vartheta}+1\right)}
\end{aligned}
$$

Proof. From Eqs. (42), (43), and (44) we obtained the adjoint equations as follows

$$
\begin{aligned}
{}_{\Upsilon}^{C}\mathcal{D}_T^{\vartheta}\lambda_1^{\odot}(\Upsilon) &= -\frac{\partial\mathcal{H}}{\partial S}(\Upsilon) = (u_1-1)\beta^{\vartheta}\left(\frac{A_m}{1+\epsilon_1^{\vartheta}A_m}+\frac{A_s}{1+\epsilon_2^{\vartheta}A_s}\right)(\lambda_1^{\odot}-\lambda_4^{\odot})\\
&\quad+\lambda_1^{\odot}(\mu^{\vartheta}+u_1+\gamma_1^{\vartheta})\\
&\quad-\lambda_2^{\odot}(u_2+\gamma_1^{\vartheta}),\\
{}_{\Upsilon}^{C}\mathcal{D}_T^{\vartheta}\lambda_2^{\odot}(\Upsilon) &= -\frac{\partial\mathcal{H}}{\partial V_1}(\Upsilon) = (u_1-1)(\tau_1^{\vartheta}-1)\beta^{\vartheta}\left(\frac{A_m}{1+\sigma^{\vartheta}V_1}+\frac{A_s}{1+\sigma^{\vartheta}V_1}\right)\\
&\quad\times(\lambda_4^{\odot}-\lambda_2^{\odot})-\lambda_3^{\odot}(u_3+\gamma_4^{\vartheta})\\
&\quad+(u_1-1)(\tau_1^{\vartheta}-1)\beta^{\vartheta}V_1\left(\frac{A_m\sigma^{\vartheta}}{(1+\sigma^{\vartheta}V_1)^2}+\frac{A_s\sigma^{\vartheta}}{(1+\sigma^{\vartheta}V_1)^2}\right)(\lambda_2^{\odot}-\lambda_4^{\odot})\\
&\quad+\lambda_2^{\odot}(\mu^{\vartheta}+u_3+\gamma_4^{\vartheta}),\\
{}_{\Upsilon}^{C}\mathcal{D}_T^{\vartheta}\lambda_3^{\odot}(\Upsilon) &= -\frac{\partial\mathcal{H}}{\partial V_2}(\Upsilon) = (u_1-1)(\tau_2^{\vartheta}-1)\beta^{\vartheta}\left(\frac{A_m}{1+\sigma^{\vartheta}V_2}+\frac{A_s}{1+\sigma^{\vartheta}V_2}\right)\\
&\quad\times(\lambda_4^{\odot}-\lambda_3^{\odot})+\lambda_3^{\odot}(\mu^{\vartheta}+\tau_2^{\vartheta}\delta_3^{\vartheta})-\lambda_8^{\odot}\tau_2^{\vartheta}\delta_3^{\vartheta}\\
&\quad+(u_1-1)(\tau_2^{\vartheta}-1)\beta^{\vartheta}V_2\left(\frac{A_m\sigma^{\vartheta}}{(1+\sigma^{\vartheta}V_2)^2}+\frac{A_s\sigma^{\vartheta}}{(1+\sigma^{\vartheta}V_2)^2}\right)(\lambda_3^{\odot}-\lambda_4^{\odot}),\\
{}_{\Upsilon}^{C}\mathcal{D}_T^{\vartheta}\lambda_4^{\odot}(\Upsilon) &= -\frac{\partial\mathcal{H}}{\partial L}(\Upsilon) = \lambda_4^{\odot}(\mu^{\vartheta}+\alpha_1^{\vartheta}+\delta_1^{\vartheta})-\lambda_5^{\odot}\alpha_1^{\vartheta}-\lambda_8^{\odot}\delta_1^{\vartheta}-B_1,\\
{}_{\Upsilon}^{C}\mathcal{D}_T^{\vartheta}\lambda_5^{\odot}(\Upsilon) &= -\frac{\partial\mathcal{H}}{\partial A_m}(\Upsilon) = \frac{(u_1-1)\beta^{\vartheta}S}{(\epsilon_1^{\vartheta}A_m+1)^2}(\lambda_1^{\odot}-\lambda_4^{\odot})\\
&\quad+(u_1-1)(1-\tau_1^{\vartheta})\left(\frac{\beta^{\vartheta}V_1}{1+\sigma^{\vartheta}V_1}\right)(\lambda_2^{\odot}-\lambda_4^{\odot})-\lambda_6^{\odot}\alpha_2^{\vartheta}\\
&\quad+(u_1-1)(1-\tau_2^{\vartheta})\left(\frac{\beta^{\vartheta}V_2}{1+\sigma^{\vartheta}V_2}\right)(\lambda_3^{\odot}-\lambda_4^{\odot})\\
&\quad+\lambda_5^{\odot}(\mu^{\vartheta}+\alpha_2^{\vartheta}+\delta_2^{\vartheta})\lambda_6^{\odot}\delta_2^{\vartheta}-B_2,\\
{}_{\Upsilon}^{C}\mathcal{D}_T^{\vartheta}\lambda_6^{\odot}(\Upsilon) &= -\frac{\partial\mathcal{H}}{\partial A_s}(\Upsilon) = \frac{(u_1-1)\beta^{\vartheta}S}{(\epsilon_2^{\vartheta}A_s+1)^2}(\lambda_1^{\odot}-\lambda_4^{\odot})\\
&\quad+(u_1-1)(1-\tau_1^{\vartheta})\left(\frac{\beta^{\vartheta}V_1}{1+\sigma^{\vartheta}V_1}\right)(\lambda_2^{\odot}-\lambda_4^{\odot})\\
&\quad-\lambda_7^{\odot}(u_4+\alpha_3^{\vartheta})\\
&\quad+(u_1-1)(1-\tau_2^{\vartheta})\left(\frac{\beta^{\vartheta}V_2}{1+\sigma^{\vartheta}V_2}\right)(\lambda_3^{\odot}-\lambda_4^{\odot})\\
&\quad+\lambda_6^{\odot}(\mu^{\vartheta}+\phi_1^{\vartheta}+u_4+\alpha_3^{\vartheta})-B_3,\\
{}_{\Upsilon}^{C}\mathcal{D}_T^{\vartheta}\lambda_7^{\odot}(\Upsilon) &= -\frac{\partial\mathcal{H}}{\partial Q}(\Upsilon) = \lambda_7^{\odot}(\mu^{\vartheta}+\phi_2^{\vartheta}+\alpha_4^{\vartheta})-\lambda_8^{\odot}\alpha_4^{\vartheta}-B_4,\\
{}_{\Upsilon}^{C}\mathcal{D}_T^{\vartheta}\lambda_8^{\odot}(\Upsilon) &= -\frac{\partial\mathcal{H}}{\partial R}(\Upsilon) = \lambda_7^{\odot}\mu^{\vartheta}.
\end{aligned}
\tag{46}
$$

The optimal controls u_1, u_2, u_3, u_4 are also obtained by equating $\frac{\partial\mathcal{H}}{\partial u_i} = 0, i = 1, 2, 3, 4$, and making the u_i's the subject, where $i = 1, 2, 3, 4$. □

6.1. Numerical simulation of Caputo optimal control model

We studied the trajectory dynamics of the proposed Caputo fractional optimal control model. The fractional optimal solution is computed using a forward–backward scheme with the predict-evaluate-correct-evaluate (PECE) approach of Adams–Bashforth–Moulton, as described by Rosa et al. [58] in their numerical study of fractional optimal control of respiratory syncytial virus infection. In our numerical simulations, we take into account the following initial conditions and weight values: The initial values are as follows: $S(0) = 33\,422\,824, V_1(0) = 20\,000, V_2(0) = 600, L(0) = 200, A_m(0) = 0, A_s(0) = 32\,246, Q(0) = 0, R_0 = 0, B_1 = 5; B_2 = 1; B_3 = 5; B_4 = 1; C_1 = 2; C_2 = 2; C_3 = 2; C_4 = 2$, with a fractional order of $\vartheta = 0.90$. The corresponding parameter values are given in Table 3. We assumed that our ultimate time for the numerical simulation would be $T = 5$ years because the World Health Organization's goals for most diseases are typically fixed for five-year periods [58]. Fig. 9 shows the fractional optimal control effects of the media campaign and isolation centers for treatment on

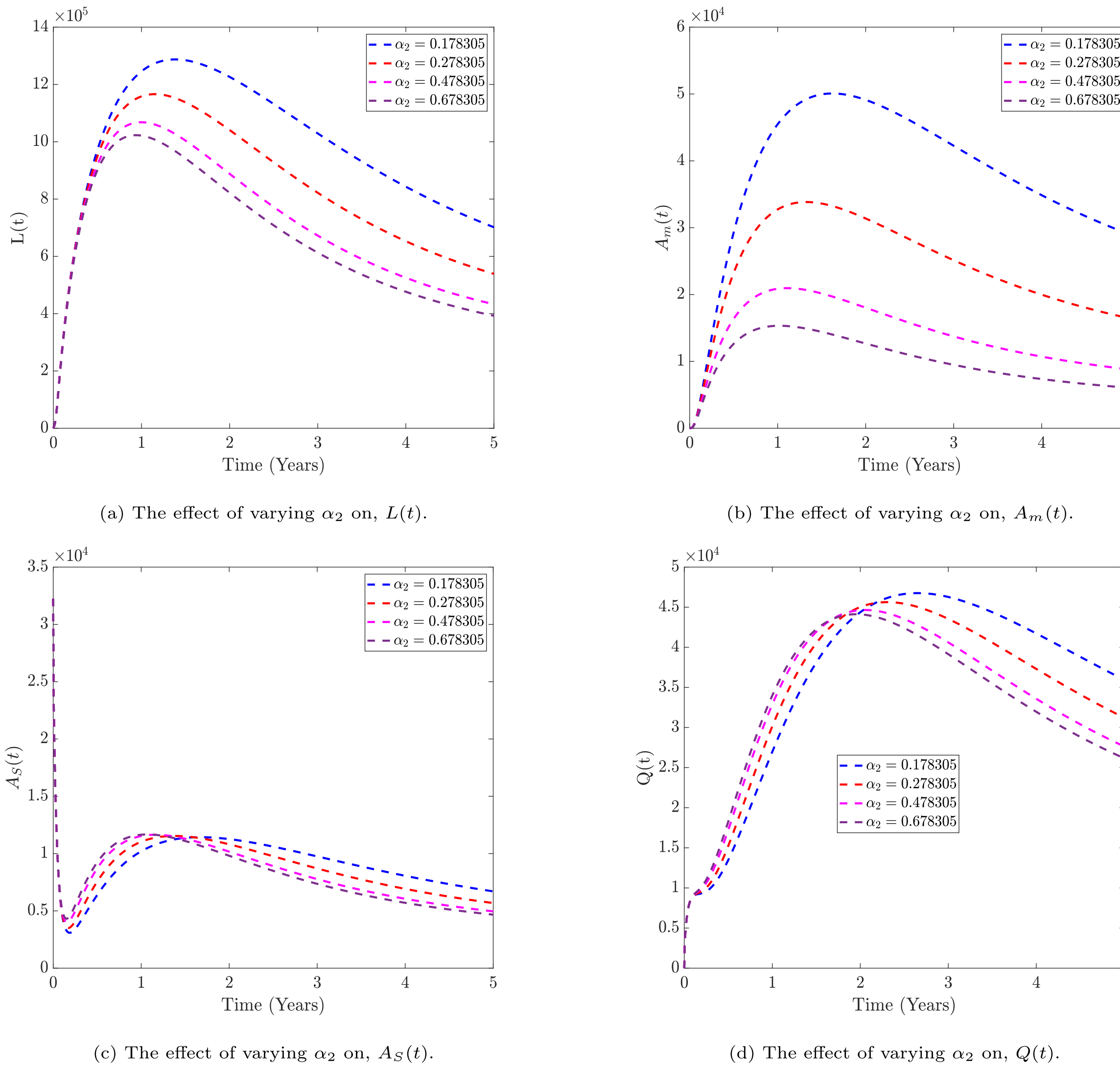

(a) The effect of varying α_2 on, $L(t)$.

(b) The effect of varying α_2 on, $A_m(t)$.

(c) The effect of varying α_2 on, $A_S(t)$.

(d) The effect of varying α_2 on, $Q(t)$.

Fig. 5. The effect of varying the rate at which individuals in the asymptomatic class become symptomatic, α_2.

the $A_m(t), A_s(t), Q(t)$, and $Q(t)$, respectively. As shown in Fig. 9(a), 9(b), 9(c), 9(d), the introduction of media campaigns and isolation centers for treatment as controls causes a decrease in the number of infected individuals. Fig. 10 shows the fractional optimal control profiles, thus considering media campaigns and isolation centers for treatment. It is noticed that to achieve the said numerical trajectories, as seen in Fig. 9(a), Fig. 9(b), Fig. 9(c), and Fig. 9(d), it is advisable to maintain media campaign control and isolation centers for treatment at an intensity of 88% for four years six months and 100% for five years respectively before lowing these two controls intensities.

Fig. 11 shows the fractional optimal control effects of first dose vaccine and second dose vaccine on the $A_m(t), A_s(t), Q(t)$, and $Q(t)$, respectively. As shown in Fig. 11(a), 11(b), 11(c), 11(d), the introduction of first dose vaccine and second dose vaccine as controls causes a decrease in the number of infected individuals. Fig. 12 shows the fractional optimal control profiles, thus considering the first and second doses. It is noticed that to achieve the said numerical trajectories, as seen in Fig. 11(a), Fig. 11(b), Fig. 11(c), and Fig. 11(d), it is advisable to maintain first dose vaccine and second dose vaccine at an intensity of 85% for five years and 100% for five years respectively, before lowing these two controls intensities. Fig. 13 shows the fractional optimal control considering media campaigns, first-dose vaccines, second-dose vaccines, and isolation centers for treatment on the $A_m(t), A_s(t), Q(t)$, and $Q(t)$, respectively. As shown in Fig. 13(a), 13(b), 13(c), 13(d), the introduction of media campaigns, first-dose vaccines, second-dose vaccines, and isolation centers for treatment as controls causes eradication of the number of infected individuals. Fig. 14 shows the fractional optimal control profiles, thus considering media campaigns, first-dose vaccines, second-dose vaccines, and isolation centers for treatment. It is noticed that to achieve the said numerical trajectories as seen in Fig. 13(a), Fig. 13(b), Fig. 13(c), and Fig. 13(d), it is advisable to maintain media campaign, first dose vaccines, second dose vaccines and isolation centers for treatment at an intensity of 98%, 85%, 100%, and 100% for five years respectively for media campaign u_1, first dose vaccines u_2, second dose vaccines u_3 and isolation centers for treatment u_4, throughout the simulation time.

7. Conclusion

We demonstrated the effectiveness of Caputo fractional optimal control analysis in understanding and managing measles outbreaks using real-world data. By employing fractional calculus techniques, we developed a comprehensive compartmental model that accurately captures the complex dynamics of measles transmission, accounting for factors

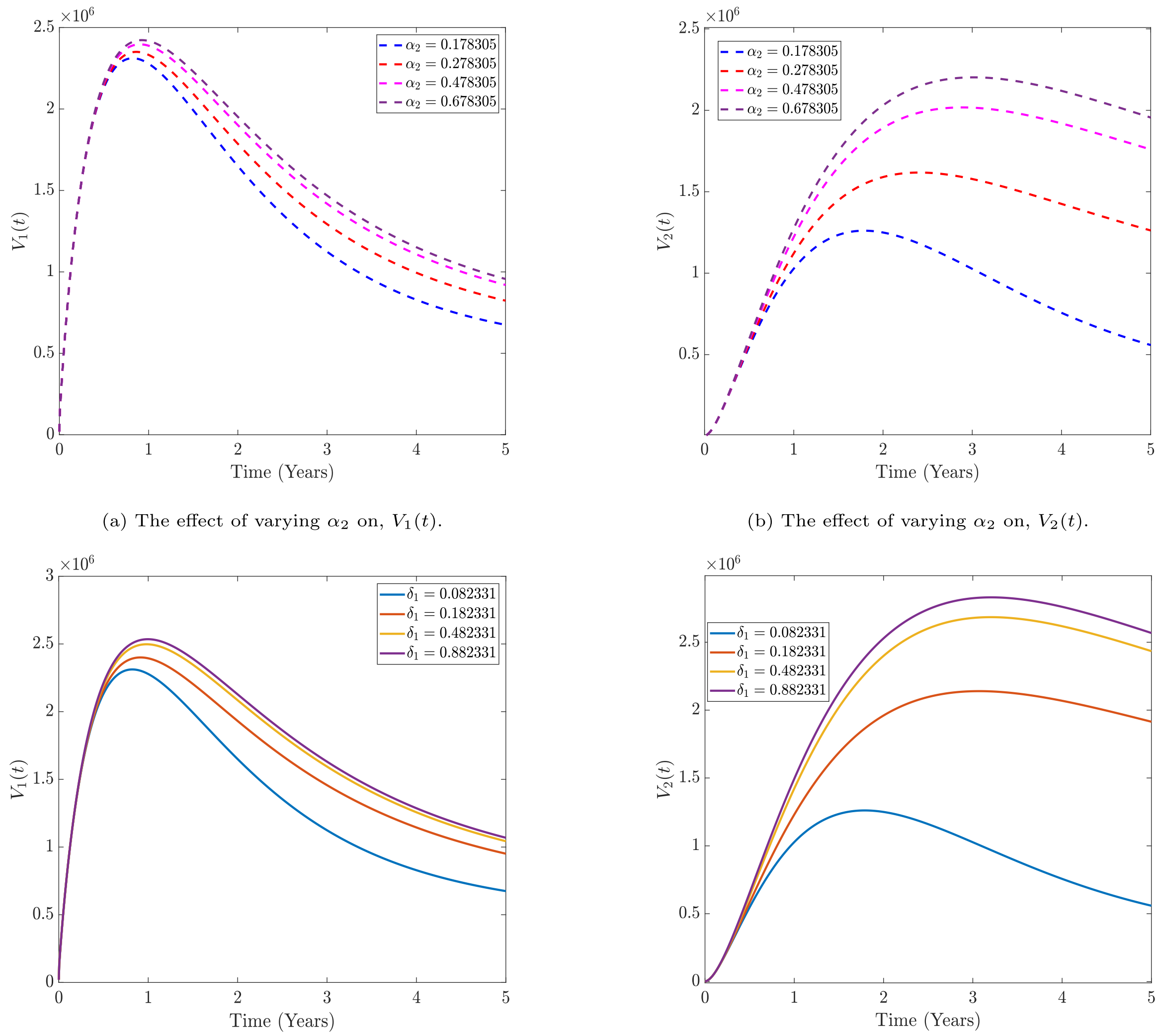

(a) The effect of varying α_2 on, $V_1(t)$.

(b) The effect of varying α_2 on, $V_2(t)$.

(c) The effect of varying δ_1 on, $V_1(t)$.

(d) The effect of varying δ_1 on, $V_2(t)$.

Fig. 6. The effect of varying the rate at which individuals in the asymptomatic class become symptomatic, α_2, and the effect of varying the rate at which individuals in the latent class recover from the measles, δ_1.

such as waning immunity and heterogeneous population interactions. Through numerical simulations and sensitivity analyses, we identified optimal control strategies that effectively minimize disease burden while considering practical constraints such as vaccination resources, isolation centers for treatment purposes, and media campaigns. We obtained the measles disease-free equilibrium point and the measles reproduction number and also proved that the proposed fractional model is stable using the Ulam–Hyers stability analysis. The sensitivity analysis of the model indicates the most sensitive parameters in the measles reproduction number. Leveraging the sensitivity analysis using Latin hypercube sampling and three-D plots, we formulated an optimal control model using Pontryagin's maximum principle. Our findings highlight the importance of adaptive and data-driven disease control and management approaches. By leveraging actual epidemiological data, we were able to tailor control strategies that are more robust and efficient in mitigating measles outbreaks. Moreover, fractional calculus provides a flexible framework for modeling and analyzing infectious disease dynamics, allowing for a more accurate representation of memory effects and non-local interactions inherent in epidemic processes. Extending this analysis to other contagious diseases and considering dynamic socio-demographic factors would contribute to a more comprehensive understanding of epidemic dynamics and inform the development of proactive public health policies.

CRediT authorship contribution statement

Fredrick Asenso Wireko: Writing – review & editing, Writing – original draft, Visualization, Validation, Methodology, Investigation, Formal analysis, Conceptualization. **Joshua Kiddy K. Asamoah:** Writing – review & editing, Writing – original draft, Visualization, Validation, Supervision, Software, Resources, Project administration, Methodology, Investigation, Formal analysis. **Isaac Kwasi Adu:** Writing – review & editing, Writing – original draft, Visualization, Validation, Methodology, Investigation, Formal analysis. **Sebastian Ndogum:** Writing – review & editing, Writing – original draft, Validation, Software, Resources, Methodology, Investigation, Formal analysis.

Declaration of competing interest

The authors declare that they have no known competing financial interests or personal relationships that could have appeared to influence the work reported in this paper.

Acknowledgment

The authors thank their respective university for the support in writing the manuscript.

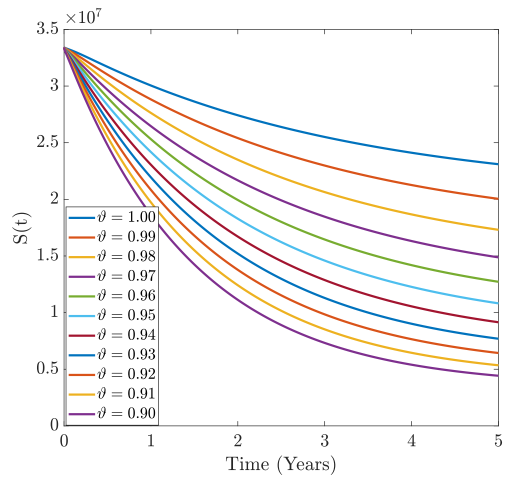

(a) Effect of memory on the susceptible compartment, $S(t)$.

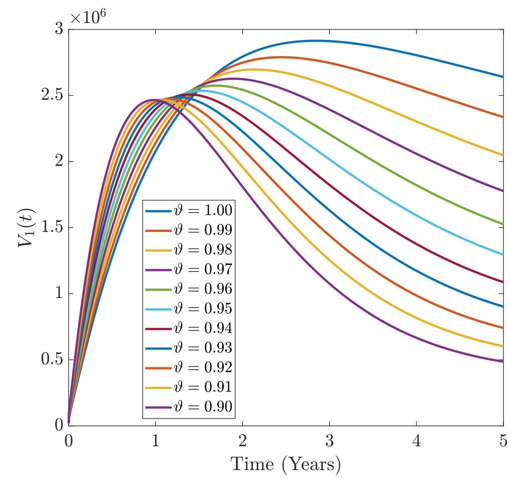

(b) Effect of memory on the first dose compartment, $V_1(t)$.

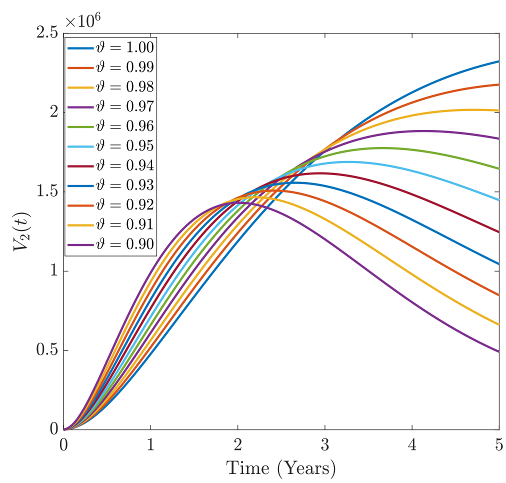

(c) Effect of memory on the second dose compartment, $V_2(t)$.

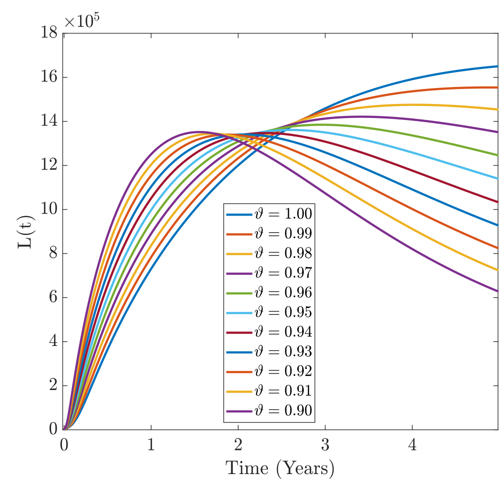

(d) Effect of memory on the latent compartment, $L(t)$.

Fig. 7. Effect of memory on the $S(t), V_1(t), V_2(t)$, and $L(t)$, respectively. Considering $\vartheta \in [0.90 : 0.01 : 1]$.

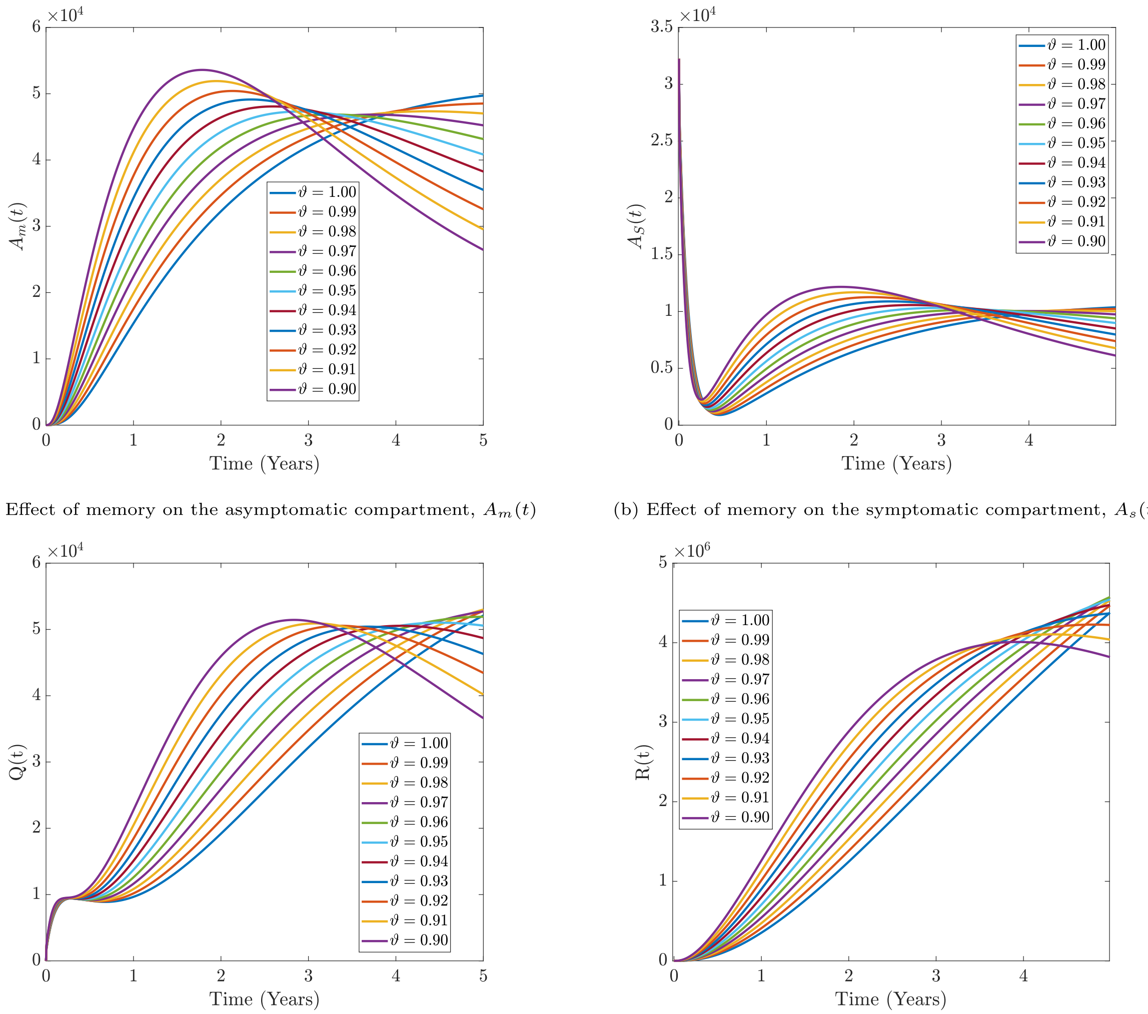

(a) Effect of memory on the asymptomatic compartment, $A_m(t)$

(b) Effect of memory on the symptomatic compartment, $A_s(t)$

(c) Effect of memory on the quarantined compartment, $Q(t)$

(d) Effect of memory on the recovered compartment, $L(t)$

Fig. 8. Effect of memory on the $A_m(t), A_s(t), Q(t)$, and $R(t)$, respectively. Considering $\vartheta \in [0.90 : 0.01 : 1]$.

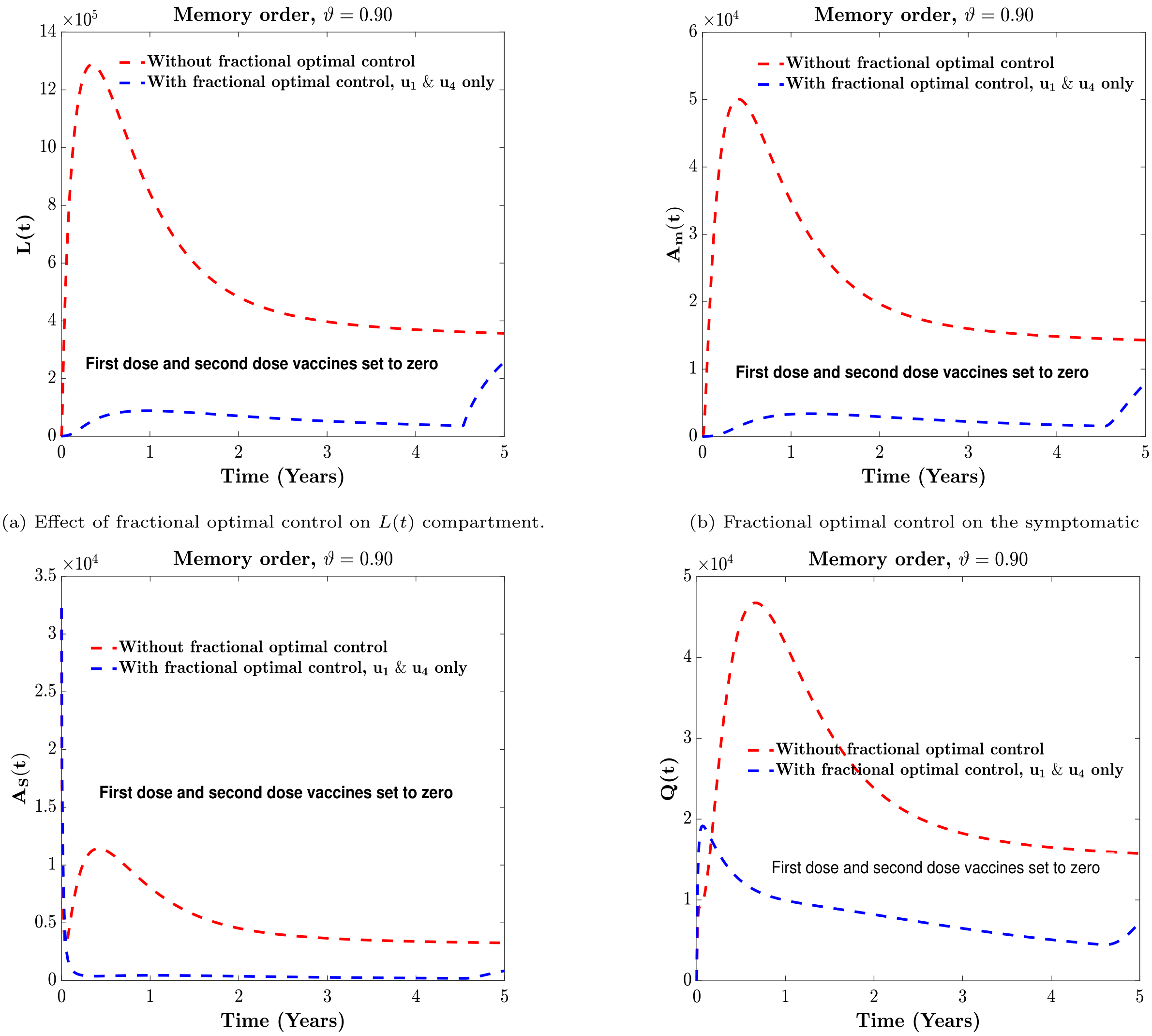

(a) Effect of fractional optimal control on $L(t)$ compartment.

(b) Fractional optimal control on the symptomatic

(c) Fractional optimal control on the asymptomatic.

(d) Fractional optimal control on the quarantined.

Fig. 9. Fractional optimal control effects of media campaign and isolation centers for treatment on the $A_m(t), A_s(t), Q(t)$, and $Q(t)$, respectively. Considering $\vartheta = 0.90$.

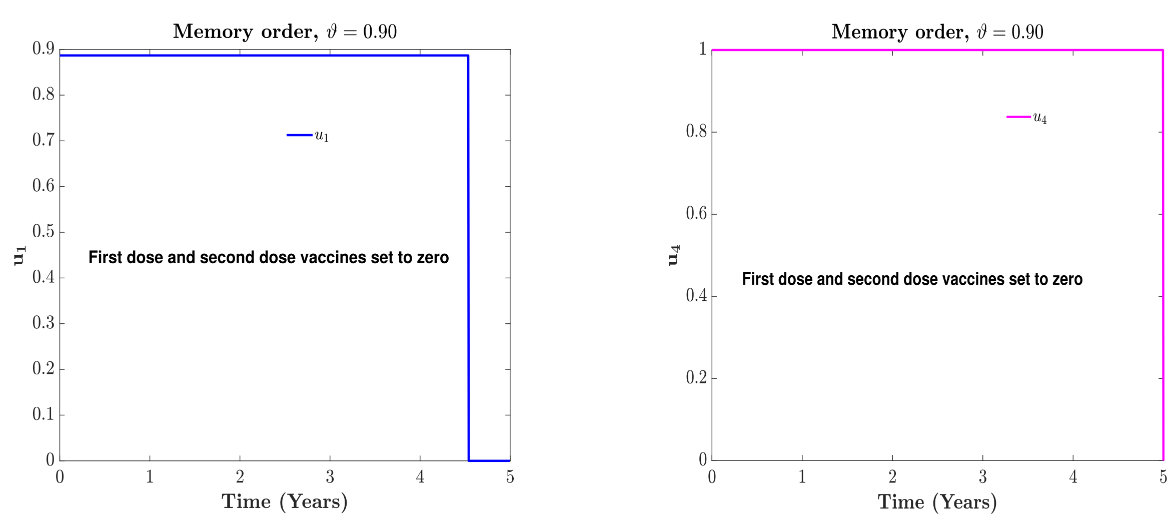

(a) Control profile, $u_1(t)$.

(b) Control profile, $u_4(t)$.

Fig. 10. Fractional optimal control profiles considering media campaign and isolation centers for treatment, with $\vartheta = 0.90$.

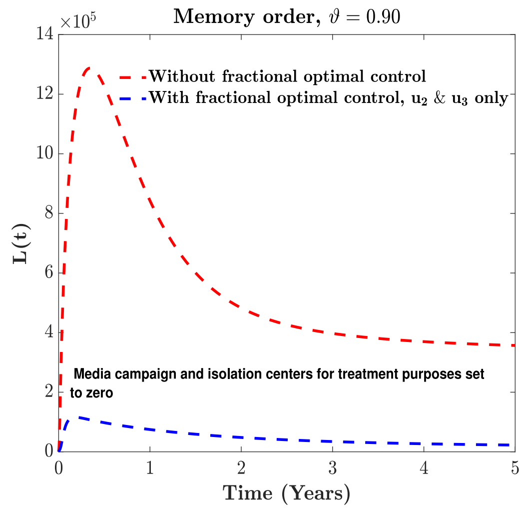

(a) Effect of fractional optimal control on $L(t)$ compartment.

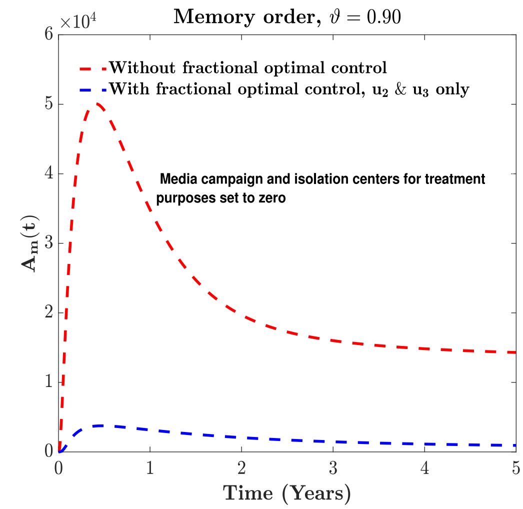

(b) Fractional optimal control on the asymptomatic

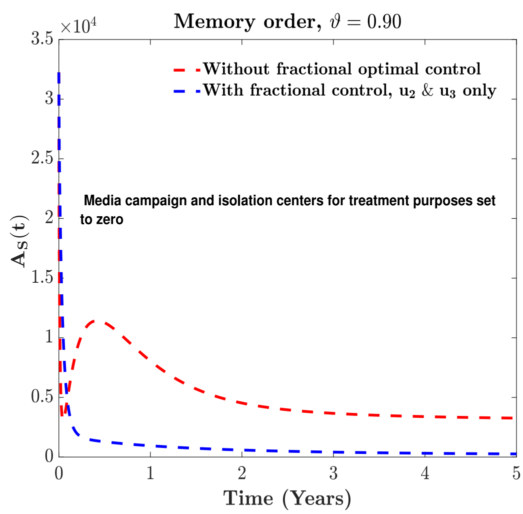

(c) Fractional optimal control on the symptomatic

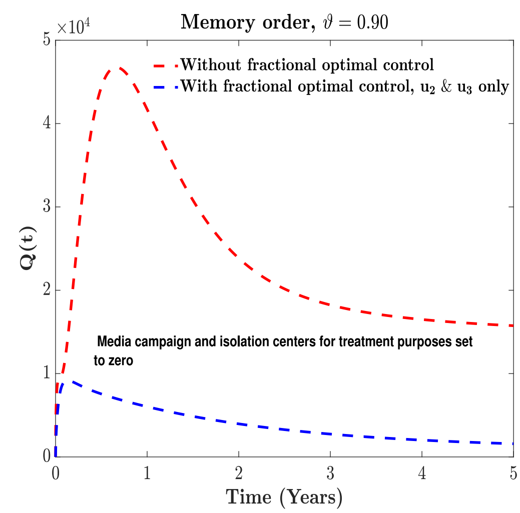

(d) Fractional optimal control on the quarantined

Fig. 11. Fractional optimal control effects of first dose vaccine and second dose vaccine on the $A_m(t), A_s(t), Q(t)$, and $Q(t)$, respectively. Considering $\vartheta = 0.90$.

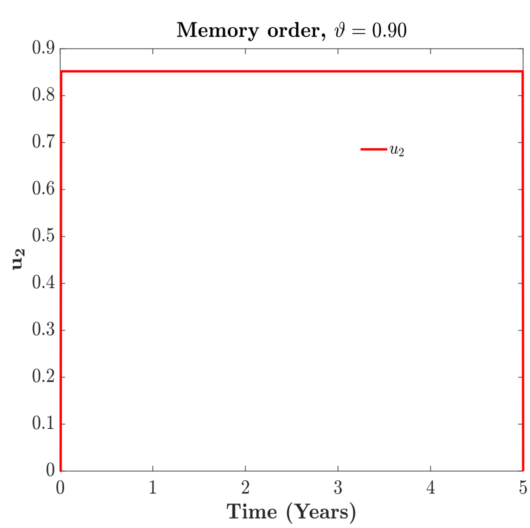

(a) Control profile, $u_2(t)$

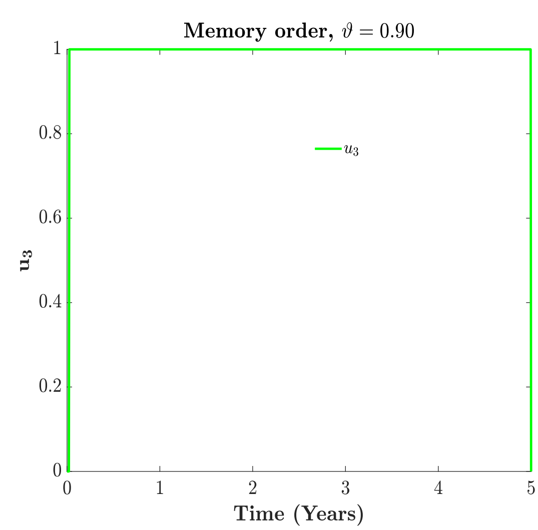

(b) Control profile, $u_3(t)$

Fig. 12. Fractional optimal control profiles considering first dose and second dose vaccines only, with $\vartheta = 0.90$.

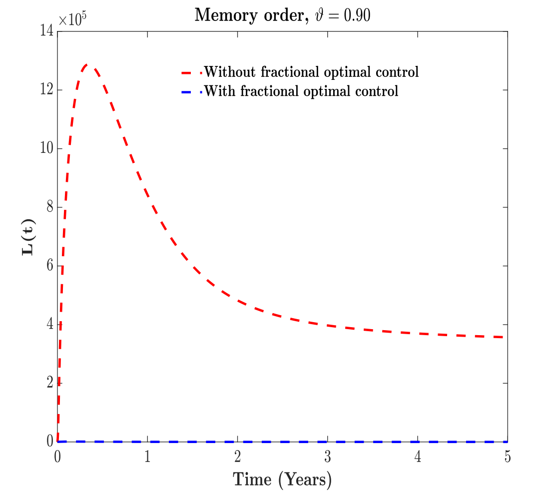

(a) Effect of fractional optimal control on $L(t)$ compartment.

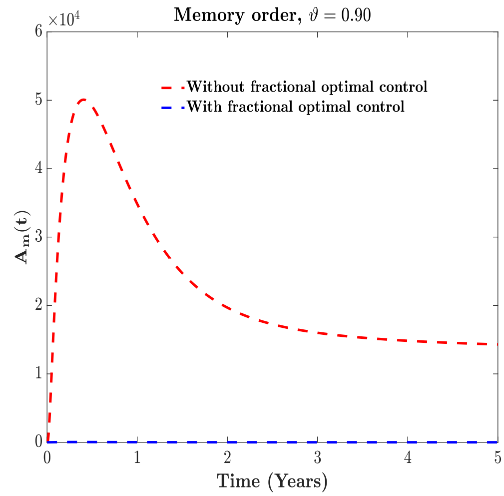

(b) Fractional optimal control on the asymptomatic

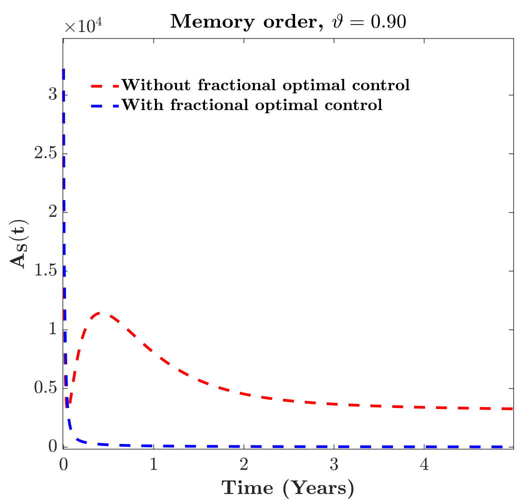

(c) Fractional optimal control on the symptomatic

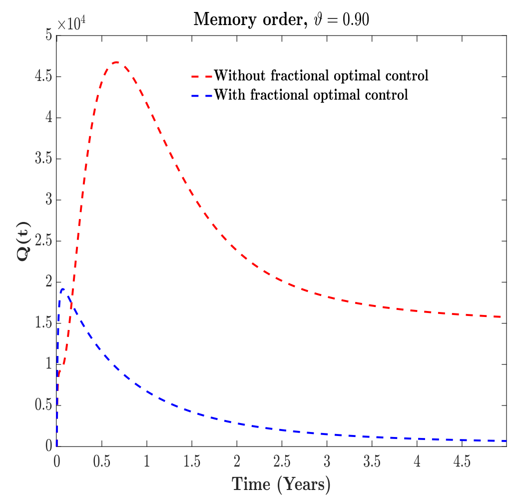

(d) Effect of fractional optimal control on the quarantined

Fig. 13. Fractional optimal control effects of all four controls on the $A_m(t), A_s(t), Q(t)$, and $Q(t)$, respectively. Considering $\vartheta = 0.90$.

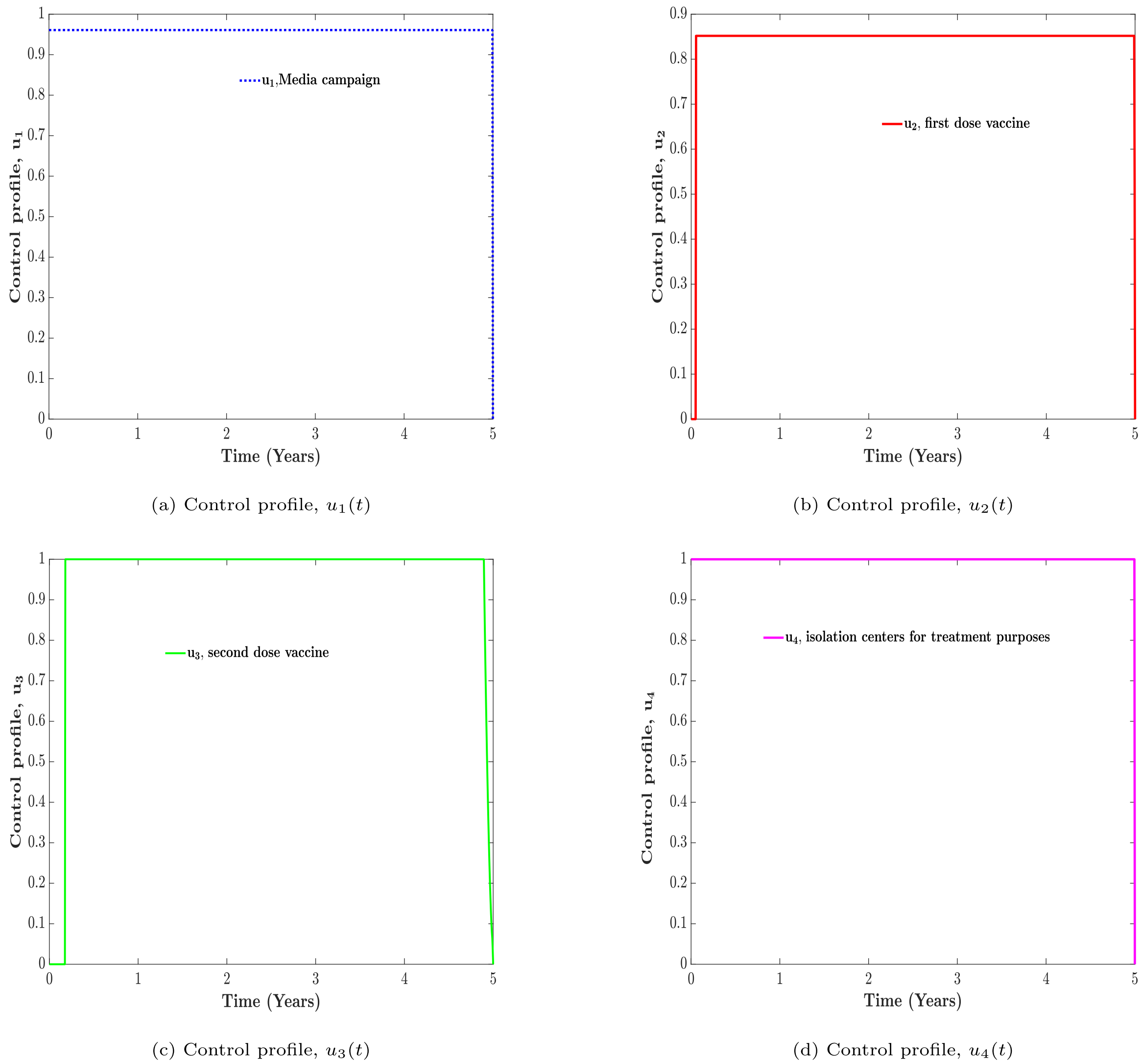

(a) Control profile, $u_1(t)$

(b) Control profile, $u_2(t)$

(c) Control profile, $u_3(t)$

(d) Control profile, $u_4(t)$

Fig. 14. Fractional optimal control profiles considering media campaign, first dose vaccines, second dose vaccines and isolation centers for treatment, with $\vartheta = 0.90$.

References

[1] Branda F, Giovanetti M, Romano C, Benvenuto D, Ciccozzi A, Sanna D, Ciccozzi M, Scarpa F. Global measles surveillance: Trends, challenges, and implications for public health interventions. Infect Dis Rep 2024;16(2):367–79.

[2] Plattet P, Alves L, Herren M, Aguilar HC. Measles virus fusion protein: structure, function and inhibition. Viruses 2016;8(4):112. http://dx.doi.org/10.3390/v8040112.

[3] CDC. Transmission of measles. Centers for Disease Control and Prevention; 2020, https://www.cdc.gov/measles/transmission.html/.

[4] Leung AK, Hon K, Leong K, Sergi C. Measles: a disease often forgotten but not gone. Hong Kong Med J 2018;24(5):512. http://dx.doi.org/10.12809/hkmj187470.

[5] Dixon MG, Ferrari M, Antoni S, Li X, Portnoy A, Lambert B, Hauryski S, Hatcher C, Nedelec Y, Patel M, et al. Progress toward regional measles elimination—worldwide, 2000–2020. Morb Mortal Wkly Rep 2021;70(45):1563. http://dx.doi.org/10.15585/mmwr.mm7045a1.

[6] WHO. Measles. World Health Organization; 2023, https://www.who.int/news-room/fact-sheets/detail/measles/.

[7] Dundar S, Gokkurt B, Soylu Y. Mathematical modelling at a glance: a theoretical study. Procedia-Soc Behav Sci 2012;46:3465–70. http://dx.doi.org/10.1016/j.sbspro.2012.06.086.

[8] Wireko FA, Adu IK, Sebil C, Asamoah JKK. A fractal–fractional order model for exploring the dynamics of monkeypox disease. Decis Anal J 2023;8:100300. http://dx.doi.org/10.1016/j.dajour.2023.100300.

[9] Asamoah JKK, Safianu B, Afrifa E, Obeng B, Seidu B, Wireko FA, Sun GQ. Optimal control dynamics of gonorrhea in a structured population. Heliyon 2023;9(10). http://dx.doi.org/10.1016/j.heliyon.2023.e20531.

[10] Tilahun GT, Demie S, Eyob A. Stochastic model of measles transmission dynamics with double dose vaccination. Infect Dis Model 2020;5:478–94. http://dx.doi.org/10.1016/j.idm.2020.06.003.

[11] James Peter O, Ojo MM, Viriyapong R, Abiodun Oguntolu F. Mathematical model of measles transmission dynamics using real data from Nigeria. J Difference Equ Appl 2022;28(6):753–70. http://dx.doi.org/10.1080/10236198.2022.2079411.

[12] WHO. Measles vaccines: WHO position paper, april 2017–recommendations. Vaccine 2019;37(2):219–22. http://dx.doi.org/10.1016/j.vaccine.2017.07.066.

[13] Kuddus MA, Mohiuddin M, Rahman A. Mathematical analysis of a measles transmission dynamics model in Bangladesh with double dose vaccination. Sci Rep 2021;11(1):16571. http://dx.doi.org/10.1038/s41598-021-95913-8.

[14] Diagne ML, Rwezaura H, Pedro S, Tchuenche JM. Theoretical analysis of a measles model with nonlinear incidence functions. Commun Nonlinear Sci Numer Simul 2023;117:106911. http://dx.doi.org/10.1016/j.cnsns.2022.106911.

[15] Addai E, Zhang L, Preko AK, Asamoah JKK. Fractional order epidemiological model of SARS-CoV-2 dynamism involving Alzheimer's disease. Healthc Anal 2022;2:100114. http://dx.doi.org/10.1016/j.health.2022.100114.

[16] Berhe HW, Makinde OD. Computational modelling and optimal control of measles epidemic in human population. Biosystems 2020;190:104102. http://dx.doi.org/10.1016/j.biosystems.2020.104102.

[17] Khajanchi S, Das DK, Kar TK. Dynamics of tuberculosis transmission with exogenous reinfections and endogenous reactivation. Phys A 2018;497:52–71. http://dx.doi.org/10.1016/j.physa.2018.01.014.

[18] Seidu B, Wiah EN, Asamoah JKK. Optimal strategies for control of cholera in the presence of hyper-infective individuals. Results Phys 2023;53:106968. http://dx.doi.org/10.1016/j.rinp.2023.106968.

[19] Raymond Fosu A, Jin Z, Yang J, Asamoah JK, et al. Cost-benefit analysis of COVID-19 vaccination model incorporating different infectivity reductions. Front Phys 12:1383357. http://dx.doi.org/10.3389/fphy.2024.1383357.

[20] Raymond Fosu A, Jin Z, Yang J, Asamoah JKK. Mathematical modeling of two strains Tuberculosis and Covid-19 vaccination model: A co-infection study with cost-effectiveness analysis. Front Appl Math Stat 10:1373565. http://dx.doi.org/10.3389/fams.2024.1373565.

[21] Das DK, Khajanchi S, Kar TK. The impact of the media awareness and optimal strategy on the prevalence of tuberculosis. Appl Math Comput 2020;366:124732. http://dx.doi.org/10.1016/j.amc.2019.124732.

[22] Khajanchi S, Bera S, Roy TK. Mathematical analysis of the global dynamics of a HTLV-I infection model, considering the role of cytotoxic T-lymphocytes. Math Comput Simulation 2021;180:354–78. http://dx.doi.org/10.1016/j.amc.2019.124732.

[23] Das DK, Khajanchi S, Kar T. Transmission dynamics of tuberculosis with multiple re-infections. Chaos Solitons Fractals 2020;130:109450. http://dx.doi.org/10.1016/j.amc.2019.124732.

[24] Misra AK, Singh RK, Tiwari PK, Khajanchi S, Kang Y. Dynamics of algae blooming: effects of budget allocation and time delay. Nonlinear Dynam 2020;100:1779–807. http://dx.doi.org/10.1007/s11071-020-05551-4.

[25] Khajanchi S, Banerjee S. A strategy of optimal efficacy of T11 target structure in the treatment of brain tumor. J Biol Systems 2019;27(02):225–55. http://dx.doi.org/10.1142/S0218339019500104.

[26] Khajanchi S. Stability analysis of a mathematical model for glioma-immune interaction under optimal therapy. Int J Nonlinear Sci Numer Simul 2019;20(3–4):269–85. http://dx.doi.org/10.1007/s11071-020-05551-4.

[27] Asamoah JKK, Jin Z, Sun GQ. Non-seasonal and seasonal relapse model for Q fever disease with comprehensive cost-effectiveness analysis. Results Phys 2021;22:103889. http://dx.doi.org/10.1016/j.rinp.2021.103889.

[28] Khajanchi S, Ghosh D. The combined effects of optimal control in cancer remission. Appl Math Comput 2015;271:375–88. http://dx.doi.org/10.1016/j.amc.2015.09.012.

[29] Adu IK, Wireko FA, Sebil C, Asamoah JKK. A fractal–fractional model of Ebola with reinfection. Results Phys 2023;52:106893. http://dx.doi.org/10.1016/j.rinp.2023.106893.

[30] Odionyenma UB, Ikenna N, Bolaji B. Analysis of a model to control the co-dynamics of Chlamydia and Gonorrhea using Caputo fractional derivative. Math Model Numer Simul Appl 2023;3(2):111–40. http://dx.doi.org/10.53391/mmnsa.1320175.

[31] Asamoah JKK, Sun GQ. Fractional Caputo and sensitivity heat map for a gonorrhea transmission model in a sex structured population. Chaos Solitons Fractals 2023;175:114026. http://dx.doi.org/10.1016/j.chaos.2023.114026.

[32] Asamoah JKK, et al. A fractional mathematical model of heartwater transmission dynamics considering nymph and adult amblyomma ticks. Chaos Solitons Fractals 2023;174:113905. http://dx.doi.org/10.1016/j.chaos.2023.113905.

[33] Emmanuel A, Zhang N, Mezue M, Rashid S, Akinnubi A, Abdul-Hamid Z, Asamoah JKK. A fractional control model to study monkeypox transport network related transmission. Int J Biomath 2024. http://dx.doi.org/10.1142/S179352452450044X.

[34] Abboubakar H, Fandio R, Sofack BS, Ekobena Fouda HP. Fractional dynamics of a measles epidemic model. Axioms 2022;11(8):363. http://dx.doi.org/10.3390/axioms11080363.

[35] Qureshi S, Jan R. Modeling of measles epidemic with optimized fractional order under Caputo differential operator. Chaos Solitons Fractals 2021;145:110766. http://dx.doi.org/10.1016/j.chaos.2021.110766.

[36] Farman M, Shehzad A, Akgül A, Baleanu D, Sen MDl. Modelling and analysis of a measles epidemic model with the constant proportional Caputo operator. Symmetry 2023;15(2):468. http://dx.doi.org/10.3390/sym15020468.

[37] Li S, Ullah S, AlQahtani SA, Asamoah JKK, et al. Examining dynamics of emerging nipah viral infection with direct and indirect transmission patterns: A simulation-based analysis via fractional and fractal-fractional derivatives. J Math Univ Tokushima 2023;2023. http://dx.doi.org/10.1155/2023/6643772.

[38] Addai E, Adeniji A, Ngungu M, Tawiah GK, Marinda E, Asamoah JKK, Khan MA. A nonlinear fractional epidemic model for the Marburg virus transmission with public health education. Sci Rep 2023;13(1):19292. http://dx.doi.org/10.1038/s41598-023-46127-7.

[39] Adu IK, Wireko FA, Mojeeb Al-R ENO, Asamoah JKK. A fractional order ebola transmission model for dogs and humans. Sci Afr 2024;e02230. http://dx.doi.org/10.1016/j.sciaf.2024.e02230.

[40] Asamoah JKK, Okyere E, Yankson E, Opoku AA, Adom-Konadu A, Acheampong E, Arthur YD. Non-fractional and fractional mathematical analysis and simulations for Q fever. Chaos Solitons Fractals 2022;156:111821. http://dx.doi.org/10.1016/j.chaos.2022.111821.

[41] Asamoah J. Fractal–fractional model and numerical scheme based on Newton polynomial for Q fever disease under Atangana–Baleanu derivative. Results Phys 2022;34:105189. http://dx.doi.org/10.1016/j.rinp.2022.105189.

[42] Aguegboh NS, Nwokoye NR, Onyiaji NE, Amanso OR, Oranugo DO. A fractional order model for the transmission dynamics of measles with vaccination. Open Access Libr J 2020;7(10):1–13. http://dx.doi.org/10.4236/oalib.1106670.

[43] Nazir G, Shah K, Alrabaiah H, Khalil H, Khan RA. Fractional dynamical analysis of measles spread model under vaccination corresponding to nonsingular fractional order derivative. Adv Difference Equ 2020;2020:1–15. http://dx.doi.org/10.1186/s13662-020-02628-7.

[44] Frederick E. How measles causes the body to 'forget' past infections by other microbes. Science; 2024, https://www.science.org/content/article/how-measles-causes-body-forget-past-infections-other-microbes#:∼:text=They%20found%20that%20measles%20infection,memory%20B's%20to%20replace%20them.

[45] Dutchen S. Measles-ravaged immune system must 'relearn' how to protect the body against infections. HMS Communications; 2024, https://news.harvard.edu/gazette/story/2019/10/how-measles-wipes-out-the-bodys-immune-memory/#:∼:text=According%20to%20this%20theory%2C%20the,its%20resistance%20to%20other%20infections.

[46] Muhammad Altaf K, Atangana A. Dynamics of Ebola disease in the framework of different fractional derivatives. Entropy 2019;21(3):303. http://dx.doi.org/10.3390/e21030303.

[47] Nisar KS, Farman M, Abdel-Aty M, Cao J. A review on epidemic models in sight of fractional calculus. Alex Eng J 2023;75:81–113. http://dx.doi.org/10.1016/j.aej.2023.05.071.

[48] Huang C, Wang J, Chen X, Cao J. Bifurcations in a fractional-order BAM neural network with four different delays. Neural Netw 2021;141:344–54. http://dx.doi.org/10.1016/j.neunet.2021.04.005.

[49] Hyers DH. On the stability of the linear functional equation. Proc Natl Acad Sci 1941;27(4):222–4. http://dx.doi.org/10.1073/pnas.27.4.222.

[50] Rassias TM. On the stability of the linear mapping in Banach spaces. Proc Amer Math Soc 1978;72(2):297–300. http://dx.doi.org/10.1090/S0002-9939-1978-0507327-1.

[51] Ackora-Prah J, Seidu B, Okyere E, Asamoah JK. Fractal-fractional Caputo maize streak virus disease model. Fractal Fract 2023;7(2):189. http://dx.doi.org/10.3390/fractalfract7020189.

[52] Rezapour S, Asamoah JKK, Hussain A, Ahmad H, Banerjee R, Etemad S, Botmart T. A theoretical and numerical analysis of a fractal–fractional two-strain model of meningitis. Results Phys 2022;39:105775. http://dx.doi.org/10.1016/j.rinp.2022.105775.

[53] Asamoah JKK, Jin Z, Sun GQ, Seidu B, Yankson E, Abidemi A, Oduro F, Moore SE, Okyere E. Sensitivity assessment and optimal economic evaluation of a new COVID-19 compartmental epidemic model with control interventions. Chaos Solitons Fractals 2021;146:110885. http://dx.doi.org/10.1016/j.chaos.2021.110885.

[54] Asamoah JKK, Owusu MA, Jin Z, Oduro F, Abidemi A, Gyasi EO. Global stability and cost-effectiveness analysis of COVID-19 considering the impact of the environment: using data from Ghana. Chaos Solitons Fractals 2020;140:110103. http://dx.doi.org/10.1016/j.chaos.2020.110103.

[55] Martcheva M. An introduction to mathematical epidemiology, vol. 61, Springer; 2015.

[56] WHO. Measles - number of reported cases. World Health Organization; 2023, https://www.who.int/data/gho/data/indicators/indicator-details/GHO/measles---number-of-reported-cases/.

[57] UNWPP. Ghana population 1950–2023. United Nations - World Population Prospects; 2023, https://www.macrotrends.net/countries/GHA/ghana/population.

[58] Rosa S, Torres DF. Numerical fractional optimal control of respiratory syncytial virus infection in octave/MATLAB. Mathematics 2023;11(6):1511. http://dx.doi.org/10.3390/math11061511.